SOME ASPECTS OF FERROHYDROSTATIC SEPARATION OF MINERALS AND THE RECYCLING OF FERROFLUID

by

STANFORD DUMBU

Thesis submitted in partial fulfilment of the requirements for the degree of

Master of Science in Engineering (Mineral Processing)

in the

Department of Chemical Engineering

at the

University of Stellenbosch

Supervised by

Dr. J. Svoboda
Prof. L. Lorenzen
Dr. K.R.P. Petersen

March, 2001

DECLARATION

I, the undersigned, declare that the work contained in this thesis is my own original work and has not been submitted previously in its entirety or in part for a degree at any university.

S Dumbu

SYNOPSIS

Ferrohydrostatic separation (FHS) of materials is a float and sink technique which utilizes ferrofluid exposed to a non-homogeneous magnetic field. The efficiency of material separation depends on numerous variables. The most important variables, which were investigated individually, are the effects of moisture content, ferrofluid level, feedrate, particle size and material density distribution on separation efficiency.

It is important to recover and recycle the ferrofluid attached to the products of separation so as to reduce the cost of the FHS technology and the amount of kerosene disposed of to the environment. This prompted research into some of the factors affecting ferrofluid recovery. The factors that were investigated are the effects of FHS operation, material moisture content, particle size and porosity.

The separation efficiency was found to be dependent on all the variables investigated. The effect of material moisture content is less pronounced for particles larger than 2.8 mm. This implies that wet feed material should be screened before ferrohydrostatic separation and material which particle size is less than 2.8 mm should preferably be treated dry. Wet material (less than 2.8 mm) floats, even though its density is greater than the cut-point density. This is owing to the immiscibility of the water coating the particles and the kerosene-based ferrofluid used for separation.

It was found that the effect of ferrofluid level on separation efficiency is a function of both the density difference of the particles to be separated and the particle size. Separation efficiency as a function of ferrofluid level is poor for particles larger than 2 mm and is good when the density difference of the material to be separated is high, for instance between 2700 kg/m^3 and 3530 kg/m^3. This shows that for efficient separation of coarse particles and near density material (material with density close to the cut-point density), the ferrofluid level should be controlled, preferably close to the maximum possible level.

The effect of feedrate on separation efficiency is also a function of the densities of the particles to be separated. An increase in feedrate leads to poor separation for particles with densities close to each other. This implies that separation of near density material requires accurate feedrate control.

It has been shown from simulation and modelling that the effective cut-point density changes as the particle moves through the chamber until it eventually reaches its terminal velocity, given that the chamber is of sufficient size for this to occur. The effective cut-point density increases to the maximum as the particle enters the ferrofluid pool but settles down to a relative constant once the particle has reached its terminal velocity. The effective cut-point density was shown to decrease with an increase in particle magnetisation. It was found that this decrease in the cut-point density determines the density difference (difference between two particles) achievable when non-magnetic material is treated together with magnetic material. It is therefore important to magnetically scalp the feed material for efficient separation. When the material is not scalped, magnetic and nonmagnetic material with the same density might report to different density fractions, which leads to poor separation. This magnetic contribution to the effective density can be utilised in the separation of material with same density but different magnetisation.

The efficiency of ferrofluid recovery was found to be dependent on all the variables investigated. The amount of ferrofluid drawn from the FHS separator was found to decrease with an increase in the magnetic field. Furthermore, the amount of ferrofluid that remains attached to the particles after allowing ferrofluid to drain from the material is the same as that attached to the FHS products of separation at high magnetic fields. This shows that it is important to operate the ferrohydrostatic separator at high magnetic fields in order to attract most of the ferrofluid back to the separator.

The amount of ferrofluid adsorbed onto and absorbed by the particles was found to decrease with an increase in the material moisture content. This is due to two factors. The first is that water occupies the vacant pores in the material. The second is that water forms a layer on the particle surface which is immiscible with kerosene-based ferrofluid. This phenomenon leads to a reduction in cost of the ferrohydrostatic separation technology when wet material as opposed to dry material is treated. As already described coarse material larger than 2.8 mm can be treated wet without detrimental effects on separation. For –8+4 mm particles, the ferrofluid loss ranges from 0.6 down to 0.14 kg/tonne of feed for 0 to 10 % material moisture content respectively.

The amount of ferrofluid lost per tonne of feed was found to range from 0.73 to 0.56 kg for –0.85+0.5 mm to –12+8 mm particle sizes respectively. The increase in ferrofluid loss in small particles is due to the increase in surface area in small particles for ferrofluid adsorption.

The increase in porosity increases the amount of ferrofluid lost due to the difficulties in recovering ferrofluid embedded in the pores of the particles.

Adding water to coarse material lowers the amount of ferrofluid lost by reducing porosity. Modelling the amount of ferrofluid lost, as a function of particle size and porosity, would assist in determining the amount of ferrofluid required to treat a known amount of material.

The quality of ferrofluid recovered was found to be the same as that initially used for material separation. This implies that the separation efficiency would not be affected by the use of recycled ferrofluid.

OPSOMMING

Ferro-hidrostatiese skeiding van materiale is 'n flotasie (dryf) en besinkingstegniek wat gebruik maak van ferro-vloeistof wat blootgestel is aan 'n magnetiese veld. Die effektiwiteit van die materiaal skeiding is afhanklik van verskeie veranderlikes. Die belangrikste veranderlikes wat die skeidingseffektiwiteit beïnvloed is individueel bestudeer, naamlik voginhoud, ferro-vloeistof vlak, voertempo, partikelgrootte en materiaal digtheid verspreiding.

Dit is belangrik om die ferro-vloeistof te herwin en te hergebruik om die koste van die proses en tegnologie te verminder en dus ook die hoeveelheid keroseen wat aan die omgewing blootgestel is. Dit het navorsing tot gevolg gehad oor die faktore wat ferro-vloeistof herwinning beïnvloed. Hierdie faktore wat ondersoek is in hierdie studie is materiaal voginhoud, partikelgrootte en porositeit.

Die skeidingseffektiwiteit was afhanklik van al die faktore wat ondersoek is. Die effek van materiaal voginhoud was minder beduidend vir partikels groter as 2.8 mm. Dit wys dat nat voermateriaal moet gesif word voor ferro-hidrostatiese skeiding, en materiaal met 'n partikelgrootte kleiner as 2.8 mm moet verkieslik gedroog word. Nat materiaal (minder as 2.8 mm) floteer selfs as die digtheid groter is as die snypunt digtheid. Dit is as gevolg van ondeurlaatbaarheid van die water wat die partikels bedek en die keroseen basis ferro-vloeistof wat gebruik word vir die skeiding.

Dit is gevind dat die invloed op die skeidingseffektiwiteit van die ferro-vloeistof vlak is 'n funksie van beide die digtheid van die partikels wat geskei word. Die partikelgrootte skeidingseffektiwiteit as 'n funksie van die ferro-vloeistof vlak, is swak vir partikels groter as 2 mm en is goed wanneer die digtheid verskil van die materiaal wat geskei moet word, hoog is, byvoorbeeld 2 700 kg/m^3 en 3 530 kg/m^3. Dit wys dat vir die effektiewe skeidings vir groter partikels en naby digtheid materiaal (materiaal net 'n digtheid naby aan die snypunt digtheid), moet die ferro-vloeistof vlak baie goed beheer word, gewoonlik naby die maksimum vlak moontlik.

Die effek van voertempo op die effektitiwiteit van skeiding is ook 'n funksie van die digtheid van die partikels wat geskei moet word. 'n Toename in die vloeitempo lei tot 'n swak skeiding van partikels met digthede wat naby mekaar lê. Dit wys weer daarop dat die skeiding van naby digtheid materiaal het die akkurate beheer van voertempo tot gevolg.

Dit is gevind deur simulasie en modulering dat die effektiewe snypuntdigtheid verander soos die partikel deur die kamer beweeg totdat dit uiteindelik sy finale snelheid bereik (gegee dat die kamer groot genoeg is). Dit effektiewe snypunt digtheid verhoog tot 'n maksimum wanneer die partikel die ferro-vloeistof binne gaan, maar bereik na 'n kort tydperk 'n kostante waarde sodra die partikel sy finale snelheid bereik het. Die effektiewe snypunt digtheid verlaag met 'n toename in partikel magnetisme. Dit is gevind dat die afname in die snypunt digtheid bepaal die digtheidsverskil (verskil tussen twee partikels) wat bereikbaar is wanneer nie-magnetiese materiaal saam met magnetiese materiaal behandel word. Dit is dus belangrik om die voer materiaal magneties te skalpeer vir effektiewe skeiding. Wanneer die materiaal so behandel word, sal magnetiese en nie-magnetiese materiaal, met die dieselfde digthede, rapporteer in verskillende digtheidsfraksies wat sal lei tot swak skeiding. Die magnetiese bydrae tot die effektiewe digtheid kan gebruik word in die skeiding van materiaal met dieselfde digtheid, maar met verskillende magnetismes.

Die effektiwiteit van ferro-vloeistof herwinning is afhanklik van al die veranderlikes wat ondersoek is. Die hoeveelheid ferro-vloeistof wat omtrek is van die ferro-hidrostatiese skeier verminder met 'n toename in die magnetiese veld. Verder is die ferro-vloeistof wat agterbly as gevolg van die feit dat hulle vas is aan die partikels na dreinering, dieselfde as die hoeveelheid wat vasgeheg is aan die die ferro-hidrostatisiese produkte van skeiding by hoë magnetiese velde. Dus is dit belangrik om die ferro-hidrostatiese skeier te bedryf by hoë magnetiese velde om sodoende die meerderheid van die ferro-vloeistof in die skeier agter te laat bly.

Die hoeveelheid ferro-vloeistof geadsorbeer aan en geabsorbeer deur die partikels verlaag met 'n toename in die materiaal voginhoud. Dit is gevolg van twee redes, nl. eerstens water wat die plek inneem van die oop porieë in die materiaal, en tweede is die feit dat water 'n lagie op die partikeloppervlakte vorm wat ondeurlaatbaar is vir keroseen-basis ferro-vloeistof. Dit lei tot die vermindering in koste van die ferro-hidrostatiese skeidingstegnologie wanneer nat materiaal in plaas van droë materiaal gebruik word. Soos alreeds genoem, partikels groter as 2.8 mm kan nat behandel word sonder enige negatiewe effekte op die skeiding. Vir –8+4 mm partikels is daar 'n ferro-vloeistof verlies van 0.6 tot 0.14 kg/ton voer vir 'n 0-10% voginhoud.

Die hoeveelheid ferro-vloeistof per ton voer materiaal wat verlore gaan wissel tussen 0.73 tot 0.56 kg vir –0.85+0.5 mm tot –12+8 mm partikelgroottes, respektiewelik. Die toename in ferro-vloeistofverlies by kleiner partikels is as gevolg van die toename in die oppervlakarea van kleinpartikels vir ferro-vloeistof adsorpsie.

Daar is 'n toename in porositeit wat gepaard gaan met 'n toename in hoeveelheid in ferro-vloeistof wat verlore gaan as gevolg van probleme met die herwinning van ferro-vloeistof wat binne-in partikelporieë vasgevang is.

Die byvoeging van water by groter materiaal verlaag die hoeveelheid ferro-vloeistof wat verlore gaan as gevolg van verminderde porositeit. Die modellering van die hoeveelheid ferro-vloeistof wat verlore gaan, as 'n funksie van die partikelgrootte en porositeit, sal help met die skatting van die hoeveelheid ferro-vloeistof benodig om 'n sekere hoeveelheid materiaal te behandel.

Dit is gevind dat die kwaliteit van die ferro-vloeistof wat herwin word dieselfde is as die wat aanvanklik gebruik is vir die materiaal skeiding. Dit wys dat die skeidingseffektiwiteit beïnvloed nie die gebruik van gehersirkuleerde ferro-vloeistof nie.

ACKNOWLEDGEMENTS

I would like to thank the following people:

- Firstly, my study leader, Dr. Jan Svoboda, for his support from the proposal stage to the final completion of the research. He was always prepared to give advice wherever necessary.
- Dr. Kurt Petersen for his assistance in formatting this thesis.
- Dr. Victor Ross for his assistance and encouragement during the course of the research.
- Prof. Leon Lorenzen for his support.
- All my colleagues at work for their encouragement, and DebTech Management for the financial and logistical support during the course of this research.
- Members of the FHS team at DebTech for the informative conversations that we had.
- Zeph Phakathi for his assistance in obtaining material for experimentation.
- My wife, Yvonne, for her encouragement when the going was tough.

TABLE of CONTENTS

CHAPTER 3
EXTENDED FHS EQUATION

CHAPTER 4
EXPERIMENTAL METHODS

CHAPTER 5
RESULTS AND DISCUSSION

CHAPTER 6
CONCLUSIONS AND RECOMMENDATIONS

SYMBOLS and ABBREVIATIONS

χ_p	Mass magnetic susceptibility of the particle
μ_o	Magnetic permeability of vacuum
κ_p	Volumetric magnetic susceptibility of the particle
ρ_p	Density of the particle
ρ_a	Apparent density of ferrofluid
ρ_{sp}	Effective density cut-point of separation
ρ_o	Natural density of ferrofluid
ρ_f	Density of diluted ferrofluid
ρ_k	Density of kerosene
ρ_c	Density of concentrated ferrofluid
H	Magnetic field strength
B	Magnetic induction
$\nabla\mathbf{B}$	Magnetic field gradient
M_f	Magnetisation of ferrofluid
M_p	Magnetisation of the particle
V_p	Volume of the particle
V_k	Volume of kerosene
V_c	Volume of concentrated ferrofluid
V_f	Volume of diluted ferrofluid
v_p	Velocity of the particle
g	Acceleration due to gravity
b	Radius of the particle
d	Diameter of the particle
η	Dynamic viscosity of ferrofluid
FHS	Ferrohydrostatic Separation
MHS	Magnetohydrostatic Separation
R & D	Research and Development
DMS	Dense Media Separation
FeSi	Ferrosilicon
Ep	Ecart Probable Moyen
TBE	Tetrabromoethane
WHIMS	Wet High Intensity Magnetic Separator

LIST of TABLES

LIST of FIGURES

CHAPTER 1

INTRODUCTION

Mineral separation remains a key activity in the recovery phase of metallurgical processes. In view of economic constraints forcing many operations to become marginal, the development of a new separation technology is pivotal to the full exploitation of mineral resources. This chapter discusses the potential use of ferrohydrostatic separation in the diamond industry, and highlights various advantages over other forms of gravity separation, such as high separation efficiency and a wide particle density processing range.

1.1 Introduction

Various techniques are employed in the recovery / extraction of minerals from their ores such as classification, flotation, gravity separation and magnetic separation. The choice of the recovery route depends on the cost and the efficiency of the technique. Coupled with declining ore grades, it is important to assess and develop methods that will keep ore processing costs to a minimum. Consequently, this has motivated companies to emphasise R&D as a means to achieve business objectives. This trend in industrial philosophy is driven by the recognition that to stay in business they must remain competitive and this requires the development of a culture of continuous improvement (May, 1995). Therefore, the coexistence of technology management and development is critical in order to sustain the balance between the necessary incremental improvements to existing processes and major technological advances.

One of the potential techniques to be applied to mineral separation based on density is the use of magnetic fluids. Commonly termed ferrohydrostatic separation, it is a float / sink technique, which employs magnetic fluid (ferrofluid), exposed to a non-homogenous magnetic field. The advantages of this technique over other gravity separation techniques are that:

(a) the cut-point density can be accurately controlled,
(b) there is no significant change in viscosity when the apparent density of the fluid is increased,
(c) the treatable density range of feed material is wider, for example, from the separator from the Ukraine, it has been shown that densities as high as 12000 kg/m^3 are realisable (Svoboda *et al.*, 1996) and

(d) they are much safer and more convenient to use.

Even though this technology has been tested in the Soviet Union and the United States since the 1960s (Lin *et al.*, 1994), many of the operational characteristics are still not clearly understood, especially in relation to metallurgical scenarios. The potential application of this technology is not only restricted to diamonds, but also applicable to areas such as coal, platinum group metals, base metals, and re-treatment of slag and recovery of metals from waste. Apart from material separation, magnetic fluids are employed in high-tech applications such as seals, lubrication, damping, printing, chemical and petrochemical processing, thermal effects and medicine (Moskowitz, 1975).

1.2 Ferrohydrostatic Separation

The ferrohydrostatic separator used for this research was imported from the Ukraine and is shown in Figure 1.1.

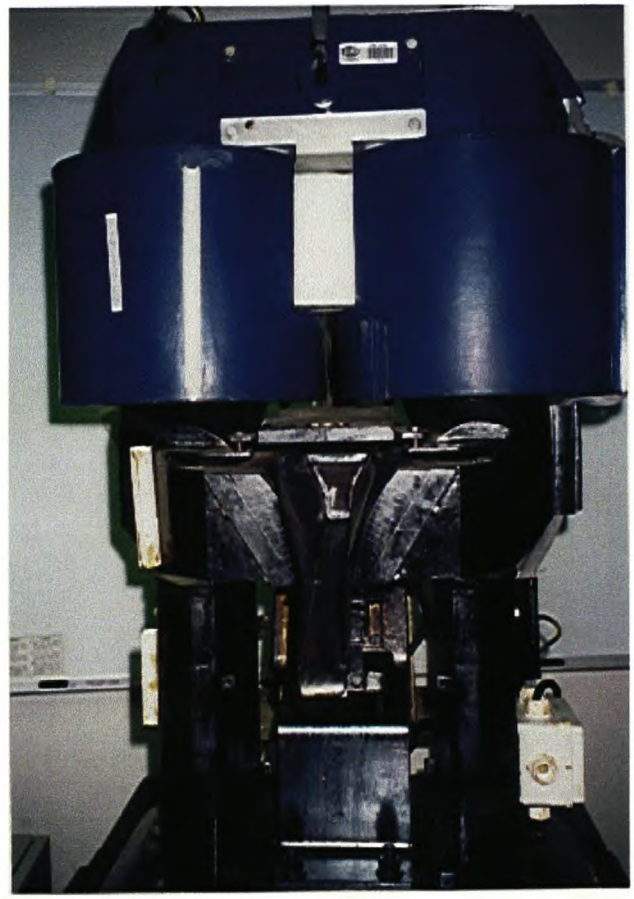

Figure 1.1 Ferrohydrostatic separator used in this research.

It consists of a set of pole tips and an iron yoke, which is magnetised by two coils. The separation chamber is located between two pole tips, and is externally vibrated so that the sink product can slide at the bottom of the chamber and discharged. The ferrofluid is placed in the separation chamber, where it is exposed to a non-homogenous magnetic field (described in more detail in Chapter 2). The resulting apparent density of ferrofluid is then exploited as the cut–point density and this can be adjusted to any required density by either changing the density of ferrofluid being used or by altering the current supplied to the coils. When separating particles with close densities, it is important to have a constant apparent density in the working volume for efficient separation. In some applications such as separation of particles with large density difference, the apparent density does not have to be constant. The foremost disadvantage of this technology is the failure to treat strongly magnetic material.

1.2.1 Operating Variables

There are numerous variables that affect the efficiency of separation. These can be classified into two categories:

(a) equipment-based variables, and
(b) variables that are dependent on the feed material.

Equipment-based variables include the splitter position, level of ferrofluid in the separation chamber and feed rate, whilst feed variables include material moisture content, density and particle size, just to name a few. A principal objective of this thesis will be to identify the significance of each variable to separation efficiency.

1.3 Magnetic Fluids

There are two types of magnetic fluids that are used to form the separating medium, namely:

- Fluids consisting of suspensions of ultrafine strong magnetic particulates in a suitable carrier fluid e.g. water or kerosene (ferrofluids), and
- Single phase fluids (mainly solutions of paramagnetic salts).

For this research, only kerosene-based ferrofluids were used.

1.3.1 Ferrofluids

Magnetic ferrofluids are ultrafine colloidal systems containing single-domain ferromagnetic or ferrimagnetic particles. Ferrofluids are superparamagnetic (have zero coercivity and zero remanence). Most ferrofluids are made up of ultrafine (10 nm) particles of magnetite (a molecular mixture of iron oxides FeO and Fe_2O_3) suspended in a carrier liquid, either kerosene, oil or water.

Good quality ferrofluids maintain their homogeneity over a long period of time due to:

(a) a coating on the magnetite particles, and
(b) the fact that the minute particles obey kinetic theory principles.

The kinetic theory states that, under certain conditions, fine particles can remain suspended indefinitely in a liquid even though the density of the particle is much higher than the liquids. The particle is subject to hindered settling because it continually collides with molecules of the liquid, which are in random thermal motion. The resulting effect is that the liquid molecules share their kinetic energy with the suspended particle.

The energy carried by the particle is equal to kT, where k is the Boltzmann constant and T is the absolute temperature. For a particle to remain in suspension indefinitely, this thermal energy must be equal to or greater than the gravitational energy needed to raise the particle to the height of the container holding the fluid. If two or more particles collide, they may stick together, effectively creating a single heavier particle and this may lead to settling (Rosenweig, 1966).

Magnetic and Van der Waals Force Interactions

The magnetic force and the van der Waals force are responsible for ferrofluid particles being attracted to one another. To avoid agglomeration due to van der Waals forces, each particle is coated with a molecular film (surfactant) that acts as an elastic cushion. This surfactant molecule has a polar chemical group, or head, that adheres to the surface of the particle and a tail that has an affinity for the carrier fluid. A widely used surfactant in kerosene based ferrofluid production is oleic acid (organic polymer).

In the absence of an external magnetic field, the magnetic moments of individual particles are randomly distributed and the fluid has no net magnetisation. When the magnetic field is applied, the moments

experience a torque and are aligned in the direction of the field. The magnetisation of the fluid depends on the degree of alignment.

Magnetically, a ferrofluid is perfectly soft. This means that when a magnetic field is applied, the magnetic moments of the particles orient along the field lines almost instantly. Thus, the magnetisation of the ferrofluid responds immediately to changes in the applied magnetic field, and when the field is removed, the moments randomise instantly.

In a uniform field, particles in a ferrofluid experience only torque and align with the field. However, in a gradient field, the entire fluid responds as a homogeneous magnetic liquid which moves to the region of highest flux (Rosenweig, 1966). As the ferrofluid remains homogenous in a gradient field, this implies that the apparent density of ferrofluid is constant in a ferrohydrostatic separator.

Kerosene vs Water based Ferrofluids

The most favourable aspect of a ferrofluid is that it can be tailored to meet a variety of needs by varying the quantity of magnetic material in the fluid and by using different carrier liquids. The saturation magnetisation (the maximum value of the magnetic moment per unit volume when all the domains are aligned) is determined by the nature of the suspended magnetic material and by the volumetric loading of the material. The greater the quantity of magnetic material in suspension, the higher the saturation magnetisation of the ferrofluid.

The literature shows that kerosene based ferrofluids with a density of as high as 1230 kg/m^3 can be prepared, which can then be diluted with kerosene to produce ferrofluids with different magnetisation and densities (Svoboda *et al.*, 1996). Fluids with high magnetisation are used for high-density separation while those with low magnetisation are employed in low-density separations.

In the case of water based ferrofluids, the quality is inferior compared to kerosene-based (Svoboda, 1996). They deteriorate with time and the suspension does not remain homogenous over long periods of time. Water-based ferrofluids have a higher viscosity and a lower magnetisation. In the ferrohydrostatic separator, cursory tests carried out in this research showed that they produce strata / regions of different densities. These fluids can only be used for less demanding applications where the density difference of the materials to be separated and the particle size is large. Because of their lower magnetisation, they can only be used for low-density separations such as coal preparation (Fofana, 1997). Water-based ferrofluids are difficult to recycle compared to kerosene based ones.

1.4 Ferrofluid Recycling and Environmental Aspects

Products from the separation process are coated with ferrofluid, which must be removed before subsequent processing. This ensures quality of product to be sold and reduces the amount of ferrofluid disposed to the environment.

The ferrofluid attached to the particles can be washed off using water and recycled for further use. Recycling is accomplished by passing the water / ferrofluid emulsion over a permanent magnetic circuit, where the ferrofluid is attracted to the magnets and the water is displaced such that it can be collected. The washed products may still contain some ferrofluid / kerosene, and consequently, there exists a need for careful disposal of the tailings. Also it is necessary to perform final cleaning of the products using a detergent in order to reduce the amount of kerosene and ferrofluid discolouring on the particles. The water used for washing the particles will typically contain some micro emulsions, which is detrimental to the environment. Consequently, the removal of contaminants is paramount before disposal of the wash water.

The efficiency of the ferrofluid recovery process depends on a number of factors such as particle size, porosity and moisture content of the particles as well as pressure of the wash water. The type of the washing agent used also contributes to the recovery of ferrofluid.

1.5 Objectives of this Study

The existing literature on ferrohydrostatic separation of minerals is not extensive and is mainly found in Russian journals. In view of this deficiency, the main objectives of the project were:

- To understand the application of FHS in mineral processing.
- To perform experiments that identify the most important variables which affect the efficiency of separation.
- To determine the interdependence of these variables.
- To identify operating procedures that maintain acceptable separation efficiency.
- To find a sufficiently efficient method for the ferrofluid recycling for different types of feed material.

1.6 Summary

Ferrohydrostatic separation technology is a highly efficient means of separating minerals based on density. However, there is little information in the literature concerning its application in mineral processing. The most critical step in this process is the design of a magnetic system that allows accurate separation of material.

This thesis will be concerned mainly with gaining an insight into the operating characteristics that are critical to the success of this technique in the minerals industry, particularly for the purposes of processing diamondiferous materials.

CHAPTER 2

SEPARATION TECHNOLOGY AND FHS BACKGROUND

The utilisation of physical properties such as particle size, density and magnetic properties for mineral separation is widely used. This chapter outlines various separation technologies commonly encountered in mineral processing, and subsequently, presents FHS technology which is a highly efficient density separation process based on the use of a fluid (ferrofluid) which density is induced magnetically.

2.1 Introduction

The process of separating minerals based on differences in density, size and magnetic properties is one of the cornerstones in mineral processing technology. Gravity separation often initiates the recovery process, whereby particles are separated according to size and / or density (typically using the phenomenon of differential settling velocity), and subsequently, supplies down-stream processes such as flotation, leaching etc. with a sufficiently concentrated valuable material. In the case of diamond processing, dense medium separation (DMS) performs separation of gangue and diamond according to a difference in density, and aims to reduce the amount of unwanted material for subsequent sorting (e.g. X-ray machines).

Magnetic separation exploits the difference in magnetic properties between the materials to be separated. Almost all materials are affected in some way when placed in a magnetic field, although with most materials, the effect is too slight to be detected. Typical areas of application include the separation of magnetite and ilmenite from rutile and zircon, magnetite from garnet, pyrite, chalcopyrite etc.

The FHS system investigated in this thesis can be classified as a gravity separation technique, in that the separation is density dependent. The novel aspect of this process is that the separating medium has a density, which is magnetically induced. Consequently, the magnetic property of materials to be processed also plays a part in the efficiency of separation but can be disadvantageous when processing highly magnetic material.

This chapter presents a review of standard mineral separation techniques, highlighting those most comparable to FHS technology. In contrast to other

techniques, it is shown that FHS is simple to operate, has high separation efficiency and can be applied to a wide range of material densities. Consequently, the application of FHS extends beyond diamond processing into areas such as recovery of metals from waste, recovery of platinum group metals, coal preparation, base metals, re-treatment of slag, etc.

2.2 Types of Gravity Separators

The minerals industry is replete with examples of novel gravity separating techniques. The most widely used include dense medium separators (DMS), heavy liquid separators, jigs, spirals, shaking tables, Nelson concentrators, sluice boxes, pans, and separation in magnetic fluids. Only DMS and heavy liquid separators will be described as they are widely used in diamond processing.

2.2.1 Dense Medium Separation

Dense medium separation is closely related to gravity separation. In the case of gravity separation, the separation is carried out in water or air, whereas in dense medium separation, the separation is in a medium of density higher than that of water and between the densities of the minerals to be separated. The most commonly used medium is a suspension in water of finely divided high-density particles such as ferrosilicon (FeSi) and magnetite (Kelly *et al.*, 1992).

Fine FeSi (density 6700 to 6900 kg/m^3) and magnetite (density 5100 kg/m^3) are used to produce a stable suspension of sufficiently high density with a reasonably low viscosity. Ferrosilicon is widely used for separating metalliferous ores whilst magnetite is mainly used in coal preparation.

Cyclones

There are many separating vessels that employ magnetite and ferrosilicon suspensions as the separating medium.

They are mainly classified as static and centrifugal vessels. The static includes the Wemco cone, drum, drewboy bath, and the norwalt washer. Dense medium cyclones are the most extensively used dynamic separators for diamond processing (Figure 2.1).

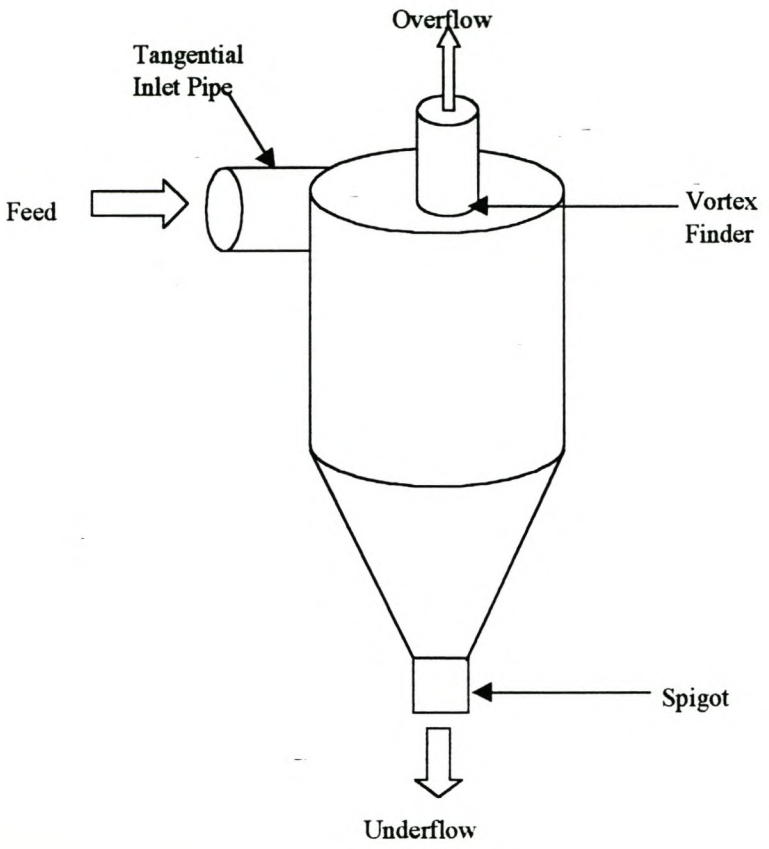

Figure 2.1 A Diagram of a cyclone.

The ore is initially mixed with a medium of fine ferrosilicon or magnetite and is introduced tangentially to the cyclone under pressure, either gravity fed via a constant head or by a pump. The larger and denser particles move along the wall of the cyclone and are discharged through the apex (spigot) or underflow, while the less dense materials pass out of the vortex or overflow. The fine medium forms a density gradient within the cyclone.

The sharpness of separation in the cyclone depends on:

(a) the hydrodynamic properties of the material to be separated,
(b) the viscosity experienced by the ore particles and
(c) the stability of the suspension (atomised ferrosilicon produces low apparent densities (Burt, 1984).

The efficiency of the cyclone is determined by plotting the Tromp curve (percent recovery of a particular density range to the sinks) and determining the Ecart Probable Moyen (Ep value). The Ep value is defined as half of the difference between the density where 75% (d_{75}) is recovered to sinks and that at which 25% (d_{25}) is recovered to the sinks, i.e.

$$Ep = 0.5(d_{75} - d_{25}) \qquad (2.1)$$

The Tromp curve is specifically used for determining the density of material at which there is an equal probability of particles reporting to the overflow or underflow (d_{50}). The Ep value is used as the main criteria for performance, or more specifically, sharpness of separation. The Ep of the cyclone is normally equal to or greater than 0.02.

A lot of work has been done to improve the Ep of the cyclone. This includes finding the optimum orientation of the cyclone and the control of the density differential between the overflow and the underflow by the use of a solenoid wound around the cyclone (Svoboda *et al.*, 1998 and Freeman *et al.*, 1994). Adjusting the magnetic field strength controls the density difference, which influence the distribution of the magnetic particles of the medium. From the work done by Svoboda *et al.*, 1998, it has been shown that the density difference decreases with an increase in the magnetic field until it reaches the minimum. A further increase in the magnetic field causes an increase in the density differential. This implies that for efficient operation of any magnetic cyclone, it is necessary to determine the minimum density differential achievable as this, besides the magnetic field strength, also depends on the medium in use.

Typical separating densities that are realisable with cyclones are in the range of 2200 to 3200 kg/m^3. Despite efforts to employ a control of material separation by density alone, particle size also proves to play a significant role in separation, where larger particles tend to separate more efficiently than small particles. Industrial scale cyclones typically treat a size range of 0.5 to 40 mm (Wills, 1992). Furthermore, feed compositions predominantly with a density close to that of the separation density will result in relatively poor separation.

Medium Recovery

Apart from cyclone wear, the replacement / addition of separating medium is one of the ongoing costs. Medium recovery is accomplished by washing it off from the products using water on the rinse screen (after separation in the cyclone). The resulting dilute medium is de-watered and purified as it might contain fine impurities from washed products. This is

commonly achieved by using drum magnetic separators (Section 2.3.1). Reported losses of ferrosilicon from a DMS circuits vary, from as little as 0.1 kg/tonne of feed treated to 2.5 kg/tonne of feed treated. The loss and recovery of the medium is dependent on size and porosity of the particles and the rate of medium corrosion. Corrosion accounts for small loses and can be prevented by maintaining FeSi in its passive state. This is accomplished by atmospheric oxygen diffusing into the medium or by the addition of small quantities of sodium nitrite (Burt, 1984).

The recovered medium retains a residual magnetism that causes flocculation of the medium unless the medium is demagnetised. This is accomplished by pumping it or by using a demagnetising coil (Wills, 1992). When magnetite medium is being recovered, the density of the recovered medium may be sufficiently high that it can be reused. However, in the case of ferrosilicon medium, densification might be necessary before re-use. If the quality of the recovered medium is different from the initial one, efficiency of separation is altered.

2.2.2 Heavy Liquid Separation

Heavy liquids are mainly used for densimetric analysis (separating material into different density fractions) and the recovery of geological indicator minerals. The liquid has a density lower than the minerals to be sunk and higher than the minerals to be floated.

There are a variety of heavy liquids that are used for mineral beneficiation, including tetrabromoethane (TBE), bromoform, 3,3-di-iodomethane, methylene iodide, lead sulphamate and clerici solution (thallium formate - thallium malonate solution) (Gustàv, 1986). These liquids can be tailored to a specific density by dilution with less dense liquids. Table 2.1 presents a variety of heavy liquids, a possible diluting medium and their density range application. The maximum cut-point density that can be achieved by using heavy liquids is 5000 kg/m^3. In contrast to dense medium cyclones, heavy liquid separation is a static process. The major disadvantage is long processing time for small particles, caused by a slow throughput of material due to the relatively large hydrodynamic drag force.

Most heavy liquids in use are toxic and should be used with extreme care. The potential health effects of some of the heavy liquids are shown in Table 2.2. Due to the toxicity of most heavy liquids, they are not commercially used, but are mainly used in laboratories where they can easily be handled with care. The foremost advantage of heavy liquids is high separation efficiency due to the static nature of the process.

Table 2.1 Heavy liquids diluting medium and range of densities.

Heavy Liquid	Diluting Medium	Density Range [kg/m^3]
Bromoform	Acetone	2000 – 2850
Lead Sulphamate	Distilled water	3000 – 3600
TBE	Acetone	2000 – 2950
Clerici Solution	Water	1000– 5000
Methylene Iodide	Acetone	2000 – 3320

Table 2.2 Potential health effects of some heavy liquids (Luxon, 1992).

Heavy Liquid	Potential Health Effects	Limit values
Bromoform	Irritant to skin, eyes and upper respiratory tract.	0.5 ppm long term
TBE	Harmful when swallowed or inhaled.	
Lead Sulphamate	Early symptoms of lead poisoning include fatigue, sleep disturbances, aching bones and muscles, and reduced appetite. Large doses affect the central nervous system and may lead to death.	0.15 ppm long term
Acetone	Inhalation of vapour may cause dizziness, narcosis, and coma. Swallowing may cause gastric irritation, narcosis and coma.	1500 ppm short term
Clerici Solution	Toxic by ingestion, skin adsorption or inhalation.	0.1 ppm long term

2.3 Magnetic Separation

Magnetic separators exploit the difference in magnetic properties between ore minerals and are used to separate either valuable mineral from non-magnetic gangue or valuable minerals from magnetic gangue material. Magnetic separation is also used to remove any unwanted magnetic materials before some metallurgical processes.

In magnetic separation, the dominant separating force is the magnetic force but other competing forces such as gravitational, hydrodynamic, inertial and centrifugal also influence the removal of the magnetic material from the less magnetic one. These forces are dependent on the mineralogy of the feed material as well as on the design of the separating device (Svoboda, 1987).

2.3.1 Magnetic Separators

There is a wide variety of magnetic separators and these serve numerous applications in the mineral processing industry. They can be classified into low- and high intensity machines, which can further be classified into dry- feed and wet- feed separators. Low intensity separators are used to treat ferromagnetic materials and some highly paramagnetic minerals. In contrast, high intensity magnetic separators are employed in the treatment of paramagnetic minerals of low magnetic susceptibility.

The principal requirement in the design of magnetic separators is the provision of a non-homogenous magnetic field. The magnetic attractive force, **F**, acting on the particle is given by:

$$\vec{\mathrm{F}} = \frac{\kappa_p}{\mu_0} V_p \left|\vec{\mathrm{B}}\right\| \nabla \vec{B} \right| \qquad (2.2)$$

where $\vec{B}$ is the magnetic field induction, $\nabla \vec{B}$ is the magnetic field gradient, κ, and V_p are the volume magnetic susceptibility and volume of the particle respectively and μ_o is the permeability of vacuum. An increase in the magnetic field induction will increase the magnetic force, both by increasing the magnetisation of the particles and, in many cases, by increasing the magnetic field gradient (Svoboda, 1987).

Low Intensity Magnetic Separators

Low intensity magnetic separators are used for the recovery of strongly magnetic material. Dry, low intensity magnetic separators are used for the treatment of coarse material range greater than 1mm, whereas wet, low intensity magnetic separators are used for fine particles. An example of a dry low-intensity magnetic separator is a dry drum magnetic separator. The material to be separated is fed at the top of the rotating drum surface. The non-magnetic fraction is discharged whilst the magnetic fraction is attracted by the magnetic force at the drum surface and discharged outside the magnetic field as shown in Figure 2.2.

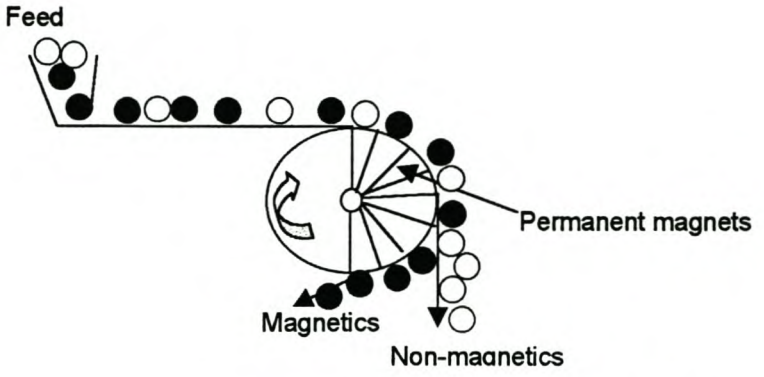

Figure 2.2 Dry drum magnetic separator.

The wet low-intensity magnetic separators are the most common magnetic separators in use. They also employ the drum magnetic separators. The drum consists of a stationary magnetic circuit and a non-magnetic casing which rotates round the magnets.

High Intensity Magnetic Separators

These are used to separate paramagnetic minerals of low magnetic susceptibility. The common versions of dry high-intensity magnetic separators are induced magnetic roll, the cross belt and the permanent magnetic roll. For wet high-intensity magnetic separation, permanent roll, induction-element (WHIMS) and high gradient magnetic separators are used.

2.4 Separation in Magnetic Fluids

Mineral separation in magnetic fluids is conducted in one of two ways,

(a) centrifugal or dynamic separation (Magstream separation), and
(b) gravitational or static separation (magneto-hydrostatic, magnetohydro-dynamic and ferrohydrostatic separation).

In centrifugal separation, separation is effected in a rotating magnetic fluid. In contrast, static separation takes place in a static ferrofluid.

2.4.1 Magstream (centrifugal) Separation

The Magstream technique is based on the separation of material in a rotating ferrofluid. The schematic diagram of the side view of the Magstream 200 separator is shown in Figure 2.3.

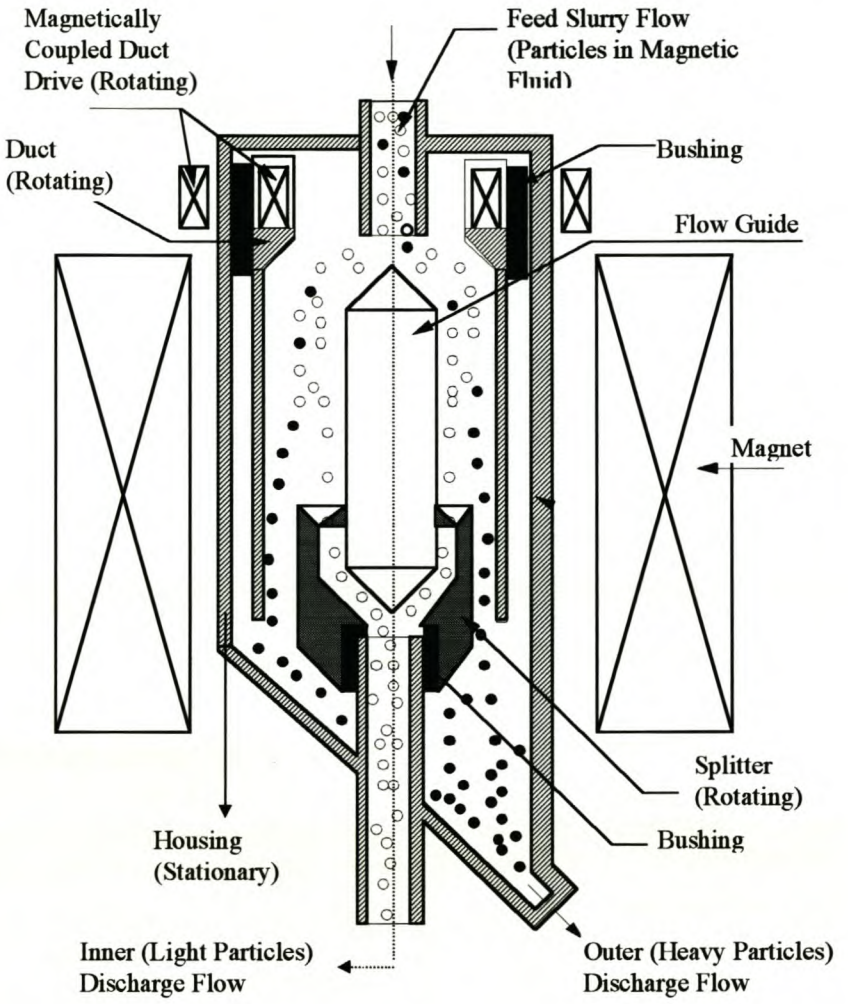

Figure 2.3 Schematic diagram of the side view of the Magstream 200 Separator.

The slurry (material to be separated in magnetic fluid) is fed downward as shown in Figure 2.3 where it rotates with the flow guide. A multipole magnet that produces a magnetic field surrounds the rotating duct. During rotation, inward and outward forces are created. Inward forces are due to the radially outward attraction of the magnetic fluid whilst the inward force is due to the centrifugal force for nonmagnetic particles.

At a set speed, the magnitudes of these two forces are different for light and heavy particles. Inward displacement forces are greater on light particles and they move radially inwards, whilst, centrifugal force is higher on heavier particles and they move radially outwards (Svoboda, 1998). The heavies are separated from the lights by a rotating splitter and collected as shown in Figure 2.3.

The separation efficiency of a Magstream is particularly sensitive to particle size and the radial position of the particle. Furthermore, the cut point density, ρ_c, can only be inferred from an appropriate model, for example equation 2.3 (Svoboda, 1996);

$$\rho_c = \rho_f + \left[\frac{\mu_0}{4\pi}\right]\left\{\frac{K}{N}\right\}^2 M_f \qquad (2.3)$$

where N is the number of revolutions of the rotating device per minute ($N = 60\omega/2\pi$), ρ_f is the density of the ferrofluid and M_f is the magnetisation of the ferrofluid and K is the parameter determined by the design of the magnetic system of the rotating separator;

$$K = 15\left\{\left(\frac{\nabla B}{\pi^3 r}\right)10^7\right\}^{0.5} \qquad (2.4)$$

where ∇B is the magnetic field gradient and r is the radial position of the particle in the separator.

An extended model which includes the hydrodynamic drag (Stokes flow) has been developed by Svoboda (1996);

$$\rho_c = \rho_f + \left(\frac{1.188x10^6}{\mu_o \pi^2 N^2}\right)\left[\frac{\mu_o}{4\pi}\right]M_f + \left(4050\eta v_p / \pi^2 b^2 N^2 r\right) \qquad (2.5)$$

where η is the dynamic viscosity of the fluid, b is the radius of the particle and v_p is the relative horizontal velocity of the particle. The important result from this model is that the cut-point density is dependent upon both particle size and particle position within the separator. Moreover, this radial variation in density has been shown to lead to poor separation.

2.4.2 Magnetohydrostatic Separation (MHS)

In this system, separation is conducted in an aqueous solution (or melt) of a paramagnetic salt (e.g. $MnCl_2$). The MHS principles are similar to that

of the FHS system described later in Section 2.4.3. The main difference between the two is that in MHS, the magnetic moment of a paramagnetic solution is much smaller (about three orders of magnitude less) than that of a magnetic fluid (Khalafalla, 1985).

As described in detail by Svoboda (1995) the paramagnetic salts poses many problems in material separation such as:

- A high magnetic field of 2 T is required to generate an apparent density of 3500 kg/m^3.
- Because of the high magnetic field required, even feebly magnetic material cannot be treated as it clogs the separator or exhibits a higher density as described in Section 2.4.3.
- The $MnCl_2$-based fluids degrade in the presence of light, they are expensive and are difficult to recycle.
- They have a high surface tension, which makes it difficult for small particles to penetrate and be wetted. This means that paramagnetic liquids can only be used for coarse material separation.

2.4.3 Ferrohydrostatic Separation

Ferrohydrostatic separation (FHS) utilises ferrofluid exposed to a non-homogenous magnetic field. The apparent density of the ferrofluid is exploited as the cut-point density of the separator. The separation efficiency depends on a number of variables such as particle size, feed rate and properties of the ferrofluid. The design of the pole tips (Figure 2.4) of the separator is critical in order to realise a constant density in the separation volume (Kaiser *et al.*, 1975).

Theoretical Principles

The schematic representation of the FHS is shown in Figure 2.4.

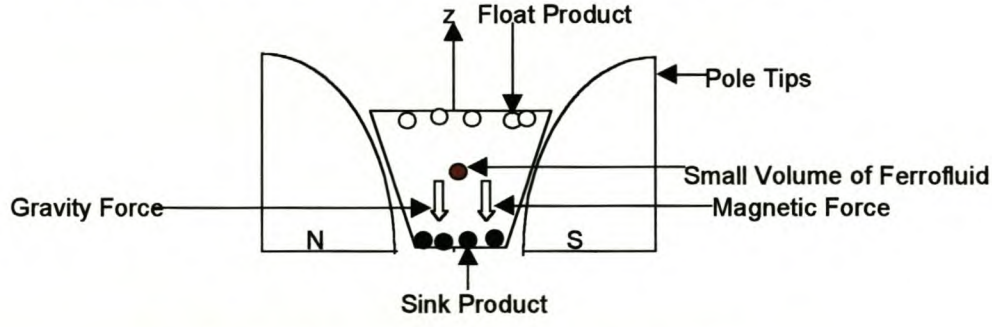

Figure 2.4 Schematic diagram of a FHS Separator.

The ferrohydrostatic separator consists of two pole tips with a separation chamber in between them. The separation chamber is filled with ferrofluid.

Forces Acting on a Small Volume of Ferrofluid

Due to the shape of pole tips (Figure 2.4), the magnetic field at the base of the poles is the highest and decreases vertically, creating a magnetic field gradient. The magnetic field gradient is parallel to gravity and of the same sense (Svoboda *et al.*, 1996). Consider a small volume (V) of ferrofluid exposed to a non-homogenous magnetic field and assume that the volume is so small that the magnetic field gradient within the volume is negligible. The total force, $\vec{F}$, acting on the volume of the ferrofluid is given by the addition of the force due to gravity ($\vec{F}_g$) and that due to the magnetic field ($\vec{F}_m$), i.e.

$$\vec{F} = \vec{F}_g + \vec{F}_m$$

$$= m\vec{g} + \frac{M_f V \left|\nabla \vec{B}\right|}{\mu_o}$$

$$= \rho_o V\vec{g} + \frac{M_f V \left|\nabla \vec{B}\right|}{\mu_o} \qquad (2.6)$$

where ρ_o is the natural density of ferrofluid in kg/m^3, M_f is the magnetisation of ferrofluid in Tesla (T), $\vec{g}$ is acceleration due gravity (ms^{-2}), B is the magnetic induction in T and $\nabla\vec{B}$ is the magnetic field gradient in T/m. Equation (2.6) can be re-written (in SI units) as:

$$\vec{\mathrm{F}} = (\rho_o + \frac{M_f}{\mu_o g}\left|\nabla \vec{B}\right|)V\vec{g} \qquad (2.7)$$

The expression in parenthesis can be viewed as an apparent density (ρ_a) of the ferrofluid exposed to an external non-homogeneous magnetic field, which can be isolated to give (in SI units):

$$\rho_a = \rho_o + \frac{M_f}{\mu_o g}\left|\nabla \vec{\mathrm{B}}\right| \qquad (2.8)$$

Equation 2.8 outlines the basic theory on which ferrohydrostatic separation is based. It is ensured that the magnetic field gradient (∇B) is constant in the separation volume by manufacturing pole tips to an appropriate shape, viz. hyperbolic. When the FHS is operated at saturation magnetisation of the ferrofluid in use, M_f is a constant, and consequently, the apparent density is constant.

Forces Acting on a Suspended Particle

A particle suspended in a ferrofluid is acted upon by a number of forces, viz. gravity ($\vec{F}_{gp}$), magnetic ($\vec{F}_{mp}$), Archimedes buoyancy due to gravity ($\vec{F}_{gb}$) and buoyancy due to the magnetic force ($\vec{F}_{mb}$). The total force acting on the particle in the vertical direction is then given by:

$$\vec{F}_{total} = \vec{F}_{gp} + \vec{F}_{mp} + \vec{F}_{gb} + \vec{F}_{mb} \tag{2.9}$$

The gravitational force acting on the particle is given by:

$$\vec{F} = \rho_p V_p \vec{g} \tag{2.10}$$

where ρ_p is the density of the particle and V_p is its volume. The magnetic force acting on the particle is given by (in SI):

$$\vec{F}_m = \frac{V_p \kappa_p B \nabla \vec{B}}{\mu_o} \tag{2.11}$$

where κ_p is the volume magnetic susceptibility of the particle. Buoyancy forces are the result of pressure differences throughout the fluid. A suspended particle experiences a pressure difference between its upperside and underside (with respect to the direction of the external force) and moves according to the volume of fluid that it displaces. The gravity related buoyancy force is given by:

$$\vec{F}_{gb} = \rho_o V_p \vec{g} \tag{2.12}$$

Similarly, the buoyancy force due to the magnetic field is given by:

$$\vec{F}_{mb} = \frac{V_p M_f \nabla \vec{B}}{\mu_o} \tag{2.13}$$

The net vertical force (equation 2.9) acting on a particle suspended in a ferrofluid and acted upon by a non-homogeneous magnetic field can therefore be written as:

$$\vec{F}_{total} = \rho_p V_p \vec{g} + \frac{V_p \kappa_p B \nabla \vec{B}}{\mu_o} - \rho_o V_p \vec{g} - \frac{V_p M_f \nabla \vec{B}}{\mu_o} \qquad (2.14)$$

Defining the effective density cut-point of separation ρ_{sp} as that particle density for which $\vec{F} = 0$ (i.e. forces acting on the particle are in equilibrium), equation 2.14 yields (in SI):

$$\rho_{sp} = \rho_o + \frac{\nabla B}{\mu_o g}[M_f - B\kappa_p] \qquad (2.15)$$

For non-magnetic particles $\kappa_p = 0$, equation 2.15 reduces to equation 2.8, which indicates that for non-magnetic particles, the density cut-point is equal to the apparent density of the ferrofluid (Svoboda *et al.*, 1996).

For paramagnetic magnetic particles, $\kappa_p > 0$, the observed apparent density is less than that for nonmagnetic particles. Similarly, the apparent density will be affected by a change in the magnetic field induction, B.

For diamagnetic particles, $\kappa_p < 0$, e.g. bismuth, copper, diamond, gold and silver, the resulting apparent density is greater compared to nonmagnetic materials. However, this effect is typically negligible as the absolute value of the magnetic susceptibility of diamagnetic particles is relatively small.

In FHS, the ferrofluid magnetisation (M_f) is usually high enough such that particles with low magnetic susceptibility can be treated. The above effects will be considered more closely in Chapter 3 in conjunction with the hydrodynamic drag force.

2.5 The Ferrohydrostatic Separator

The ferrohydrostatic separator used in this research is shown in Figure 1.1. It consists of a set of pole tips that generate the magnetic field gradient. Two sets of pole tips are available for use, both generating different magnetic field gradients. The first set can be used to generate an apparent ferrofluid density ranging from 2500 to 6500 kg/m^3, while the other set covers the range from 3000 to 12000 kg/m^3. These ranges of densities are attained using 950 kg/m^3 density ferrofluid. The separator is also equipped with an iron yoke for the magnet, which is magnetised by two coils.

The separation chamber is situated between the pole tips of the magnet and an external vibrator vibrates the chamber. The separation chamber contains a splitter that separates the sink product from the float.

The separation chamber is filled with ferrofluid (approximately 0.9 litres). The power supply unit (PSU) feeds current to the two coils, which in turn magnetises an iron yoke. This magnetises the ferrofluid to produce an apparent density different from the natural density of the ferrofluid.

2.5.1 The Control System

For efficient separation, the apparent cut-point density should be strictly maintained. Consequently, a steady magnetic field is vital, and requires consistent and reliable supply of current to the coils. Secondly, and most importantly, a strain gauge (shown in Figure 2.5) is used to control the apparent density by detecting any change in the apparent density and sending a signal to the PSU either to reduce or to increase the current. The current is increased when the detected density is lower than the required density and decreased when it is higher.

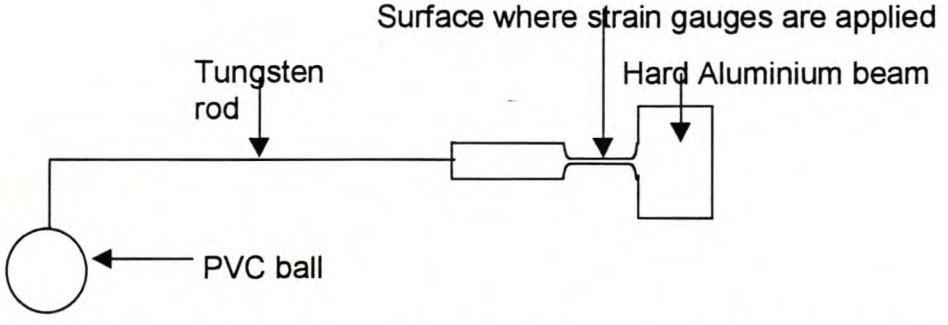

Figure 2.5 Schematic diagram of the strain gauge assembly. The PVC ball is always immersed in ferrofluid during FHS Separator operation.

The strain gauge is calibrated using density tracers and the separator can either be operated under closed- or open-loop conditions. Open-loop operation is when the strain gauge is disabled. Under closed loop, the PC controller captures the strain gauge measurements, then using the software program, drives the PSU to supply a fixed current to the coils, ensuring that the required apparent density is maintained. Closed loop operation ensures that any density variation due to evaporation of kerosene from the ferrofluid or temperature increase in ferrofluid, creates an appropriate change in the current supplied to the coils (Svoboda *et al.*, 1996). However, the success of closed loop operation is intimately linked to the

settings of the strain gauge range. For example, a very sensitive strain gauge is required when fine density (separating particles of close densities) cuts are required during material processing.

2.5.2 Factors Affecting the Efficiency of FHS

The efficiency of FHS separation is dependent on a number of variables, such as particle size, feed rate, feed moisture content and the level of ferrofluid in the separation chamber. This section gives a background on these various factors, which form the bulk of the experimental investigation in this thesis (Chapters 4 and 5).

Particle Size

The particle size plays an important role in the efficiency of ferrohydrostatic separation. The motion of the particles in the ferrofluid is determined by the interaction of a variety of forces acting on the particles, viz., gravity, the magnetically and gravity driven buoyancy forces and hydrodynamic drag. The balance of these forces determines the trajectory of the particle in the ferrofluid. In particular, particle diameter is pivotal to particle motion. For example, all the forces mentioned in Section 2.4.3 are a function of particle volume (d^3). The drag force, described in detail in Chapter 3, only depends upon particle diameter (d). Consequently, the drag force is only significant in terms of trajectory when considering small sized particles (Svoboda *et al.*, 1996). In view of this phenomenon, the separation efficiency would benefit from separating the feed material into narrow size ranges such that treated particles are subject to similar prevailing force conditions.

Feed rate / Optimum Operating Capacity

In practice, it is difficult to establish a rule-of-thumb as to the optimum operating capacity, as this largely depends on factors such as particle size, density difference of the minerals to be separated and also the viability of the process. For example, achieving near perfect separation at the cost of throughput might prove to be economically not viable. Similarly, high throughput at low efficiency might achieve the same results. Consequently, economically optimum operating conditions must be determined for each specific application. However, experience has shown that high feed rates result in hindered settling, which ultimately reduces efficiency as described in more detail in Chapter 5.

Ferrofluid Level

During the course of operation, the fluid level decreases as a result of fluid losses, which are the result of:

(1) ferrofluid coating emerging material from the separation chamber and, to a smaller extent,
(2) evaporation of kerosene.

The resulting drop in ferrofluid level will affect the selectivity of separation. In order to maintain a constant and optimum efficiency of separation, the fluid level must be kept above a minimum level. It will be shown in Chapter 5 that the required minimum level is a function of the particle size and the density difference of the minerals to be separated.

Material Feeding and Discharge

The vibrating feeder is used to feed material onto an inclined platform, which then slides into the ferrofluid filled separation chamber. The material can also be fed directly into the ferrofluid pool, but this typically results in poor separation for particles greater than 1 mm (Svoboda *et al.*, 1996). The float product is removed from the top of the splitter while the sink product exits from the separation chamber along the sloped bottom.

Particle Shape

The shape of a particle may be important in a number of situations, in that it can affect properties such as surface area, bulk density, and flow. In this research, such quantitative descriptions as angular, flaky and modular will be used. A flaky particle, such as mica, may float even though its density may be greater than the cut-point density. The particle fails to penetrate the ferrofluid surface tension.

Moisture Content

The moisture content affects separation efficiency in that water coating the particles is immiscible with kerosene-based ferrofluid. Consequently, the water-coated particle might float even though its density is higher than the cut-point density. The effect of moisture content should decrease with an increase in particle size as well as the density difference of the material to be separated.

Viscosity of Ferrofluid

The viscosity of kerosene-based ferrofluids depends on the density of the diluted ferrofluid, which in turn, varies according to the magnetic field (Gubarevich, 1987). The increase in viscosity affects selectivity of separation due to an increase in the hydrodynamic drag force. This is more pronounced for smaller particles. An account of the effect of the drag force is dealt with in Chapter 3. As described in detail by Khalafalla (1973) and Lin (1994) ferrofluids retain their fluid properties under all applied fields and field gradients.

2.5.3 Applications of FHS Technology

FHS can be used extensively for material separation as long as the material constituents to be separated differ in density or magnetic susceptibility. The magnetic component should be small as to avoid the clogging of the separator due to high magnetic material. The magnetic effect of the feed material is considered in detail in Chapter 3.

The FHS can be used for the recovery of diamonds, gold and PGMs, non-ferrous metals, automobile and electronic scrap, coal preparation and the recovery of indicator mineral in diamond exploration. Even though FHS is being employed in these various applications, the designs of the separators differ. High selectivity separators are employed in the recovery of close density material whilst modest separation selectivity is used in the separation of materials with large density differences, e.g. aluminum and copper. In low-selectivity separators, the apparent density in the separation volume is not constant (Svoboda, 1998).

2.6 The Loss and Recovery of Ferrofluid

In ferrohydrostatic separation, particles emerge from the separator covered with ferrofluid, which can be recovered and re-used. If the mineral being sought is of high value, the recovery of the ferrofluid might not be required whereas in low-value processes, the regeneration of the ferrofluid is of paramount importance. Moreover, the ferrofluid-coated particles might make the product unsuitable for sale if not removed.

The use of kerosene based ferrofluids in ferrohydrostatic separation also poses a threat to the environment if proper methods of ferrofluid management are not developed. The amount of ferrofluid attached to the products depends on moisture content, particle size, porosity and operating conditions of the FHS. When the FHS is being operated at a density (related to applied magnetic field

intensity) at which the ferrofluid is just about to flow out of the separation chamber, more of it will be drawn from the separator, compared to when it is operated at a higher magnetic field intensity (Dumbu, 1999).

2.6.1 The Recovery Agents

A number of techniques can be used for the recovery of kerosene based ferrofluids. These include washing with water and recovering the emulsion over magnets or washing with an organic solvent and then recovering ferrofluid using ultra-filtration. The use of an organic solvent is not viable, as most of these are toxic and also it is difficult to recover ferrofluid from the mixture. Water seems to be the best agent to recover kerosene-based ferrofluid. It is non-toxic and ferrofluid can easily be recovered from the emulsion. For this research, only water was used as a ferrofluid recovery agent.

Ferrofluid Recovery using Water

Kerosene-based ferrofluid attached to the particles can be washed off using water. The resulting ferrofluid / water emulsion can then be passed over a magnetic circuit to recover the ferrofluid (see Figures 2.6 and 4.3), and then recycled back to the FHS chamber. The water component is displaced to the top of the emulsion separation chamber, and subsequently reused.

The amount of ferrofluid recovered from the emulsion depends mainly on three factors:

(1) the magnetic field intensity.
(2) size of ferrofluid droplets in the emulsion and
(3) the residence time of the emulsion in the recovery / separation chamber.

The ferrofluid / kerosene that remains in wash water can then be recovered by allowing it to float and collect at the top of the water reservoir.

The quality of ferrofluid recovered is of prime importance because it will be reused for mineral separation. Poor quality ferrofluid can have detrimental effects on the efficiency of separation (Dumbu, 1999).

Figure 2.6 Magnetic circuit for the recovery of ferrofluid from ferrofluid / water mixture. The recovered ferrofluid drains at the bottom of the emulsion separation chamber.

2.6.2 Factors Affecting the Loss and Recovery of Ferrofluid

The loss and recovery of ferrofluid is dependent on a number of factors such as particle size, moisture content and porosity of particles.

Particle Size

Experience shows that small particles "consume" relatively more ferrofluid than larger particles (described in detail in Chapter 5) in terms of the material volume processed. Assuming that the ferrofluid losses are proportional to the surface area, the simple ratio of particle surface area ($A=4\pi b^2$) to volume ($V=\frac{4}{3}\pi b^3$) yields $\frac{A}{V}=\frac{3}{b}$, which indicates that smaller particles have a higher surface to volume ratio. Consequently, processing

Porosity

A more porous sample will exhibit a greater ferrofluid loss than a less porous one, typically as a result of a greater availability of the attachment sites. The recovery of this embedded ferrofluid might be very difficult due to the immiscibility of ferrofluid and water.

Moisture Content

Moisture reduces the porosity of the particles as water molecules occupy the vacant pores in the particle. In turn, this reduces the amount of ferrofluid removed by the particles during the processing of a sample.

2.7 Summary

Ferrohydrostatic separation of material is superior to DMS and heavy liquid separation in that:

(1) it can attain higher separation densities.
(2) it is safer than heavy liquids due to non-toxicity of the ferrofluid medium used.
(3) it has higher separation efficiency.
(4) a wide range of separation densities can be attained without changing the medium.
(5) it is easy to recover and recycle the ferrofluid.

The efficiency of material separation using the FHS depends on a number of factors such as particle size, material feed rate and moisture content, ferrofluid level in the separation chamber, etc. The effect of these factors will be investigated in this research as well as those that affect ferrofluid recovery such as particle size, material moisture content and porosity.

CHAPTER 3

THEORETICAL ANALYSIS OF THE FHS EQUATION

Various factors influence the efficiency of separation in a ferrohydrostatic separator. These include particle size, ferrofluid viscosity and feed moisture content just to mention a few. In this Chapter, the effects of drag force and feed magnetisation on separation efficiency are analysed. The analysis has shown that the effective cut-point density of particles in the FHS separator is generally high for small particles. It has also been shown that the effective cut-point density decreases with an increase in particle magnetisation. The initial particle conditions such as velocity and drop height play a major role in the efficiency of material separation in the FHS.

3.1 Introduction

The FHS equation in Chapter 2 is developed on the premise of a static force balance, which assumes an equilibrium state has been obtained, However, the FHS separator represents only a finite volume and length while particle residence time is in the order of seconds. This implies that the particle trajectory is a significant contributor to eventual separation efficiency. Figure 3.1 illustrates this phenomenon where three different sized particles, say 2, 4 and 10 mm, are fed into the separator with an identical particle density, feed angle and velocity. Given that a 50/50 split is achieved on the 4 mm (for a given cut-point density) particle due to calibration, it is then obvious that the 10 mm particle will tend to cut towards the heavier fraction (decreased cut-point density) due to the inherent relatively larger momentum of a bigger particle (Badescu, et al. 1999). This phenomenon is particularly important when considering relatively low-density particles, which should exclusively report to above the splitter.

Separation efficiency also depends on the magnetisation of the feed material (Svoboda, 1996) as is also shown graphically in Figure 3.1. It can be seen that the effective cut-point density decreases with an increase of particle magnetisation. The quantification of this effect on separation efficiency will be dealt with later in this Chapter. This Chapter also extends the FHS equation in Chapter 2 by incorporating the hydrodynamic drag force.

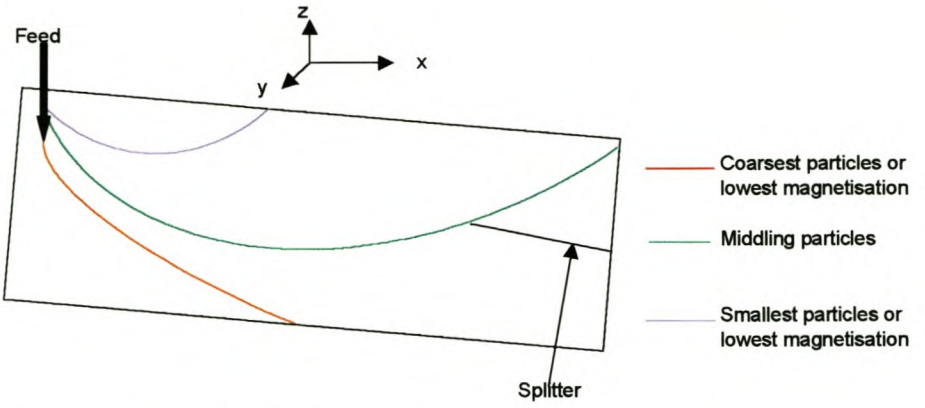

Figure 3.1 Trajectories of particles of the same density but different size or magnetic susceptibilities.

3.2 Hydrodynamic Drag

In order to incorporate particle drag forces into the FHS equation, the force balance must be resolved into the z component. The simplified force balance in the z-direction (vertical direction: see Figure 3.1) is given by:

$$\vec{F}_z = \vec{F}_{gp} + \vec{F}_{mp} + \vec{F}_{gb} + \vec{F}_{bm} + \vec{F}_d \qquad (3.1)$$

where $\vec{F}_d$ is the hydrodynamic drag in the z direction.

The x direction is along the length of the chamber and y is along the width of the separation chamber.

Assuming that Stokes law applies and the particle has reached its terminal velocity, the drag force is given by:

$$F_d = 6\pi\eta b v_p \qquad (3.2)$$

where η is the viscosity of ferrofluid in the magnetic field.

The final form (net vertical force acting on a particle) of z component is given by:

$$\vec{F}_z = \vec{F}_{gp} + \vec{F}_{mp} + \vec{F}_{gb} + \vec{F}_{bm} - 6\pi\eta b v_p$$

$$\vec{F}_z = \rho_p V_p \vec{g} + \frac{V_p \kappa_p B \nabla \vec{B}}{\mu_o} - \rho_o V_p g - \frac{V_p M_f \nabla \vec{B}}{\mu_o} - 6\pi\eta b v_p \qquad (3.3)$$

Defining the effective cut-point density, ρ_{sp}, as that particle density for which the net vertical force is zero, equation 3.3 yields (for non-magnetic particles):

$$\rho_{sp} = \rho_o + \frac{M_f}{\mu_o g}\left|\nabla \vec{B}\right| + \frac{9\eta v_p}{2gb^2} \qquad (3.4)$$

3.2.1 Significance of Hydrodynamic drag

Without considering other properties of the FHS equation, a simple analysis of the drag term in equation 3.4 (third term on the right hand side) reveals that smaller particles will experience a higher cut-point density than bigger particles. This phenomenon is illustrated in Figure 3.2, which shows plots of the effective cut-point density for different size particles (non-magnetic) assuming they have reached a terminal velocity of 0.001 m/s. It is also assumed that the ferrofluid viscosity, η = 0.003 Pa.s, ferrofluid magnetisation is 0.0150 T, ferrofluid natural density is 960 kg/m^3 and the magnetic field gradient (∇B) is 2 T/m. It should be noted that Svoboda (1996) employed the same technique in calculating the effective cut-point density of different size particles in a Magstream separator.

Figure 3.2 reveals that the hydrodynamic drag is pronounced for particle radius, b, smaller than 100 µm for a terminal velocity of 0.001 m/s, below this radius, the cut-point density increases exponentially. This implies that particles smaller than 100 µm in radius will tend to float when the cut-point density is set from the FHS theory. In the application of FHS to diamond recovery, only particles greater than 1 mm will be treated, therefore drag is not expected to have a major influence on separation results.

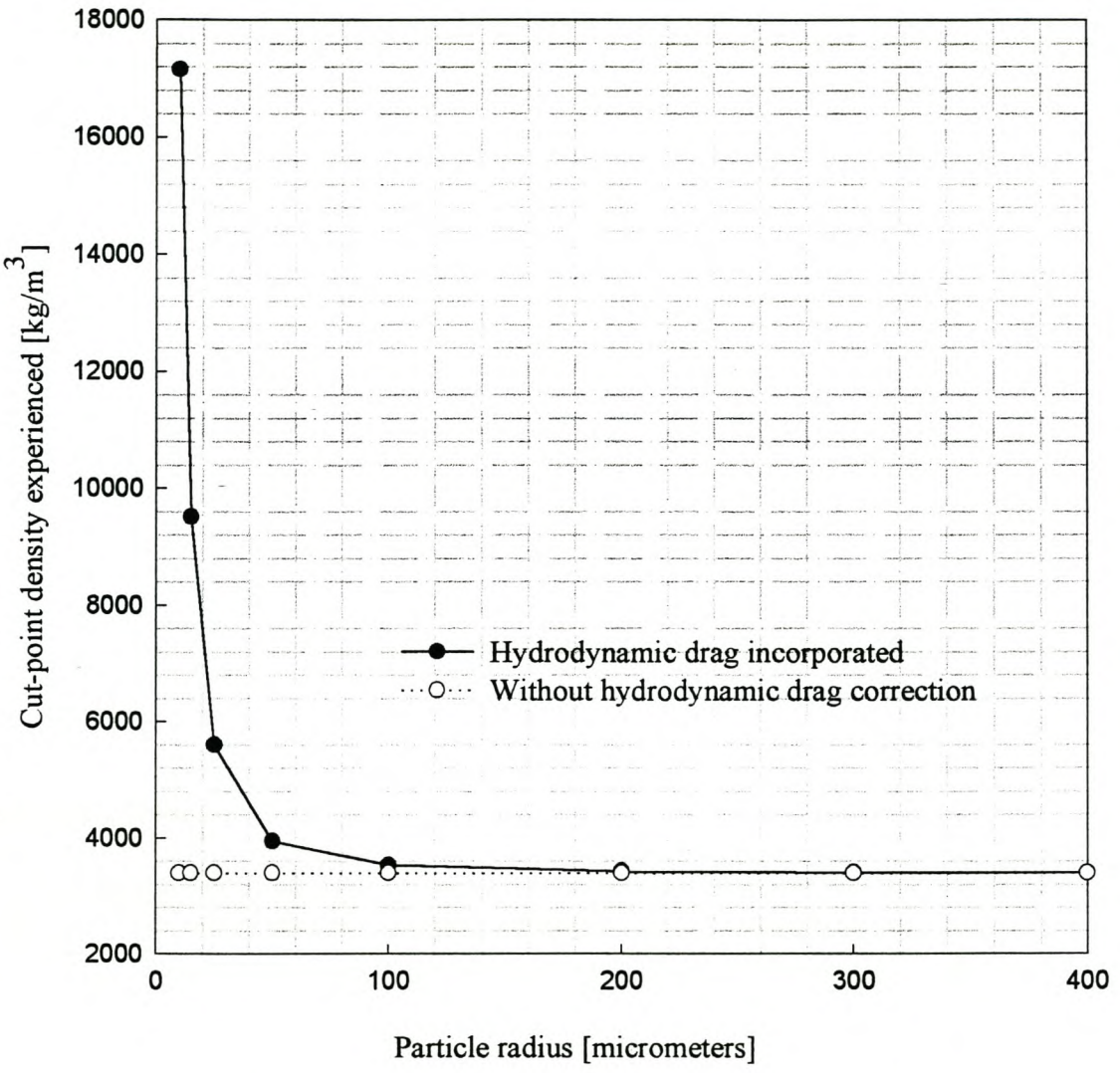

Figure 3.2 Cut-point density experienced as a function of particle size

3.2.2 Dynamic Effects

From the above consideration, it is evident that the effective cut-point density will also be determined through the initial particle velocity conditions and the size of the separation chamber. The initial velocity conditions depend on drop height and the initial particle velocity on the feeder. For example, particles of identical densities will exhibit different initial velocities if dropped from different heights.

The dynamic form of equation 3.4 is given by:

$$\rho_{sp} = \rho_o + \frac{M_f}{\mu_o \vec{g}} \left|\nabla \vec{B}\right| + \frac{9\eta}{2gb^2} \frac{dz}{dt} \qquad (3.5)$$

The result from equation 3.5 is that the effective cut-point density will change as the particle moves through the chamber and eventually goes to terminal velocity, given that the chamber is of sufficient size for this to occur. Figure 3.3 shows plots of the effective cut-point density for different size particles as they move through the ferrofluid pool before reaching their terminal velocity. The results in Figure 3.3 were obtained by numerically coding the equations of motion in the z and x directions. The conditions assumed in the simulation are as follows:

- The apparent density of the ferrofluid ($\rho_o + \frac{M_f}{\mu_o \vec{g}} \left|\nabla \vec{B}\right|$) = 3390 kg/m^3
- Density of the particles is 3250 kg/m^3
- Drop level is 8 mm
- Viscosity of ferrofluid in the magnetic field is 3 x 10^{-3} Pa.s
- 50/50 split was simulated using 4 mm size particles
- Size of particles used were 2, 3, 4, 6 and 10 mm

The characteristic initial increase in apparent density is due to the downward motion of the particle. The extent to which the apparent density increases is related to the influence of hydrodynamic drag.

As the particle starts to rise in the fluid, the effective cut-point density is then lower than that of the ferrofluid apparent density (3390 kg/m^3 in Figure 3.3). When the particle reaches terminal velocity, the added effect of drag is then diminished.

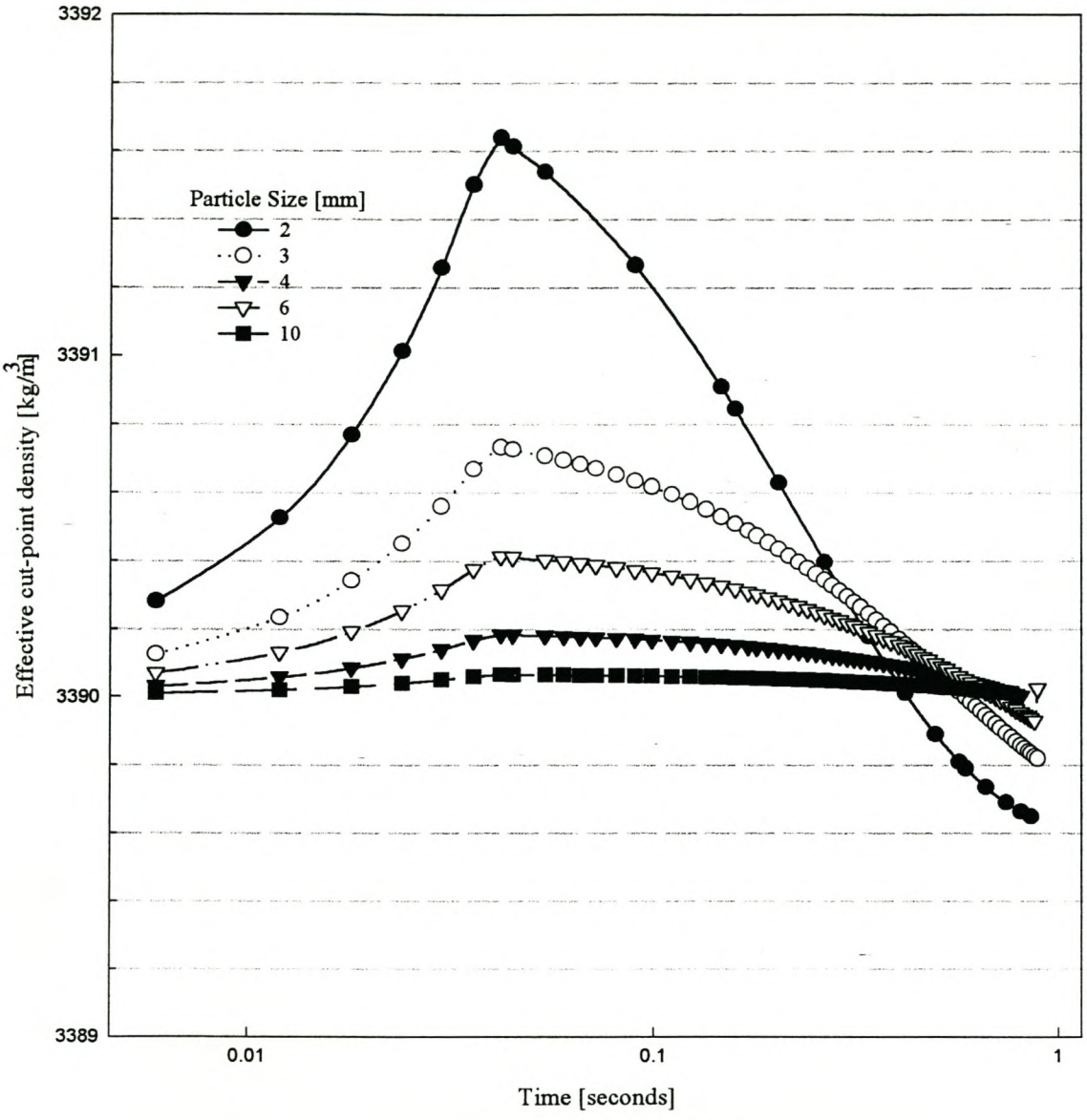

Figure 3.3 Effective cut-point densities for different size particles as they move in the ferrofluid pool.

It was found from the simulation that the smallest particles, in this instance 2 mm particle, experience the highest effective cut-point density while the largest particles (10 mm) experience the least. Ten-mm particles experience a constant effective cut-point density due to their size (bigger than 4 mm particles used for the 50/50 split) as they report to the sink products.

It can also be seen from Figure 3.3 that small particles, such as 2 mm, experience a lower cut-point density than the ferrofluid apparent density as they move through the ferrofluid pool. This can be derived from equation 3.5, which was arrived at after considering the sinking particles (moving down ward in the z-direction). However, when the particles are moving in the upward z-direction, the drag force is in the opposite direction. This implies that the third term in equation 3.5 is negative, hence lower effective cut-point density than ferrofluid apparent density is experienced. It can be seen from Figure 3.3 that if the chamber is made sufficiently long, i.e. longer residence time, all the particles eventually experience the same cut-point density. This implies that the separation chamber should be long enough for particles to attain terminal velocity for efficient separation of material.

It is important to remember that the trajectories of particles in the ferrofluid pool depend on the drop height. When particles of identical densities and size are dropped from different heights, they will report to different products if their density is close to the cut-point density. Particles dropped from a higher level will report to the sink product while particles dropped from a lower level will report to the float product. This is ascribed to the initial velocity conditions, as particles dropped from a higher level will exhibit a higher initial velocity than particles dropped from a lower level. Particles dropped from a lower level will also attain a lower effective cut-point density and will reach their terminal velocity faster than particles dropped from a higher level. This implies that it is important to maintain the drop height close to the ferrofluid level for efficient material separation using the FHS. Alternatively, there should be no drop height at all, such that this effect is eradicated from the system.

3.3 Magnetic Susceptibility

For large particles, greater than 100 μm in the example in Section 3.2, the effect of the hydrodynamic drag is negligible and equation 3.3 yields (in SI units):

$$\rho_{sp} = \rho_o + \frac{\nabla \vec{B}}{\mu_o \vec{g}}[M_f - \kappa_p B] \qquad (3.6)$$

Simple analysis of equation 3.6 indicates that an increase in the volume magnetic susceptibility of the feed material reduces the effective cut-point density of the particles. This is confirmed by Table 3.1 and Figure 3.4, which show the effective cut-point density for a range of volume magnetic susceptibilities, 0 to 1000 x 10^{-4}. It is also assumed that the natural density of ferrofluid is 960 kg/m^3, magnetic field gradient is 2 T/m, ferrofluid magnetisation is 0.015 T and the magnetic field induction is 0.2 T. The result of this analysis highlights that the treatment of nonmagnetic material together with magnetic material would result in misplaced material in the sinks.

The magnetisation of the particle (M_p) is given by:

$$M_p = \kappa_p B \qquad (3.7)$$

It can be seen from Figure 3.4 that the effect of material magnetic properties is pronounced for volume magnetic susceptibility, κ_p, greater than 20 x 10^{-4}. It can be seen that the cut-point density of 3394 kg/m^3 is only valid up to a volume magnetic susceptibility 20 x 10^{-4}. Employing equation 3.7 and the above magnetic induction assumption, the maximum magnetisation of the particle that can be treated together with non-magnetic particles is 4 x 10^{-4} T.

Table 3.1 Cut-point density as a function of volume magnetic susceptibility.

Particle Volume Magnetic Susceptibility [x 10^{-4}]	Cut-point Density Experienced [kg/m^3]
0	3394
1	3390
5	3377
10	3361
20	3329
30	3296
60	3199
100	3069
200	2745
300	2420
500	1771
750	960

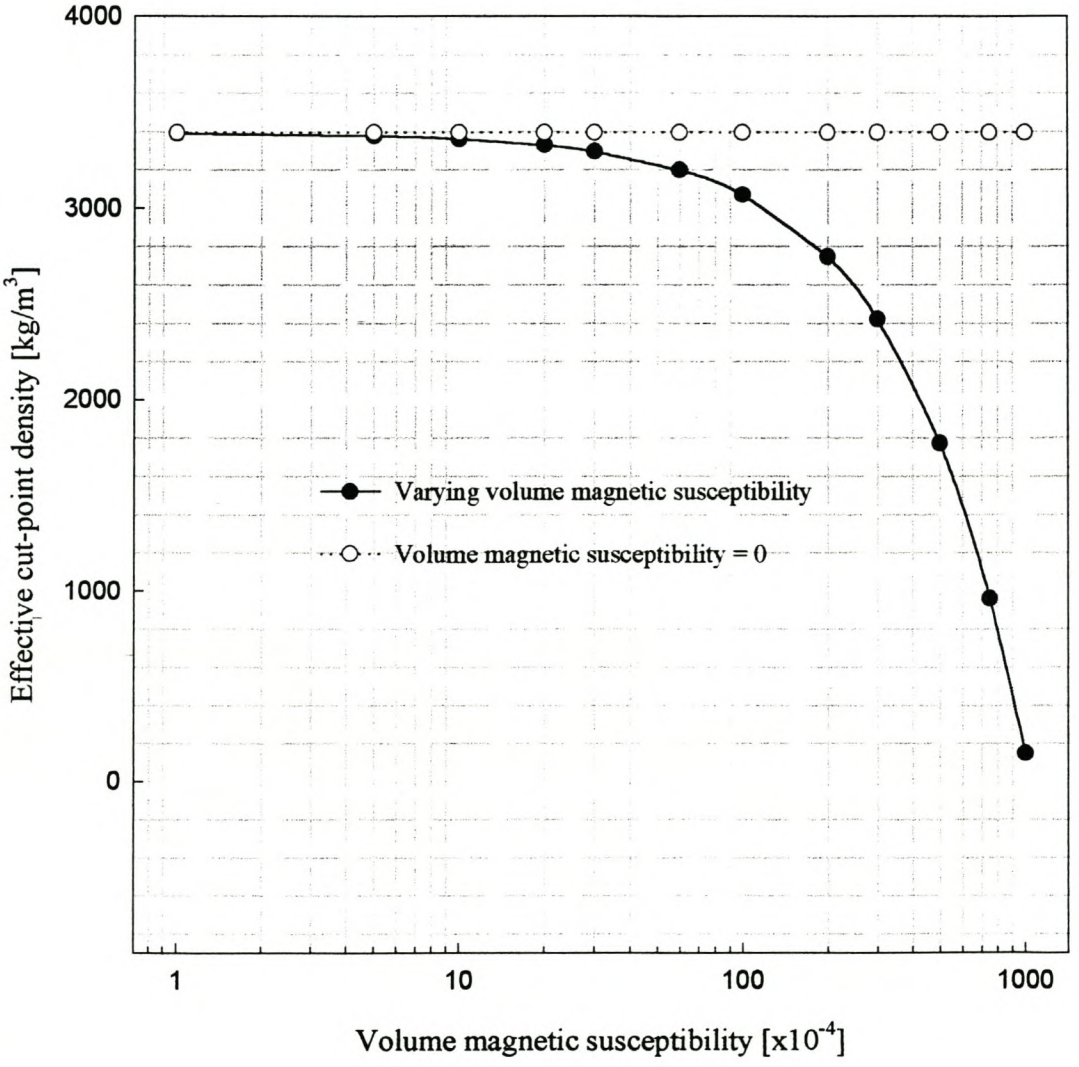

Figure 3.4 Effective cut-point denstity as a function of volume magnetic susceptibility of the particle

It can be seen from Figure 3.4 and Table 3.1 that if the volume magnetic susceptibility is 750 x 10^{-4}, which is equivalent to a particle magnetisation of 150 x 10^{-4} T, the effective cut-point density is the same as the natural density of the ferrofluid used, in this instance, 960 kg/m^3.

If the density difference of the materials to be separated is wide, the maximum volume magnetic susceptibility that can be treated can be increased. This is illustrated in Table 3.1 and Figure 3.4. It can be seen from Table 3.1 that if the density difference of the materials (non-magnetic and magnetic) to be separated is 325 kg/m^3 (3394-3069 kg/m^3) the maximum volume magnetic susceptibility is 100 x 10^{-4}.

If the maximum volume magnetic susceptibility is 20 x 10^{-4}, the maximum mass magnetic susceptibility of the particle that can be treated can be calculated from:

$$\chi_p = \frac{\kappa_p}{\rho_p} \tag{3.8}$$

where χ_p is the mass magnetic susceptibility of the particle.

Equation 3.8 shows that the maximum mass magnetic susceptibility of the particle decreases with an increase in the density of the particle. This is illustrated in Figure 3.5.

It can be seen from Figure 3.5 that the maximum mass magnetic susceptibility of the particles that can be treated together with nonmagnetic particles decreases with an increase in the density of the particles. This implies that for low-density separations such as coal and diamonds, the magnetic susceptibility of the material to be treated can be higher than that for high density separations, e.g. lead and gold. It can be seen from Figure 3.5 that the maximum mass magnetic susceptibility for particles of density 19000 kg/m^3 (e.g. gold) is 0.1 x 10^{-6} m^3/kg while that for 3520 kg/m^3 density particles, such as diamond, is 0.57 x 10^{-6} m^3/kg.

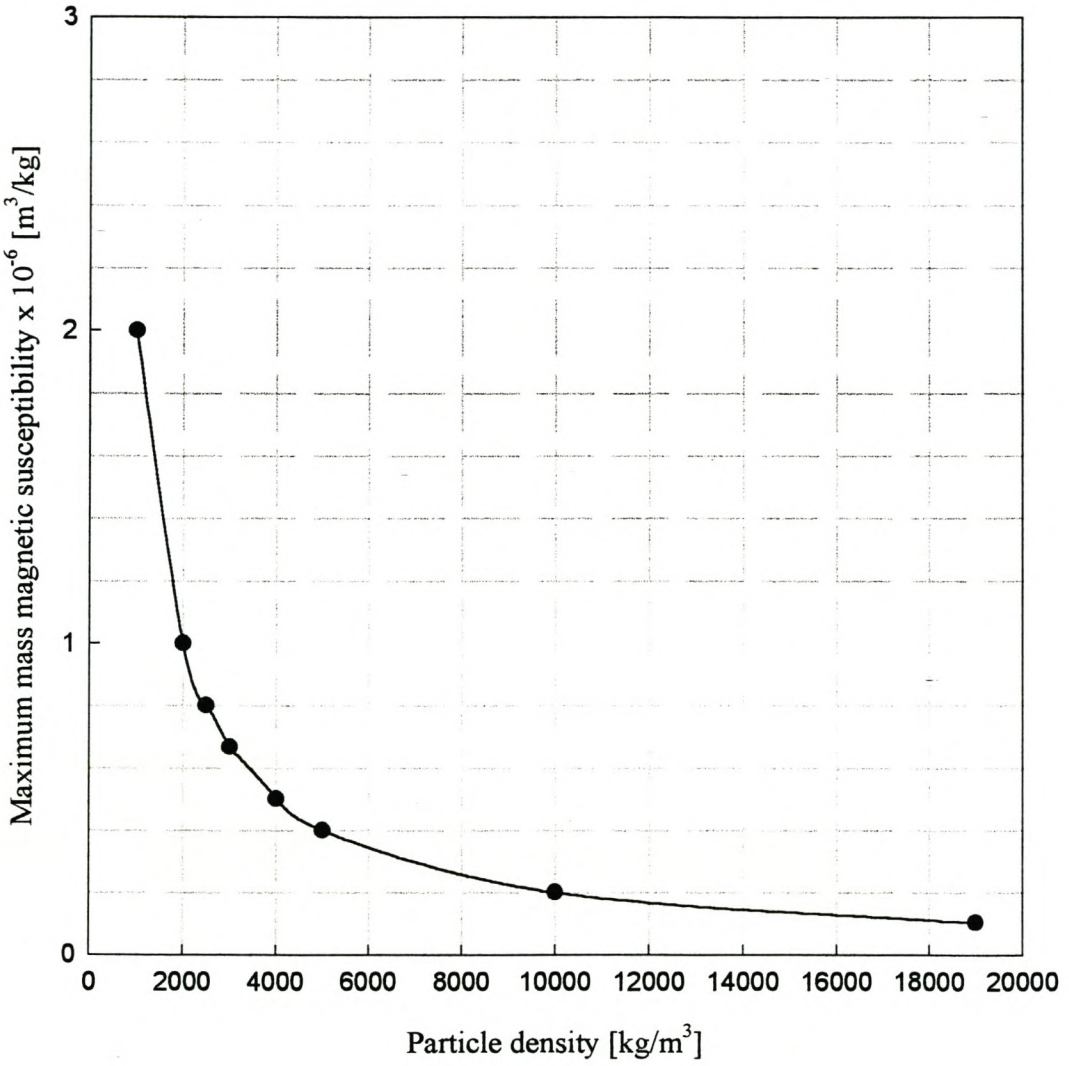

Figure 3.5 Maximum mass magnetic susceptibility of different density particles that can be treated in the FHS Separator

3.4 Ferrofluid Magnetisation and Magnetic Field Gradient

It has been shown in Chapter 2, equation 2.8, that the ferrofluid apparent density depends on the magnetisation of the ferrofluid and also on the magnetic field gradient. The effect of ferrofluid magnetisation on ferrofluid apparent density is illustrated in Figure 3.6 while that for magnetic field gradient is illustrated in Figure 3.7.

It is assumed that the ferrofluid natural density is 960 kg/m^3 and the magnetic field gradient was kept constant at 2 T/m when the ferrofluid magnetisation was varied. Ferrofluid magnetisation was kept constant at 0.015 T when the magnetic field was varied.

It can be seen from Figures 3.6 and 3.7 that the apparent density increases exponentially with an increase in ferrofluid magnetisation and/or magnetic field gradient. The magnetisation of kerosene-based ferrofluid normally used for material separation is greater than 0.01 T and the magnetic field gradient is normally greater than 1 T/m. This implies that a small change in either the magnetisation of ferrofluid or magnetic field gradient will result in a significant change in the ferrofluid apparent density. This has resulted in the FHS technology being attractive for high-density separations due to significant increase in the ferrofluid apparent density when either the ferrofluid magnetisation or the magnetic field gradient is increased.

3.5 Calculated Apparent Density and Effective Density of Density Tracers

Equation (2.8) described in detail in Chapter 2 is only applicable to a static process where the separation chamber and the pole tips are horizontal. For the separator used in this research (Figure 1.1), the magnetic field and the separation chamber are inclined to the horizontal (described in detail in Chapter 4) i.e. along the length of the separation chamber. The separation chamber is also vibrated to remove the sink products. This deviation from static conditions affect the separation of particles and therefore it is necessary to determine the effective cut-point density of density tracers and compare with the apparent ferrofluid density calculated from equation 2.8.

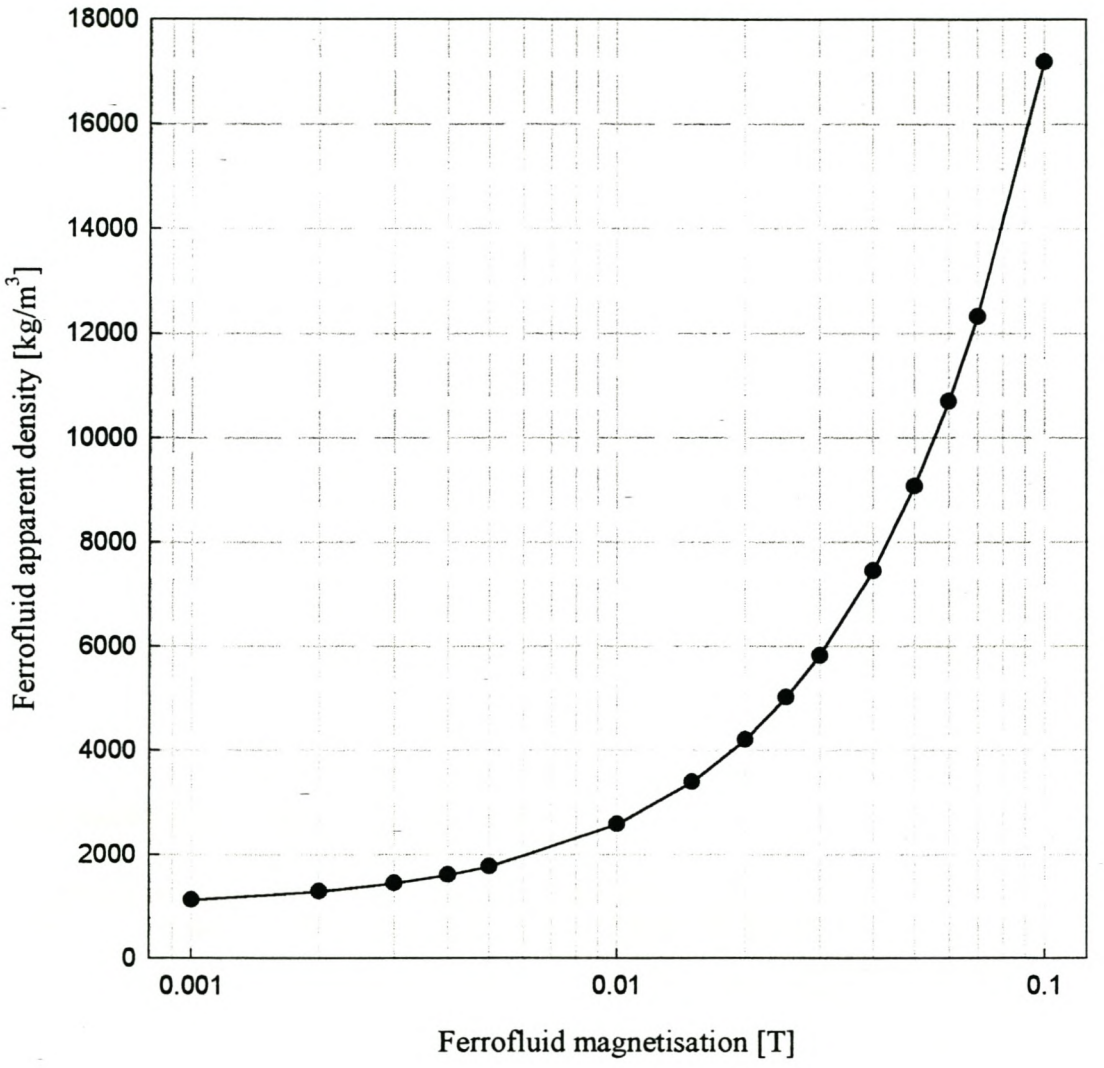

Figure 3.6 Effect of ferrofluid magnetisation on ferrofluid apparent density

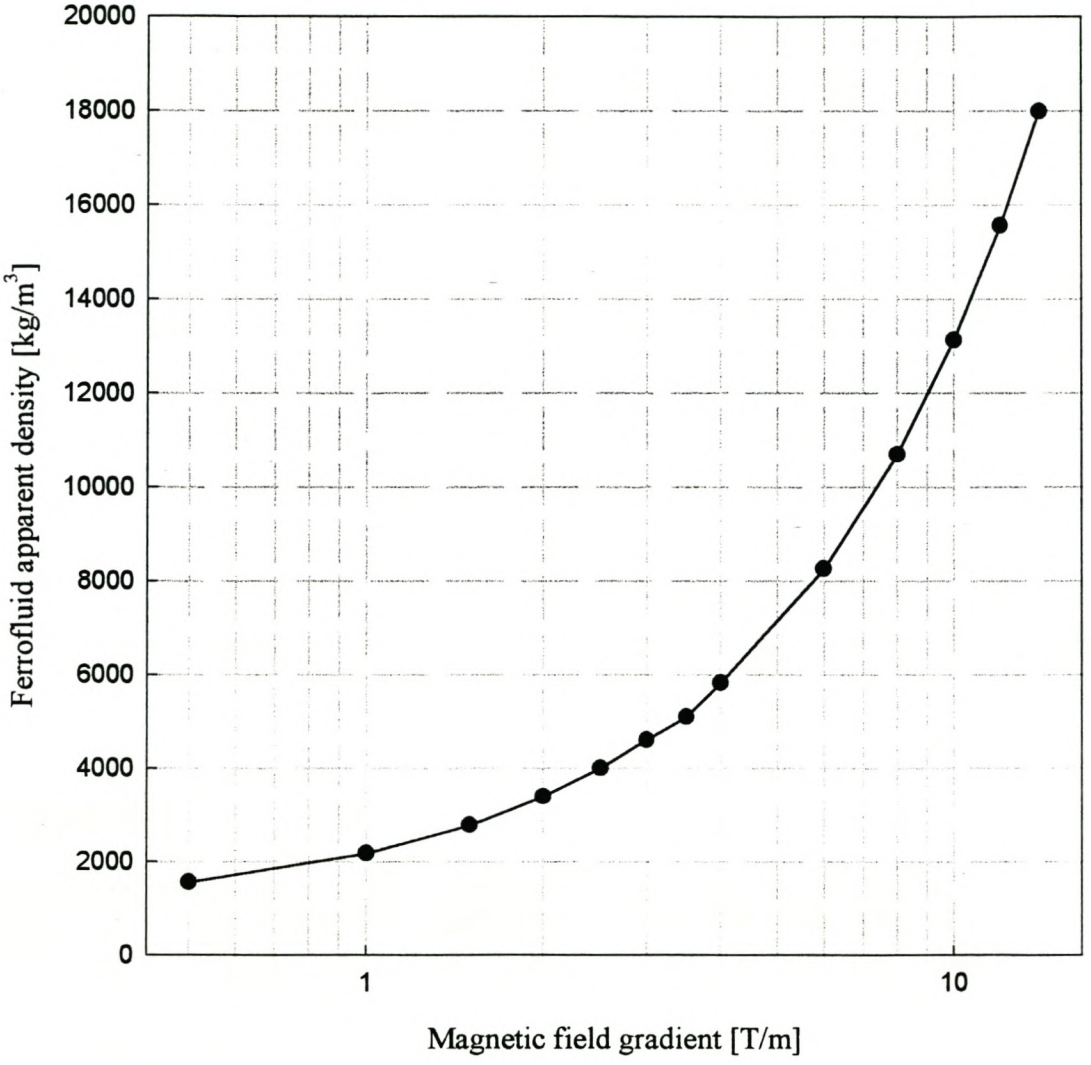

Figure 3.7 Effect of magnetic field gradient on ferrofluid apparent density

The determination of the tracer cut-point density involved setting the cut-point density at 3450 kg/m^3 using 2-mm density tracers. This was achieved at a current of 6 A using 950 kg/m^3 ferrofluid. The magnetic field, the magnetisation of ferrofluid at different positions in the separator and the calculated cut-point density is shown in Table 3.2 and Figure 3.8.

The magnetic field was measured along the vertical at the centre between the pole tips from the point of highest magnetic field using a Gauss meter. The procedure is described in detail in Chapter 4.

Table 3.2 Calculated cut-point densities at different positions between the poles of the FHS Separator using 950 kg/m^3 density ferrofluid.

Vertical Distance From the Point of Highest Magnetic Field [mm]	Magnetic Field Induction [T]	Magnetic Field Gradient [T/m]	Magnetisation of 950 kg/m^3 Ferrofluid [T]	Calculated Cut-point Density [kg/m^3]
0	0.26	-	0.0155	-
10	0.25	1.00	0.0155	2207
20	0.23	2.00	0.0154	3448
30	0.21	2.00	0.0153	3432
40	0.19	2.00	0.0150	3384
50	0.17	2.00	0.0148	3351
60	0.15	2.00	0.0146	3319
70	0.12	3.00	0.0142	4406
80	0.10	2.00	0.0137	3173
90	0.07	3.00	0.0126	4016
100	0.05	2.00	0.0112	2767

It can be seen from Figure 3.8 that the calculated cut-point density is within the tracer-determined density between 20 and 60 mm from the point of highest magnetic field. This implies that the cut-point density can be arrived at by calculating the ferrofluid apparent density at 20 mm from the point of highest magnetic field. Error bars are included due to the accuracy of the density tracers, +-30 kg/m^3. Separation takes place in this region as the splitter is positioned approximately 30 mm from the point of highest magnetic field. It can be seen from Figure 3.8 that the calculated density is the lowest at 10 mm from the point of highest magnetic field. This is due to the lowest magnetic field gradient of 1T/m at this point (see Table 3.2). The calculated density is the highest at 20 mm and then gradually decreases thereafter. The decrease in density is due to the decrease in the ferrofluid magnetisation as a result of a decrease in the magnetic field as can be seen in Table 3.2.

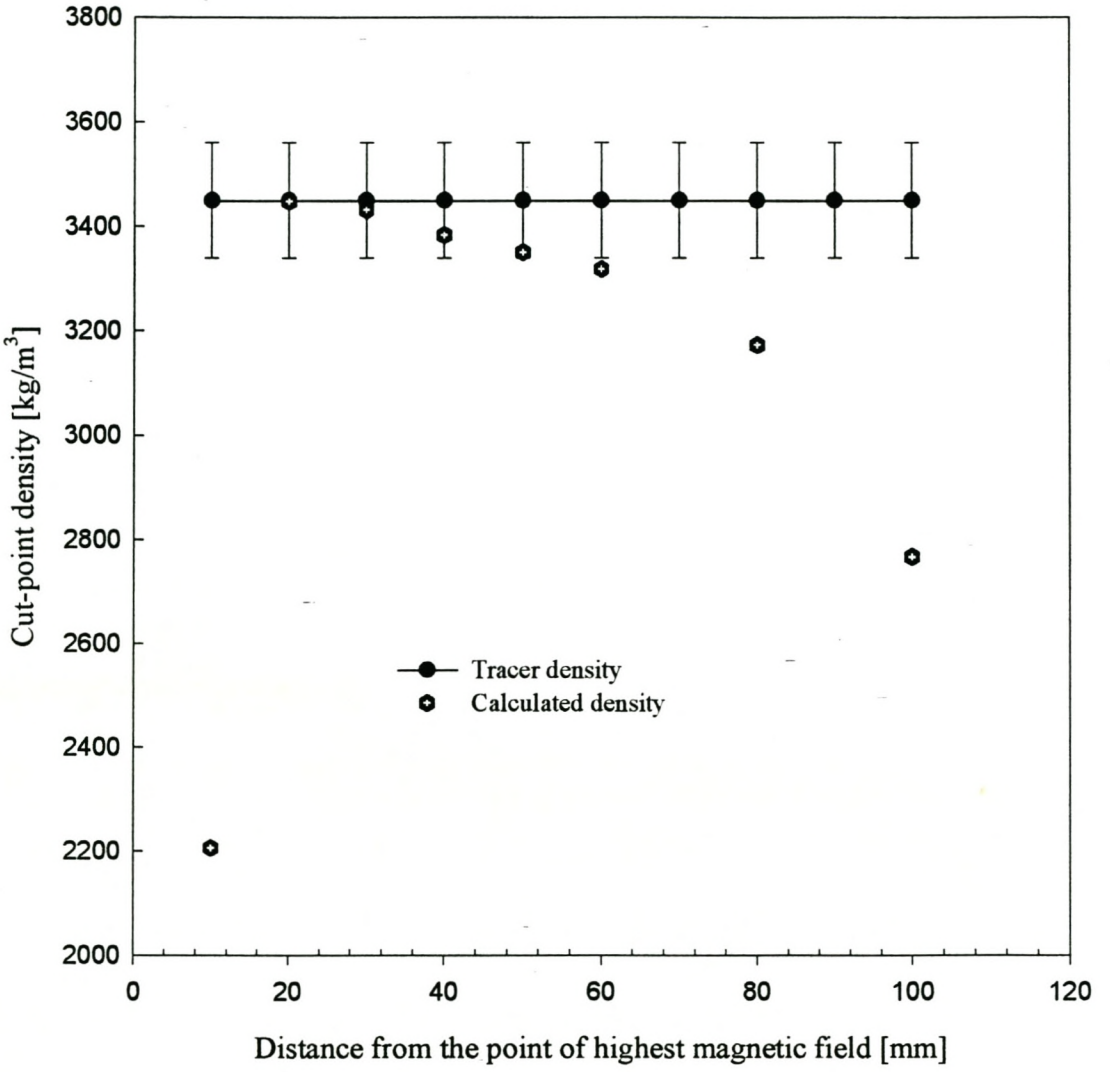

Figure 3.8 Comparison of calculated apparent density with effective density of 2 mm density tracers

3.6 Summary and Conclusions

It has been shown that the effect of hydrodynamic drag in FHS separation is significant for particles smaller than 100 μm in radius. This is good news for diamond operations, which typically treat material greater than 1 mm. It was shown that the treatment of nonmagnetic material together with magnetic material would result in misplaced material in the sinks. It has been shown that the maximum volume magnetic susceptibility that can be treated in the FHS separator is 20×10^{-4}. The misplacement of magnetic material into the sinks can be beneficial if the sinks products are to be discarded and the misplaced magnetic material are part of the gangue. The result is that there is a reduction in the gangue material reporting to the float concentrate.

CHAPTER 4

EXPERIMENTAL METHODS AND PROCEDURES

This chapter describes the test samples used, sample preparation and details the test procedures followed. Initially, the magnetic field generated at different electrical currents was measured and the magnetic field gradient calculated. The FHS Tromp curve was determined using 2 mm density tracers. The feed rate, particle size and ferrofluid level tests were performed to determine the effect of these variables on the separation efficiency. The ferrofluid drawn from the separator at different operating conditions was determined. The effect of particle size, material porosity and material moisture content on the loss of ferrofluid was also quantified. The results for all the experiments performed are described in Chapter 5.

4.1 Introduction

The choice of samples for use in experimentation is critical in order to gain most benefit from the experiments. The design of experiments before carrying them out avoids unnecessary flaws during the course of experimentation and thus fewer experiments can be conducted. A proper test procedure should be followed in order to standardise experiments and have comparable results.

Initially, preliminary research was carried out with the objective of understanding more about the FHS process, gaining a better understanding of important variables influencing the performance of the separator and those affecting ferrofluid recovery. Both separation and ferrofluid recovery preliminary investigations were very valuable in designing a systematic experimental procedure for carrying out thorough investigations into the selected variables.

All separation experiments were carried out using the ferrohydrostatic separator shown in Figure 1.1. The kerosene-based ferrofluid was used for separation and ferrofluid recovery experiments. Most separation experiments were carried out using ferrofluid of density 980 kg/m^3 and 960 kg/m^3, whilst all ferrofluid recovery tests were performed using 960 kg/m^3 density ferrofluid.

Ferrofluid used for separation and ferrofluid recovery experiments was obtained by diluting a concentrated ferrofluid of density 1230 kg/m^3 with kerosene. The dilution ratio of kerosene to concentrated ferrofluid is given by:

$$\frac{V_k}{V_c} = \frac{(\rho_c - \rho_f)}{(\rho_f - \rho_k)} \tag{4.1}$$

where V_k and V_c are the volume in m^3 of kerosene and concentrated ferrofluid respectively and ρ_k, ρ_c, and ρ_f are the densities in kg/m^3 of kerosene, concentrated ferrofluid and dilute ferrofluid respectively.

4.2 Materials

A range of kimberlite samples and density tracers (courtesy of De Beers) were used in the experimental investigation. Most of the separation experiments were carried out using density tracers whilst kimberlite samples were mainly used for ferrofluid recovery experiments. The size of density tracers ranged from 0.5 mm to 10 mm whilst the gravel size ranged from 0.3 mm to 12 mm.

4.2.1 Material Preparation

The feed material into the FHS was initially magnetically scalped using a barium ferrite permanent magnetic roll separator to remove strongly magnetic material. This was essential as strongly magnetic material clogs the separator as it is attracted to the magnetised pole tips of the ferrohydrostatic separator. A barium ferrite roll was used because a maximum magnetic field it generates is 0.25 T, the same as that generated by the FHS. Since the density tracers are diamagnetic, they were not scalped (Svoboda, 1996). Only non-magnetic fractions from the permanent roll magnetic separator were treated in the separator. Samples were treated at room temperature as hot feed into the separator reduces the apparent density of the ferrofluid.

The gravel samples were screened into different size ranges using square aperture sieves. These were –0.5+0.3 mm, -0.85+0.50 mm, -1.00+0.85 mm, -1.7+1.0 mm, -2.8+2.0 mm, -4+2 mm, -8+4 mm and -12+8 mm.

4.3 Magnetic Field Measurements

The magnetic field was measured using a gaussmeter positioned at the centre between the pole tips along the vertical, h, axis as shown in Figure 4.1. The first

point of measurement was the highest magnetic field point, which was 10 mm from the base of the pole tips. The field was measured for 2.8A, 3.3A, 4.3A, 5A, and 6A supplied to the coils and the results are shown in Appendix A.

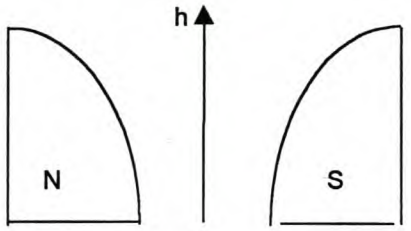

Figure 4.1 Schematic diagram of FHS Separator pole tips.

4.4 Experimental Procedure for Separation

As described in Chapter Two, the ferrohydrostatic separator can operate under either closed loop conditions (density control) where the current supplied to the coils depends on the input from the strain gauge or under current control where the closed loop circuit is disabled. Most separation experiments were carried out under density control, except for the determination of the effect of ferrofluid level on separation efficiency and comparison of water and kerosene-based ferrofluids. This was due to the change in the strain gauge reading with a change in ferrofluid level.

The current was initially ramped up to a certain value dependent on the density of ferrofluid to be used. Low default currents were set for high-density ferrofluids whilst high default currents were set for low-density ferrofluids. This is due to the fact that low-density ferrofluids require higher magnetic fields to be held between the pole tips whilst high-density ferrofluids require lower magnetic fields.

The required cut-point density was then set and the ferrofluid introduced into the separation chamber. The density control mode (closed loop) was then activated and the required cut-point density was then verified by the use of density tracers. If the apparent density experienced by the strain gauge was different from the cut-point density determined by the density tracers, the strain gauge was then calibrated to match the density tracers. This was achieved by entering the density experienced by the tracers, which then prompts the software to adjust the current to suit the required cut-point density.

The minimum level of ferrofluid in the separation chamber was entered and an ultrasonic level sensor was used to monitor the ferrofluid level. When the ferrofluid level dropped below the set minimum, a red light was shown on the computer screen and more ferrofluid was manually added.

The material / tracers were fed into the separation chamber (Figure 4.2) via the hopper and the feeder tray. The material could be introduced directly into the ferrofluid pool or onto the separation chamber feed plate and slide into the ferrofluid pool (see Figure 4.2). The latter technique was used for most separation experiments, as the size of the material treated was coarse, i.e. greater than 1 mm. Fine particles less than 1 mm should be fed directly into the ferrofluid pool to overcome surface tension and also to avoid the lumping of material on the separation chamber feed plate. There is no lumping of coarse particles and feeding onto the plate reduces the velocity of the particles as they enter the ferrofluid pool and hence improve separation efficiency (see Chapter 3).

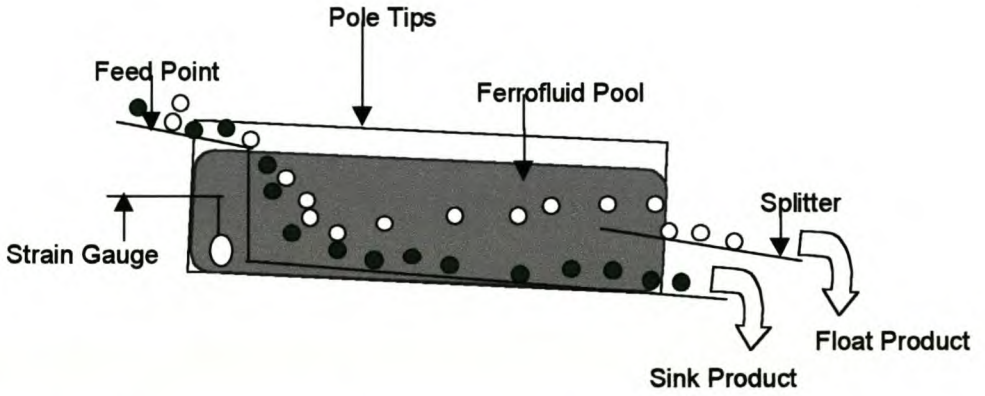

Figure 4.2 Side view of the pole tips and the separation chamber. The length of the separation volume was 195 mm.

4.4.1 FHS Tromp Curve

The FHS tromp curve was determined by setting the cut-point density at 4450 kg/m^3 and feeding 2 mm tracers of each of the following densities: 4070 kg/m^3, 4210 kg/m^3, 4340 kg/m^3, 4440 kg/m^3, 4470 kg/m^3, 4540 kg/m^3, 4640 kg/m^3 and 4740 kg/m^3. The tracer recovery into the sinks was noted.

4.4.2 Feed rate / Optimum Operating Capacity

During the feed rate experiments, particle size and ferrofluid level (94 mm) were kept constant. Adjusting the feeder vibrator varied the feed rate and the time taken to feed a known amount of tracers was measured using a stopwatch. Sixty tracers, mass measured, of each density (ranging from 2700 kg/m^3 to 3530 kg/m^3) were used and 7 runs were carried out for

each test. The sizes of tracers used for feed rate test were 2 mm and 4 mm. The tracer recovery into the sinks was noted and the results are shown in Appendix B.

Two gravel samples of particle sizes, -1.00+0.85 mm and -0.5+0.3 mm were treated at a cut-point density of 3150 kg/m^3 at various feed rates. The cut-point density was set using 2 mm tracers. Seven runs were carried per feed rate and average recovery into sinks was noted.

4.4.3 Effect of Particle Size on Separation

Fluid level (94 mm) and feed rate (1.3 kg/h) were kept constant during the determination of the effect of particle size on separation efficiency. Sixty tracers of densities ranging from 3000 kg/m^3 to 3530 kg/m^3 at a cut-point density of 3350 kg/m^3 were fed into the separator and seven runs were carried out for each test. The sizes of tracers used for particle size test were 0.5 mm, 0.85 mm, 1 mm, 2 mm, 4 mm, 6 mm, 8 mm and 10 mm. The tracer recovery into the sinks was noted and the results are shown in Appendix C.

4.4.4 Effect of Ferrofluid Level on Separation

For this experiment, the particle size, the current supplied to the coils and the feed rate (1.3 kg/h) were kept constant whilst the ferrofluid level was reduced in small aliquots from 94 mm using a pipette. The current was kept constant as the strain gauge reading decreases with a decrease in ferrofluid height. The decrease in the reading causes an increase in the current supplied to the coils and hence an increase in the apparent density of ferrofluid in the separation chamber. It was assumed that at constant current, the apparent density was constant in the separation volume. The ferrofluid level was measured from the bottom of the separation chamber close to the splitter.

Sixty tracers of each density (ranging from 3000 kg/m^3 to 3530 kg/m^3) were used for the experiment and seven runs were carried out for each test. The sizes of tracers used for the test were 2 mm and 6 mm. The ferrofluid level and the tracer recovery into the sinks was noted as shown in Appendix D.

4.4.5 The Effect of Material Density Distribution on Separation

The size of tracers used for this experiment was 2 mm and their density distribution is shown in Table 4.1.

Table 4.1 Density distribution of tracers used to determine the effect of density distribution on FHS efficiency.

Density of Tracers [kg/m^3]	2900	3000	3100	3200	3300	3400	3530
Number of Tracers Treated	10	20	30	40	30	20	10

The cut-point density was initially set at 2950 kg/m^3 and all density tracers were treated. The ferrofluid level was kept constant at 94 mm as well as the feed rate of 1.3 kg/h. The tracer recovery into the sinks was noted. The same procedure was repeated at a cut-point density of 3050 kg/m^3, 3150 kg/m^3, 3250 kg/m^3, 3350 kg/m^3, and 3450 kg/m^3 and the results are described in detail in Chapter 5.

4.4.6 Effective Cut-point Density of Different Size Tracers

This test was prompted by the fact that the effective cut-point density experienced by particles in the FHS separator is a function of particle size. The results from this test will show the deviations in the effective cut-point densities for varying particle sizes.

Initially, the cut-point density was set at 3150 k/m^3 using 2 mm tracers. Sixty, 0.85 mm, 1 mm, 4 mm, 6 mm, 8 mm and 10 mm density tracers were treated at the same cut-point density. The density of the tracers ranged from 2900 kg/m^3 to 3530 kg/m^3.

The same procedure was repeated at a cut-point density of 3350 kg/m^3 and 3450 kg/m^3 set using 2 mm density tracers and the results will be described later in Chapter 5.

4.4.7 The Effect of Material Moisture Content on Separation

Gravel from the Premier Mine was used for this experiment. The sample was treated at a constant feed rate (1.3 kg/h) and ferrofluid level (94 mm). The cut-point density was maintained at 3350 kg/m^3. The gravel moisture

content was varied from 0 % to 10 %. The material moisture content was calculated from:

$$\%Moisture = \frac{(Weight\ of\ water\ added)}{(Weight\ of\ Sample + water)} x100 \qquad (4.2)$$

The amount of gravel recovered into the sink product was noted.

4.4.8 Comparison of FHS with Heavy Liquids

The Premier Mine gravel (particle size –0.5+0.3 mm) was treated in the FHS at a cut-point density of 3250 kg/m^3 and a feed rate of 1.3 kg/h with the level of fluid maintained constant at 94 mm. Two runs were performed. FHS floats were then treated in heavy liquids of density 3300 kg/m^3 whilst sinks were treated at a heavy liquid density of 3200 kg/m^3 to check for the misplacement of material. The results are described later in Chapter 5.

4.4.9 The Effect of Ferrofluid Viscosity on Separation

The viscosities of 1230 kg/m^3, 1110 kg/m^3, 1000 kg/m^3, 980 kg/m^3, 950 kg/m^3, and 900 kg/m^3 ferrofluids were measured using a Mettler RM180 Rheomat. Shear rates of 300 s^{-1} and 1000 s^{-1} were used. The values were normalised by dividing all viscosity values with that for 900 kg/m^3, The absolute values of viscosity were not used because there are many effects influencing the viscosity inside the separation chamber i.e., magnetic field, velocity of particle.

A sample of particle size –1.0+0.3 mm was used to determine the effect of viscosity on separation. One hundred-gram samples were treated at a constant feed rate (1.3 kg/h), fluid level (94 mm) and cut-point density (3900 kg/m^3). The recovery into the sinks was noted and results are detailed in Chapter 5.

4.4.10 Comparison of Water-based with Kerosene-based Ferrofluids

The cut-point densities that could be attained at different currents using different types of ferrofluids were determined. The cut point density was verified by using 2 mm tracers.

When it was observed that water-based ferrofluids produced some stratas in the FHS, the density of ferrofluid at different regions was measured. This was achieved by extracting ferrofluid using a syringe and the density was measured using a density meter, model DMA 38. This test was carried out at a constant current of 6 A and ferrofluid was extracted after 10 minutes of introducing it into the separation chamber.

The ferrofluid was extracted from two regions:

- On the surface of the ferrofluid
- Between the poles (centre) and at the point of highest magnetic field.

The results are presented in Section 5.3.10.

4.5 Experimental Procedure for Ferrofluid Loss and Recovery

The ferrofluid recovery system is shown in Figure 4.3. The ferrofluid-recycling plant consists of two inlet chutes, which transfer sink and float products from the FHS to the partitioned screen. Attached to the screen is an Eriez vibrator, which assists in the movement of particles on the screen. The vibrator is adjustable to accommodate different size particles that require different feed rate for thorough cleaning.

Firstly, the material is washed with water. After water wash, a detergent is sprayed onto the particles to clean them. The material is then collected in two canisters (floats and sinks). Below the screen are two collecting chambers, one for the created ferrofluid / kerosene emulsion and the other for the detergent. The mixing of the emulsion and the detergent is avoided by placing a separating plate below the screen.

The emulsion is passed over a permanent magnetic circuit where ferrofluid is attracted to the magnets and wash water is displaced to the top and reused. A chamber is situated between two permanent magnets and is designed in a way to allow water to be displaced to the top and ferrofluid to drain at the bottom. The emulsion separation chamber is primed initially with ferrofluid used for separation. The water outlet is positioned slightly above the level of ferrofluid to allow a thin layer of water above the ferrofluid for efficient ferrofluid recovery.

The gap between the two magnets is vital as it determines the amount of ferrofluid to be used to prime the chamber. It also determines the level of different density ferrofluids in the chamber as more concentrated ones attain a higher level than less concentrated ones. The recovered ferrofluid is then pumped back to the ferrohydrostatic separator.

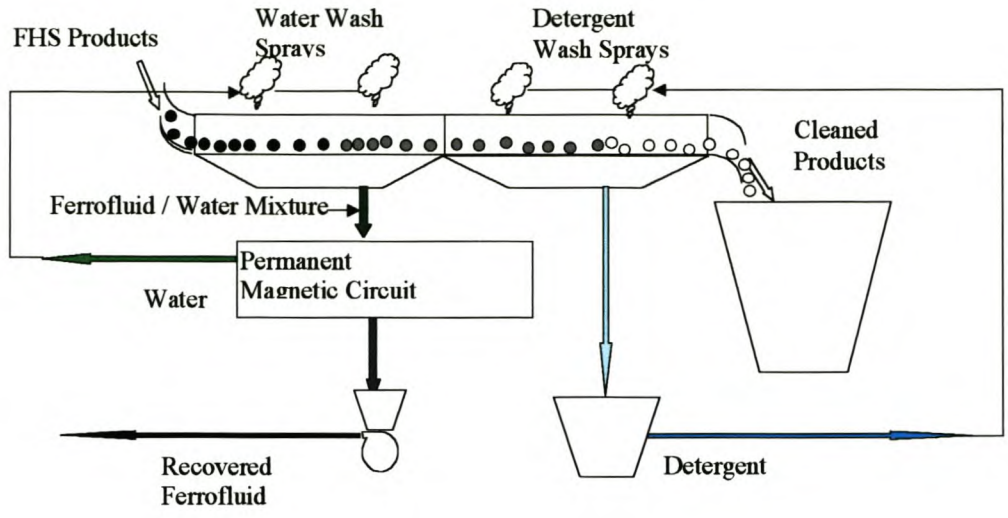

Figure 4.3 General layout of the ferrofluid recycling plant.

4.5.1 Ferrofluid Drawn from the Separator at Different Operating Conditions

Before carrying out ferrofluid recovery experiments, it was important to determine the amount of ferrofluid drawn from the separator at different operating conditions. The test procedure followed was as follows:

- The cut-point density was set at 2600 kg/m^3. The initial mass of the sample was noted and then the sample was fed into the separator. The products were collected into one tray and the mass measured. The amount of ferrofluid drawn from the separator was calculated by subtracting the initial mass of the sample from the final mass after FHS treatment.
- The same procedure was repeated at a cut-point density of 3250 kg/m^3.

  The same mass of sample was then soaked in ferrofluid and allowed to drain for 300 seconds. The amount of ferrofluid adsorbed was noted and results are described in Chapter 5.

4.5.2 Ferrofluid Recovery as a Function of Particle Size

The particle size of gravel used ranged from 0.85 mm to 12 mm. The test procedure involved:

- Washing the sample with water to remove the fines and sun drying it.
- The sample (1 kg) was then soaked in ferrofluid. The ferrofluid was allowed to drain and the mass of sample was noted.
- The sample was then washed in the ferrofluid-recycling plant with water to remove ferrofluid.
- The sample was then sun dried and weighed.

The mass of ferrofluid lost m_f in grams can be written as:

$$m_f = \frac{100(\rho_f)(m_M)}{(V_M)(\rho_M)} \tag{4.3}$$

where m_M is the mass of magnetite lost, ρ_f and ρ_M are the density of working ferrofluid and magnetite respectively, and V_M is the volumetric percentage of magnetite in the working ferrofluid used.

The results are shown in Appendix E.

4.5.3 Ferrofluid Recovery as a Function of Material Porosity

Samples were taken from kimberlite OD76, OD83, Kimberley and Venetia as well as local sand all with size of –1.7+0.85 mm.

The following procedure was used to determine the gravel porosity:

- The samples were dried at 60 °C and weighed.
- Each sample was put under vacuum overnight to extract air from the pores.
- While still under vacuum, the samples were saturated with a fluid and left under vacuum for at least three hours.
- The vacuum was removed and the samples left submerged in the fluid overnight.
- The saturated samples were weighed after removing the excess fluid on the surface by way of cladding.
- The density of the fluid was determined.

- By subtracting the dry mass of the samples from the saturated mass, the mass of fluid that filled the voids was determined.
- From this mass, the volume of fluid, which is also the volume of voids, was determined, using the density.
- The total volumes of the samples were calculated from the dry mass and the dry density.
- Having the total volume and the voids' volume, the porosity was determined.

The porosity for different samples is shown in Table 4.2.

Table 4.2 Porosities of samples. The particle size of the samples was –1.7+0.85 mm.

Sample	Porosity [%]
OD76	8.78
OD83	0.27
Local Sand	0.18
Kimberley	11.34
Venetia	0.50

The ferrofluid recovery test procedure on the samples was the same as that for Section 4.5.2 and the results are shown in Appendix G.

4.5.4 Ferrofluid Recovery as a Function of Material Moisture Content

The sample (particle size –8+4 mm) was initially washed in water to remove the fines and then sun-dried. The moisture content was varied from 0 to 10 % as described in Section 4.4.7. The sample (1 kg) was then soaked in ferrofluid and allowed to drain and the mass noted.

The procedure as per Section 4.5.2 was then followed.

4.6 Summary and Conclusions

Preliminary experiments were very valuable in the proper planning of detailed ones. Most separation experiments were carried out using ferrofluid of density 980 kg/m^3 and 960 kg/m^3. The tests were performed using these ferrofluids as 980 kg/m^3 density ferrofluid is mainly used for diamond separation while

960 kg/m^3 density ferrofluid is used for geological application. Less dense ferrofluids are used for geological applications because low viscosities are required for efficient separation of small particles. The gravel samples used for experimentation were magnetically scalped to reduce the effect of material magnetisation on the effective cut-point density of material in the magnetic field. Ferrofluid recovery tests were performed using 960 kg/m^3 density ferrofluids.

CHAPTER 5

RESULTS AND DISCUSSION

The results obtained in this research are presented and discussed in this chapter. The magnetic field and magnetic field gradient were found to increase with an increase in the electrical current supplied to the coils. The separation efficiency was found to depend on the feed rate, particle size, ferrofluid level and the feed moisture content. The separation efficiency was also found to depend on the density difference of the particles to be separated. The separation efficiency also decreases with a decrease in the density difference due to the misplacement of the near density material (density of material close to the cut-point density). An increase in feed rate results in an increase in the interaction of particles in the separation volume; hence particles are recovered to the incorrect fraction.

The separation efficiency is poor if the particle size range of the feed material is wide, due to different particle trajectories of different sizes in the separator. Coarse particles follow a deeper and longer trajectory compared to small ones. For the particles smaller than 2.8 mm, the separation efficiency deteriorates with an increase in the amount of water coating the particles. This is due to the immiscibility of water and kerosene-based ferrofluid.

The separation efficiency was also found to depend on the natural density of the ferrofluid when treating fine particles smaller than 1 mm. This is due to an increase in hydrodynamic drag effects in small particles. Dense ferrofluids have high viscosities as compared to less dense ones.

The ferrofluid drawn from the separator decreases with an increase in the magnetic field as most of it is retained in the separator. The amount of ferrofluid lost with products of separation increases with a decrease in particle size. This is due to an increase in specific surface area of small particles. Ferrofluid losses also increase with an increase in material porosity and a decrease in material moisture content due to an increase in vacant pore volume.

5.1. Introduction

As described in Chapter 4, a number of tests were carried out to determine the importance of certain factors on ferrohydrostatic separation efficiency and the variables that affect the loss and recovery of ferrofluid. Magnetic measurements were also carried out to establish the distribution of the magnetic field induction between the two pole tips described in detail in Chapter 2.

The separation variables investigated were:

(1) Feed rate
(2) Feed moisture content
(3) Particle size
(4) Ferrofluid level
(5) Feed density distribution
(6) Ferrofluid viscosity

whereas the factors investigated for the loss and recovery of ferrofluid were:

(1) FHS operation
(2) Particle size
(3) Material porosity
(4) Material moisture content

5.2 Magnetic Field Measurements

5.2.1 Magnetic Field Induction

The magnetic field induction measurement results are shown in Figure 5.1.

As can be seen from Figure 5.1, the magnetic field induction decreases along the vertical from the point of highest magnetic field induction (at the centre between the poles) due to the hyperbolic shape of the pole tips. The magnetic field induction is also higher for higher electrical currents due to increased magnetisation of the iron yoke.

5.2.2 Magnetic Field Gradient

The magnetic field gradient was derived from the magnetic field induction measurements (measure gradient of curves in Figure 5.1) and is shown in Figure 5.2 and Appendix A.

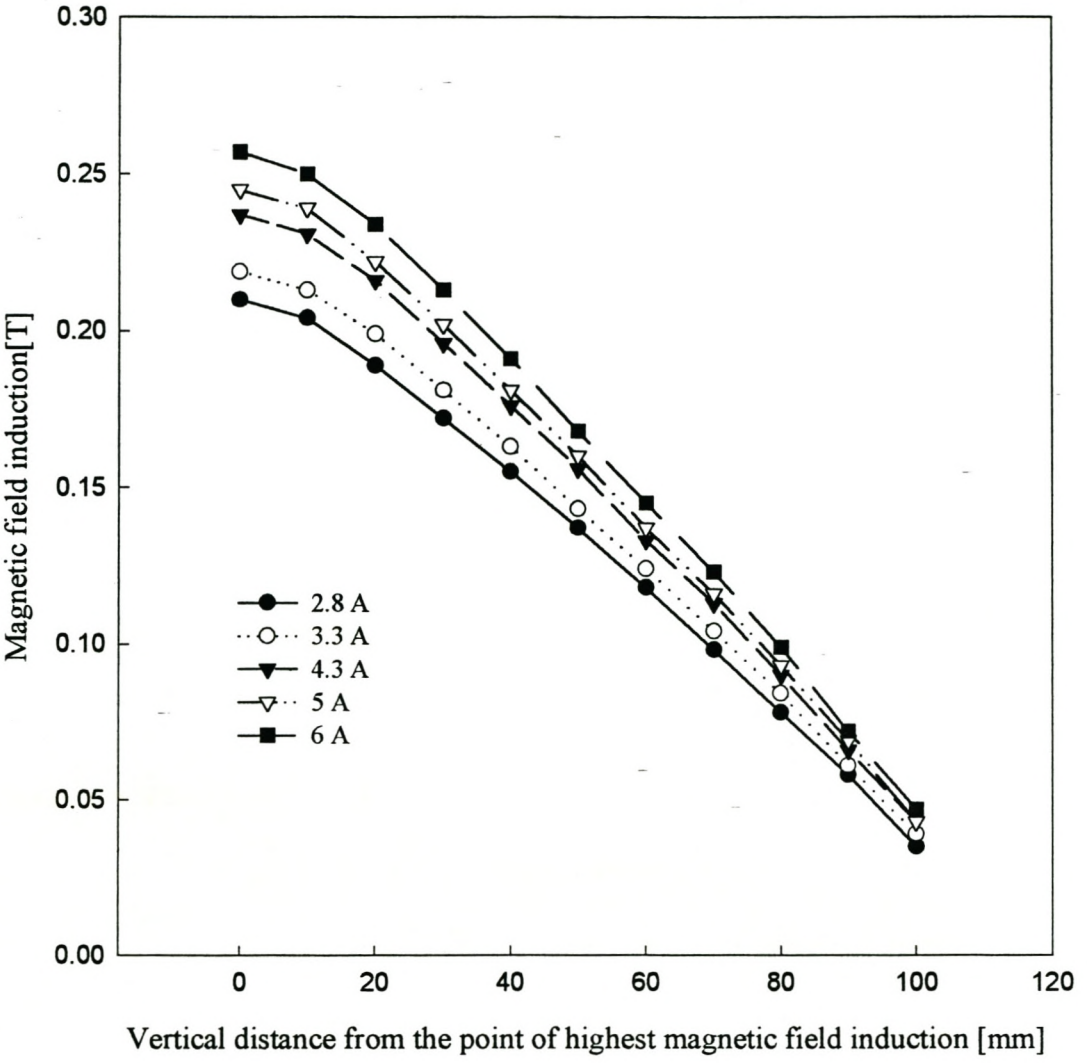

Figure 5.1 Magnetic field measurements at different electrical currents

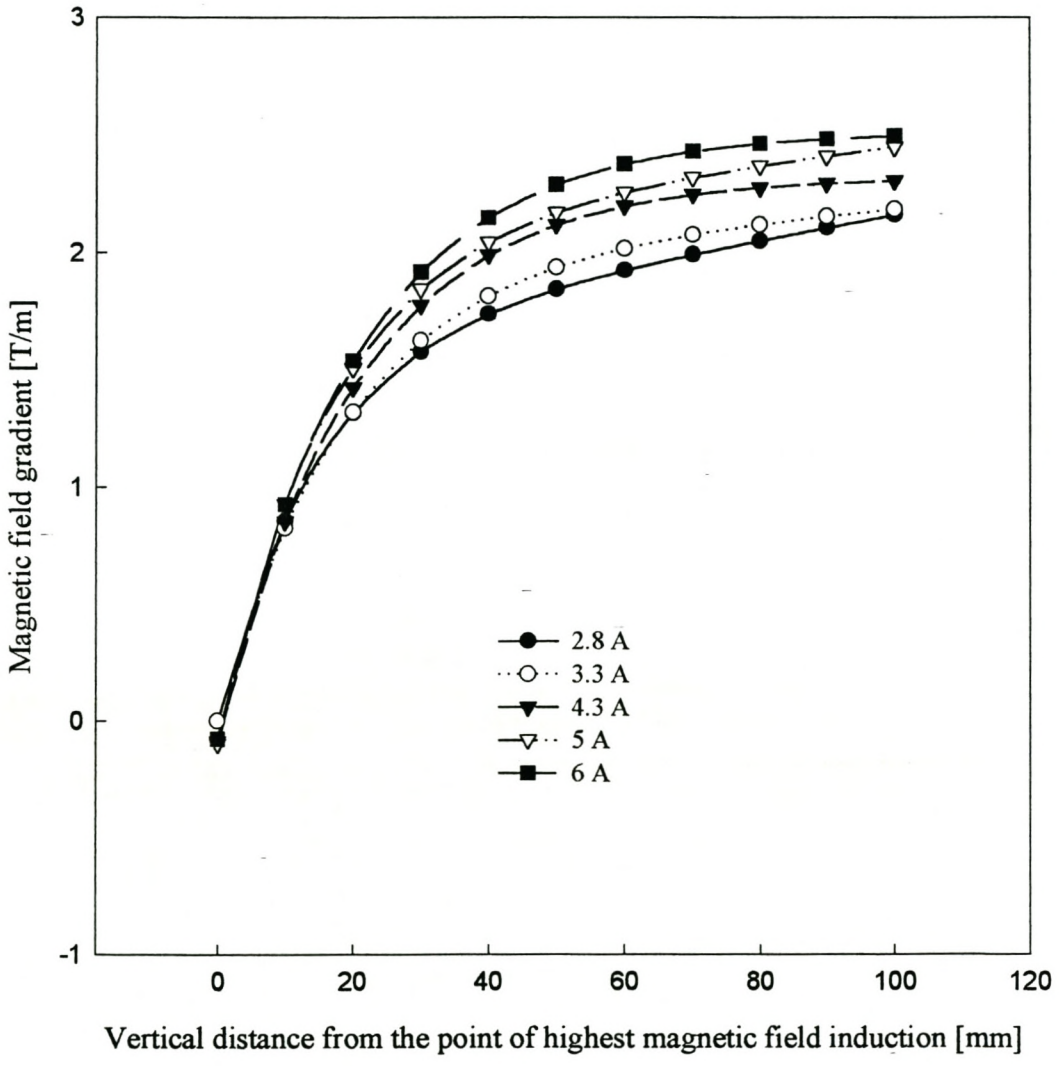

Figure 5.2 Magnetic field gradient measurements at different electrical currents

The magnetic field gradient increases from the point of highest magnetic field induction up to 40 mm. Beyond this point, the increase in the magnetic field gradient is generally negligible (for electrical currents used) for a similar increase in the vertical distance. As described in Chapter 2, it is critical to generate a constant apparent density in the FHS separation volume for efficient material separation. If the separator is operated with ferrofluids at saturation magnetisation, for constant apparent density, the magnetic field gradient should be constant (equation 2.8). This means that the ferrofluid apparent density is not constant up to 40 mm from the point of highest magnetic field induction and is nearly constant thereafter. The non-constancy in the magnetic field gradient might be due to the following:

- Inaccurate design or manufacture of the pole tips
- The Hall probe not in a correct position. For accurate measurements, the Hall probe should be equidistant from both pole tips along the vertical.
- The probe not properly aligned. The probe should be perpendicular to the magnetic flux along the vertical.

As shown in Chapter 3, Table 3.2, separation is not carried out at saturation magnetisation of the ferrofluid, which means that there is a slight variation in the apparent density in the working volume. It was also found that the magnetic field gradient increases with the increase in electrical current, which implies that high apparent densities can be achieved at high currents using the same density ferrofluid. This is particularly important for high-density separation such as discriminating lead from gold.

5.3 Separation Results

5.3.1 FHS Tromp Curve

The FHS Tromp curve is shown in Figure 5.3. It was found that the density difference distinguishable by the separator is 30 kg/m^3 or better, using 2 mm density tracers. This was achieved by separating 4440 kg/m^3 and 4470 kg/m^3 density tracers, with 100 % efficiency.

It can be deduced from the Tromp curve that the Ep is better than 0.008. This Ep is two and half times better than that obtained from a cyclone, which is usually 0.02. This implies that there is less misplacement of the near density material in ferrohydrostatic separation when compared with dense medium cyclones. When the FHS is used in diamond recovery processes, the cut-point density can be set close to the diamond density.

This leads to reduced mass of gangue material in the diamond concentrate. A high-grade diamond concentrate can be sorted faster than a conventional lower-grade diamond concentrate. This also reduces the security risks in diamond handling, as the number of personnel required in the sorthouse is reduced.

5.3.2 Separation as a Function of Feed rate

The effect of feed rate on separation efficiency is shown in Figures 5.4 to 5.8.

It can be seen from Figures 5.4 to 5.6 (2 mm: 3150 kg/m^3, 2 mm: 3400 kg/m^3, 4 mm: 3350 kg/m^3) that the separation efficiency is dependent on feed rate. This is due partly to an increase in the interaction of particles in the separator; the sinking particles collide with the particles that are floating and change their trajectory path. In addition, an increase in feed rate shortens the residence time for separation in the fluid pool, hence an increase in particle misplacement is observed.

The separation efficiency is also influenced by the density difference of the particles to be separated. It is poor when close density particles are to be separated as opposed to when the density difference is wide. It was found that the separation of 2700 kg/m^3 and 3530 kg/m^3 density tracers at a cut-point density of 3150 kg/m^3 (set using 2 mm tracers: Figure 5.4) was independent of the feed rate tested (0 to 22 kg/h). All tracers reported to their correct fractions, float and sink, for 2700 kg/m^3 and 3530 kg/m^3 density tracers respectively. This is due to the high upward force on the 2700 kg/m^3 density tracers and the resultant downward force on the 3530 kg/m^3, which sink immediately when they enter the ferrofluid pool.

For 3100 kg/m^3 and 3200 kg/m^3 density tracers, there was pronounced misplacement at very low feed rates less than 5 kg/h. The behavior is due to the close densities of 3100 kg/m^3 and 3200 kg/m^3 to the cut-point density (3150 kg/m^3). The buoyancy forces on 3100 kg/m^3 density tracers are lower than that on 2700 kg/m^3 and the downward forces on 3200 kg/m^3 are lower than that on 3530 kg/m^3. The cut-point density of 3150 kg/m^3 was set using 3100 kg/m^3 and 3200 kg/m^3 density tracers. This implies that the exact cut-point density can be close to 3100 kg/m^3 or 3200 kg/m^3. The misplacement is also enhanced by the limited accuracy of density tracers, which is ±30 kg/m^3. Taking the accuracy of density tracers into account, the density of 3100 kg/m^3 tracers could be 3130 kg/m^3, which overlaps with the possible cut-point density. The density of 3200 kg/m^3 density tracers could be 3170 kg/m^3, which also overlaps with the possible cut-point density.

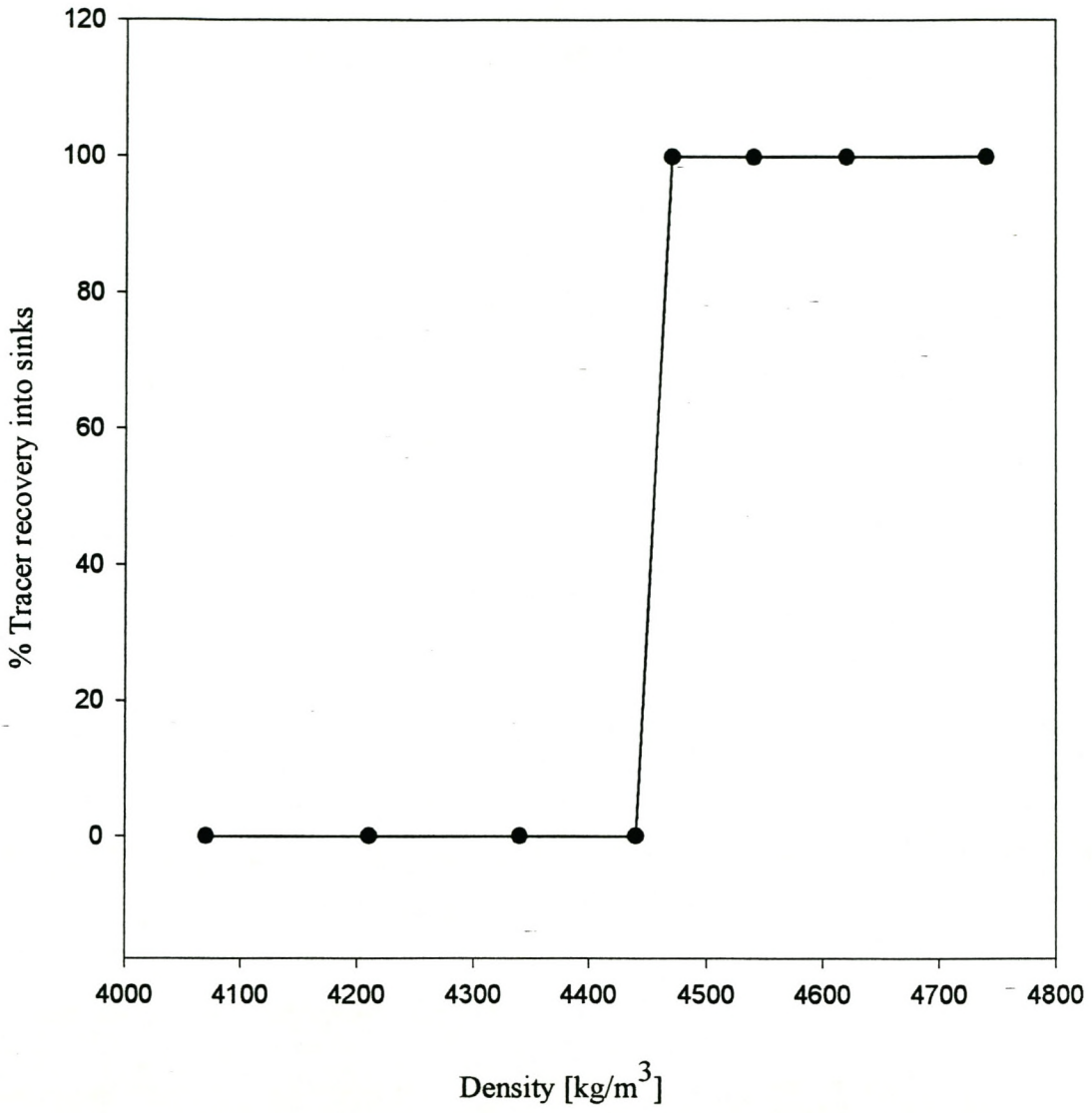

Figure 5.3 FHS Tromp Curve using 2 mm tracers at a cut-point density of 4450 kg/m^3

The separation efficiency as a function of feed rate is also dependent on the particle size as indicated by Figures 5.5 and 5.6. The 4 mm density tracers show a higher misplacement to the sink fraction at high feed rate as compared to 2 mm tracers. This is due to the lower apparent densities in the lower portion of the separation chamber as shown in Figure 5.2. Larger particles follow a deeper trajectory than small particles, hence reach the lower density regions and can potentially discharge as sink product. Even if these large tracers do not reach the lower density region, they might not have enough time to float due to the limited residence time.

Figure 5.7 shows the feed rate experiments for gravel (-1.00+0.85 mm). The percentage recovery into the sinks decreases slightly from 0.6 kg/h to 4.3 kg/h. This may due to the reduced residence time resulting in flaky-shaped particles floating. Above 4.3 kg/h, the recovery into the sinks remains constant up to 36 kg/h and then increases significantly (see Figure 5.7). This increase might be due to the increase in velocity of the feed material as it enters the ferrofluid pool coupled with a large increase in the volume of the feed material leading to increased interaction of material in the ferrofluid pool. Due to the high momentum, the particles reach the low-density zone and sink, or the particles do not have enough time to float as a result of the limited length of the separation chamber. The maximum feed rate is 36 kg/h for the sample treated.

The feed rate test graph (Figure 5.8) for the gravel size –0.5+0.3 mm indicates that there is a slight decrease in recovery into the sinks when the feed rate is slightly greater than 1.4 kg/h. It remains constant up to a feed rate of 6.2 kg/h. When the feed rate is greater than 6.2 kg/h, in contrast to Figure 5.7, there is a sharp decrease in the recovery into sinks. This decrease is due to the reduced residence time of gravel in the separation chamber. Small particles experience a high hydrodynamic drag as shown in Chapter 3 and thus follow a shallow trajectory. This means that they reach the splitter position before reporting to the correct sink product. The increase in momentum of the feed material further reduces the residence time hence an increase in the float product. The optimum feed rate for the fine particle size material treated is 6.2 kg/h.

It can be concluded from Figures 5.7 and 5.8 that coarse material will tend to sink at high feed rate while fines will tend to float.

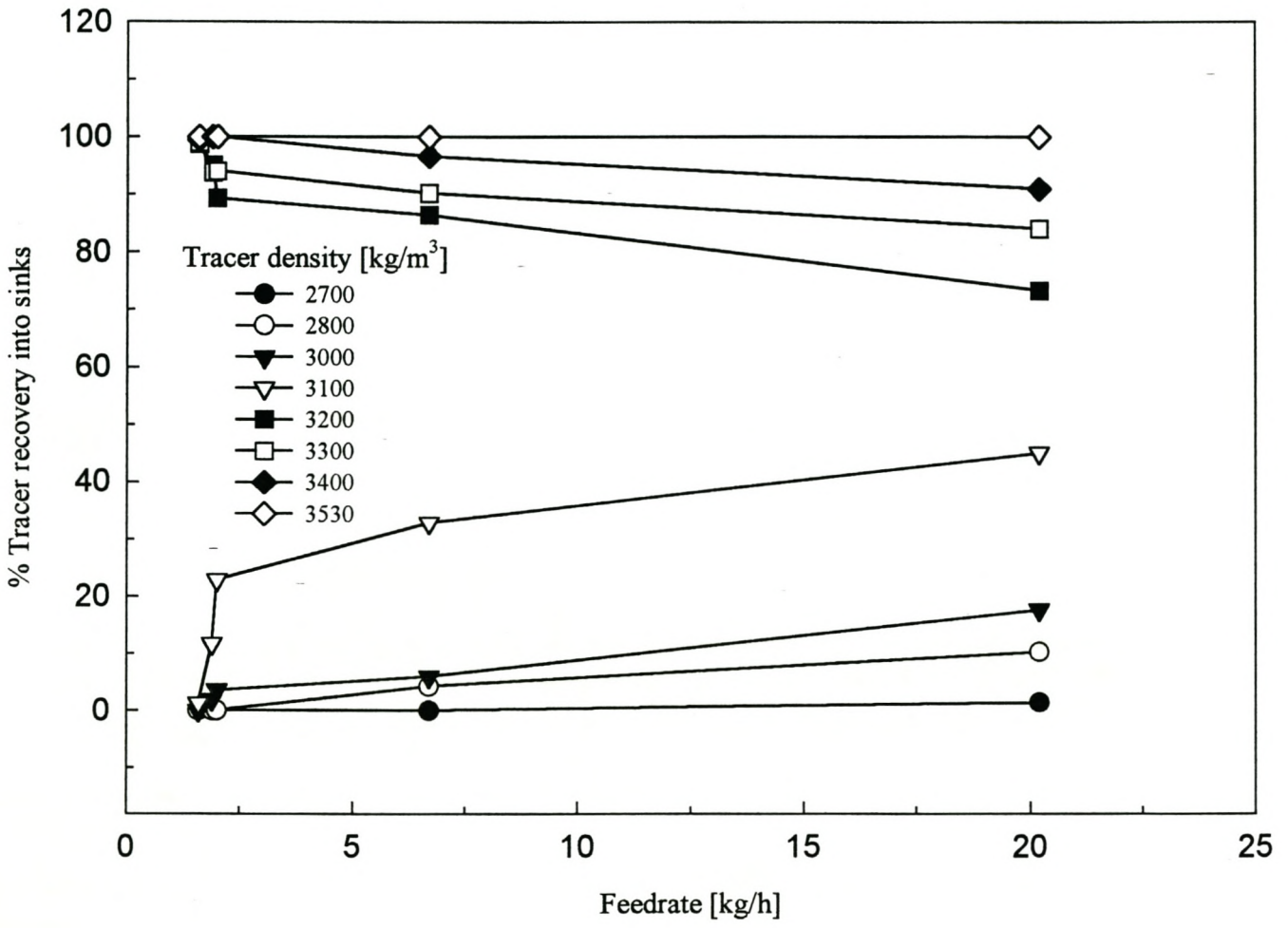

Figure 5.4 Separation as a function of feedrate using 2 mm tracers at a cut-point density of 3150 kg/m^3.

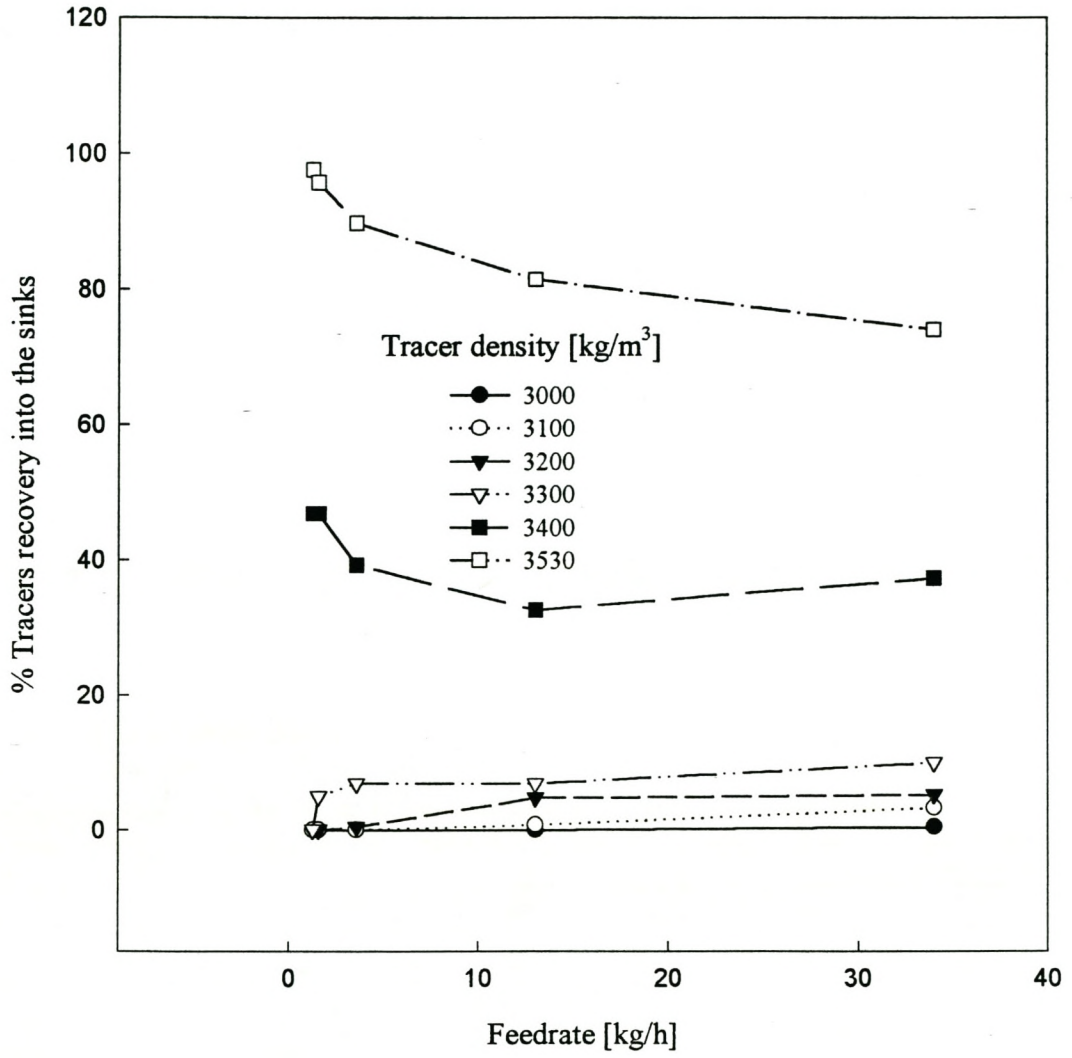

Figure 5.5 Separation as a function of feedrate using 2 mm tracers at a cut-point density of 3400 kg/m^3.

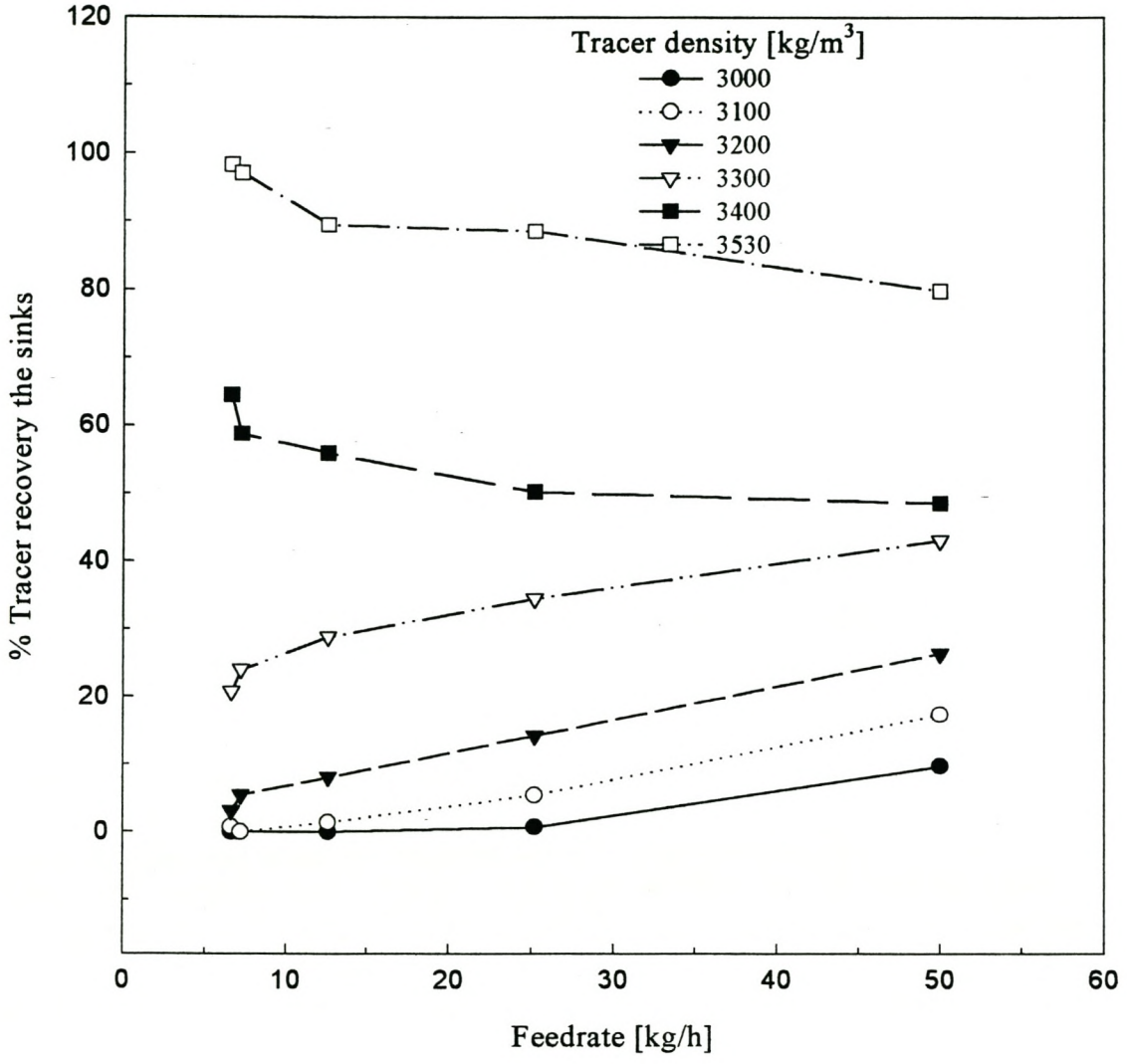

Figure 5.6 Separation as a function of feedrate using 4 mm tracers at a cut-point density of 3350 kg/m^3.

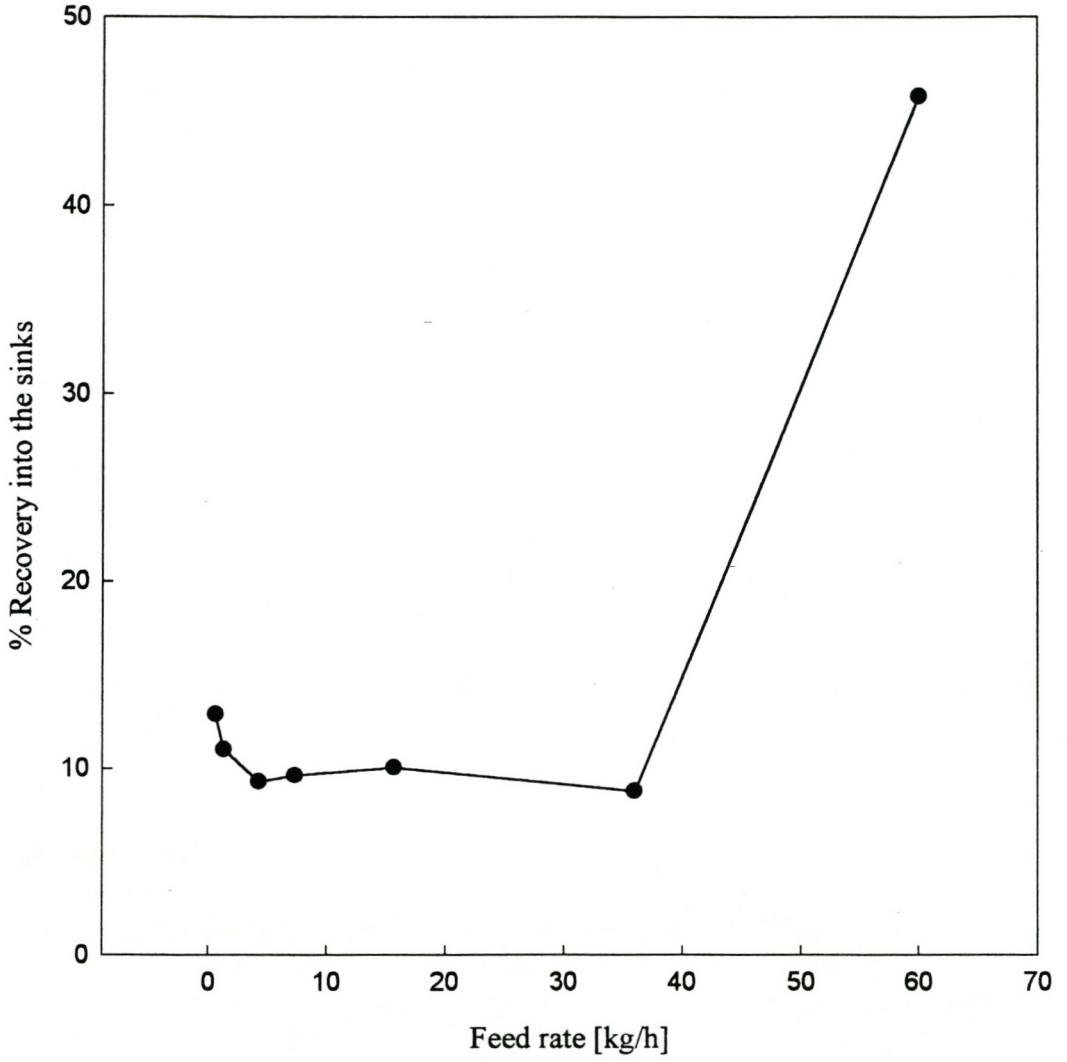

Figure 5.7 Gravel separation as a function of feed rate. The particle size treated was -1.0+0.85 mm at a cut-point density of 3150 kg/m^3.

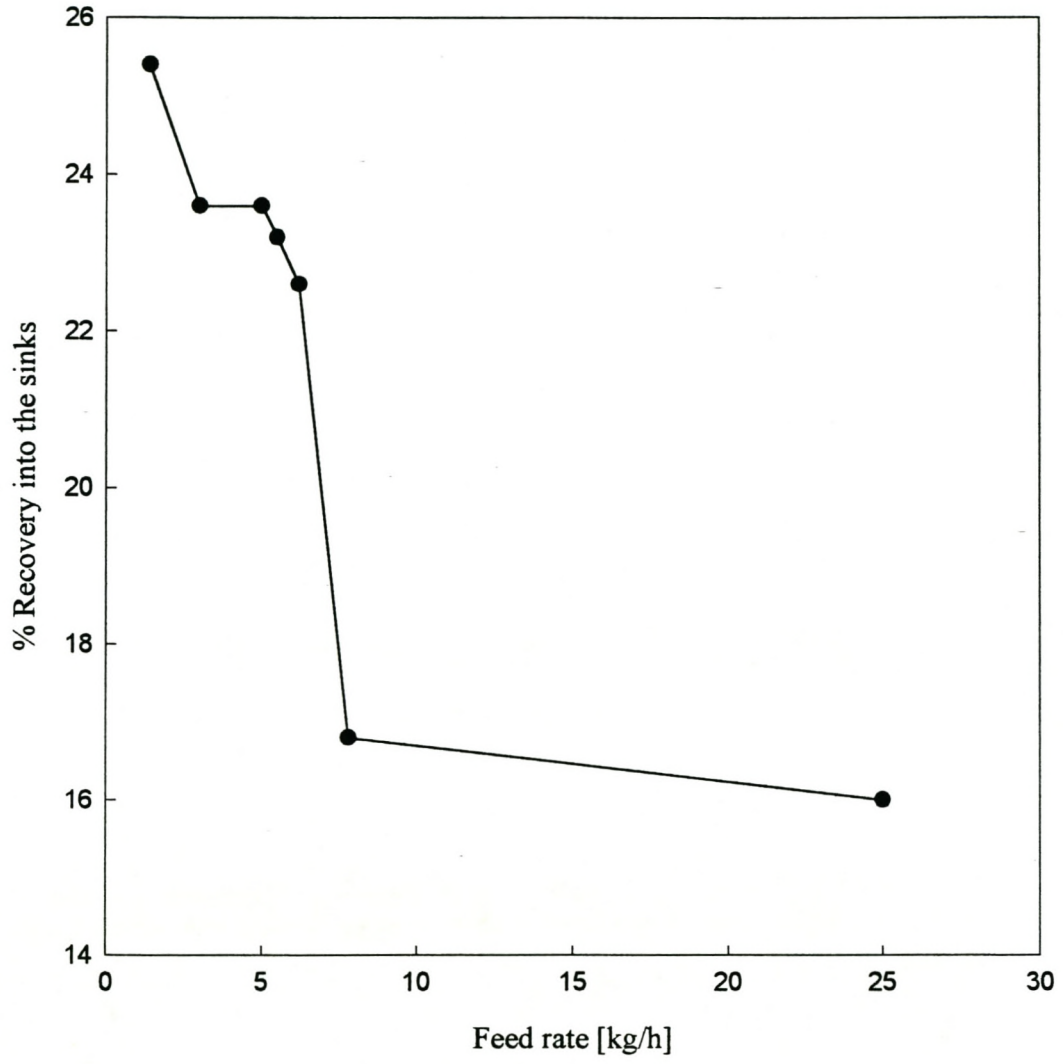

Figure 5.8 Gravel separation as a function of feed rate. The particle size treated was -0.5+0.3 mm at a cut-point density of 3150 kg/m^3.

5.3.3 Separation as a Function of Particle Size

Separation as a function of particle size at a cut point density of 3350 kg/m^3 is shown in Figure 5.9.

It was observed that separation efficiency decreased with an increase in particle size. Some of the 4 mm and 6 mm 3200 kg/m^3 and 3300 kg/m^3 density tracers sank at a cut-point density of 3350 kg/m^3 while all 8 mm and 10 mm 3300 kg/m^3 density tracers sank at the same cut-point density. It was also found that some of the 6 mm 3100 kg/m^3 density tracers and 8 mm and 10 mm 3000 kg/m^3 density tracers were sinking at 3350 kg/m^3. This shows that coarse tracers tend to sink in the FHS when small tracers are used to set the cut point density. This can be ascribed to the fact that coarser particles follow a deeper and longer trajectory in the separator than smaller ones. Due to the finite separation length (195 mm), the coarse tracers reach the splitter position before reporting to the correct float product for collection.

The sinking of coarse particles is also enhanced by the fact that the ferrofluid apparent density, as described in Section 5.2.2, is not constant at the bottom part of the separation chamber (about 30 mm from the bottom). Coarse particles reach the lower level, where they experience a lower cut-point density and thus sink even though their density is lower than the cut-point density. It can be concluded that it is important to separate the feed into the separator into narrow size ranges.

It was found that it is feasible to treat 0.5 mm to 6 mm particles if they have 53 kg/m^3 density difference (see Figure 5.9). DebTech has built a two-stage separator (two separators in series). These separators can treat a wide size range of material at the expense of an increase in yield (material recovered with the sought minerals). An example for this might be a double stage separator with the first chamber set at a cut-point density of 3600 kg/m^3 and the second chamber at 3350 kg/m^3 to treat –12+1 mm particles. For efficient recovery of all the sought materials between 3350 kg/m^3 and 3600 kg/m^3, 1 mm tracers should be used to set the cut-point density of the second chamber while 12 mm tracers should be used to set that of the first. If a smaller tracer reports to the sink product so will be a big tracer of the same density and also if a large tracer floats so will be the small one of similar density.

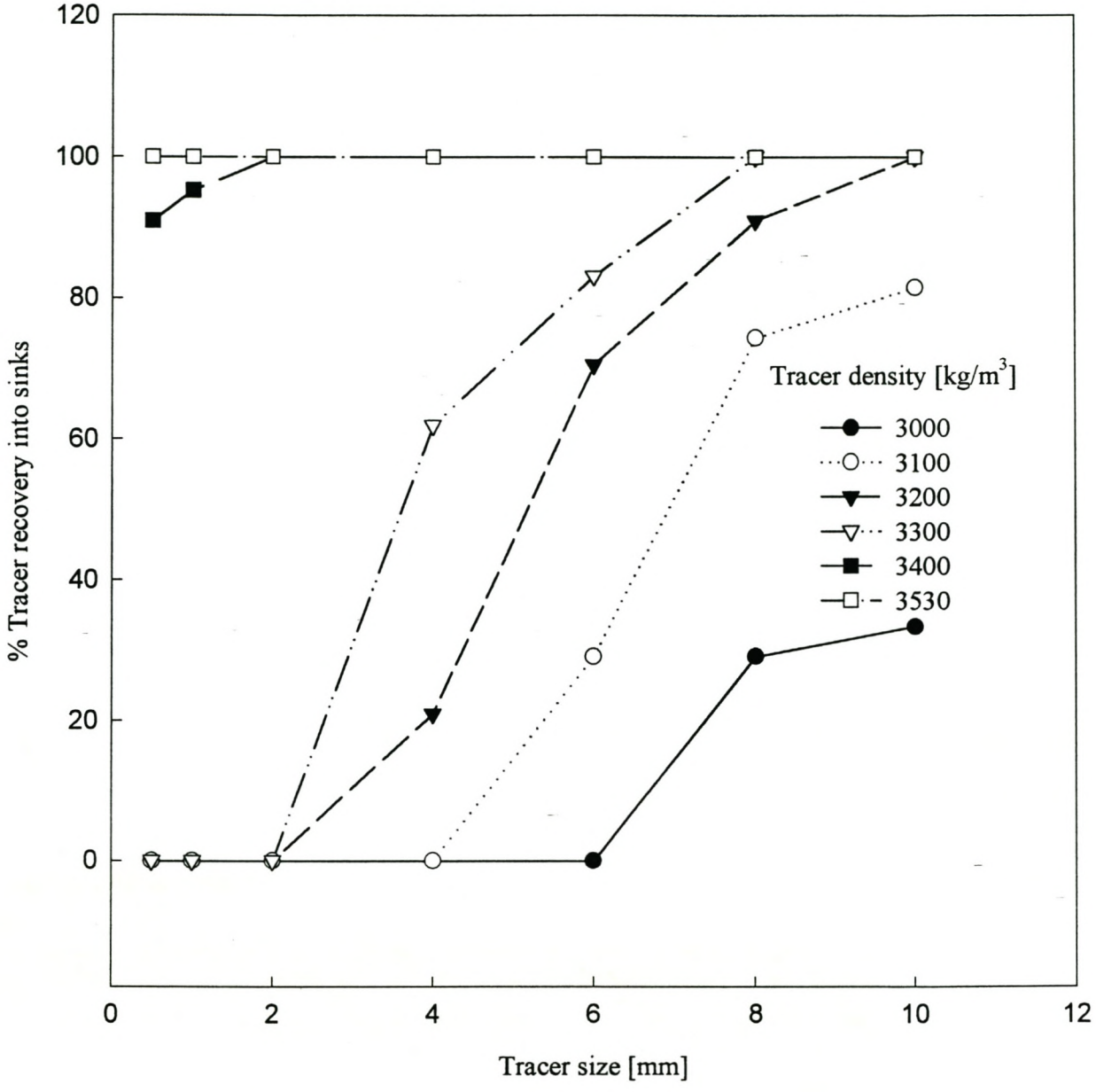

Figure 5.9 Separation as a function of particle size. Two-mm tracers used to set cut-point density at 3350 kg/m^3

5.3.4 Separation as a Function of Fluid Level

The dependence of separation efficiency on ferrofluid level is shown in Figures 5.10 and 5.11.

It can be seen from Figure 5.10 that the separation efficiency deteriorates with a decrease in the ferrofluid level. This is evident for ferrofluid level less than 87 mm (7 mm from the maximum height). The effect of ferrofluid level is also enhanced by the density difference of the density tracers to be separated. The effect is more pronounced for tracers with density close to the cut-point density and negligible for tracers with relatively large density differences. From Figure 5.10, it can be seen that 3400 kg/m^3 density tracers were affected by the lowering of ferrofluid height at a higher level than 3300 kg/m^3.

The dependence of separation efficiency on ferrofluid level is due to the trajectory followed by the tracers in the separator. As the level of ferrofluid drops, the tracers that floated at a higher level reach the splitter position before reporting to the correct float product. As described in Section 5.3.3, when a tracer finds itself in a low-density zone, it will sink. For very fine separations, e.g., 3400 kg/m^3 and 3530 kg/m^3, it is imperative to maintain the ferrofluid level within 7 mm from the maximum but this control can be relaxed for wider density separations. As can be seen from Figure 5.10, the effect of ferrofluid level only becomes a concern when it has been reduced by more than 15 mm when separating 3530 kg/m^3 and 3000 kg/m^3 density tracers.

When Figure 5.10 is compared with Figure 5.11, it can be seen that the dependence of separation efficiency on ferrofluid level is more pronounced for larger tracers. As described in detail in Section 5.3.3, coarse tracers, because of their weight, find themselves in a low-density region and thus are collected as a sink product irrespective of the fact that their densities are lower than the cut-point density. This implies that for this particular separator, it is important to control the level of ferrofluid within a narrow range (7 mm). It should be noted that the error of ±30 kg/m^3, on the density tracers, is more pronounced the larger tracers, and thus, increases misplacement of coarse tracers.

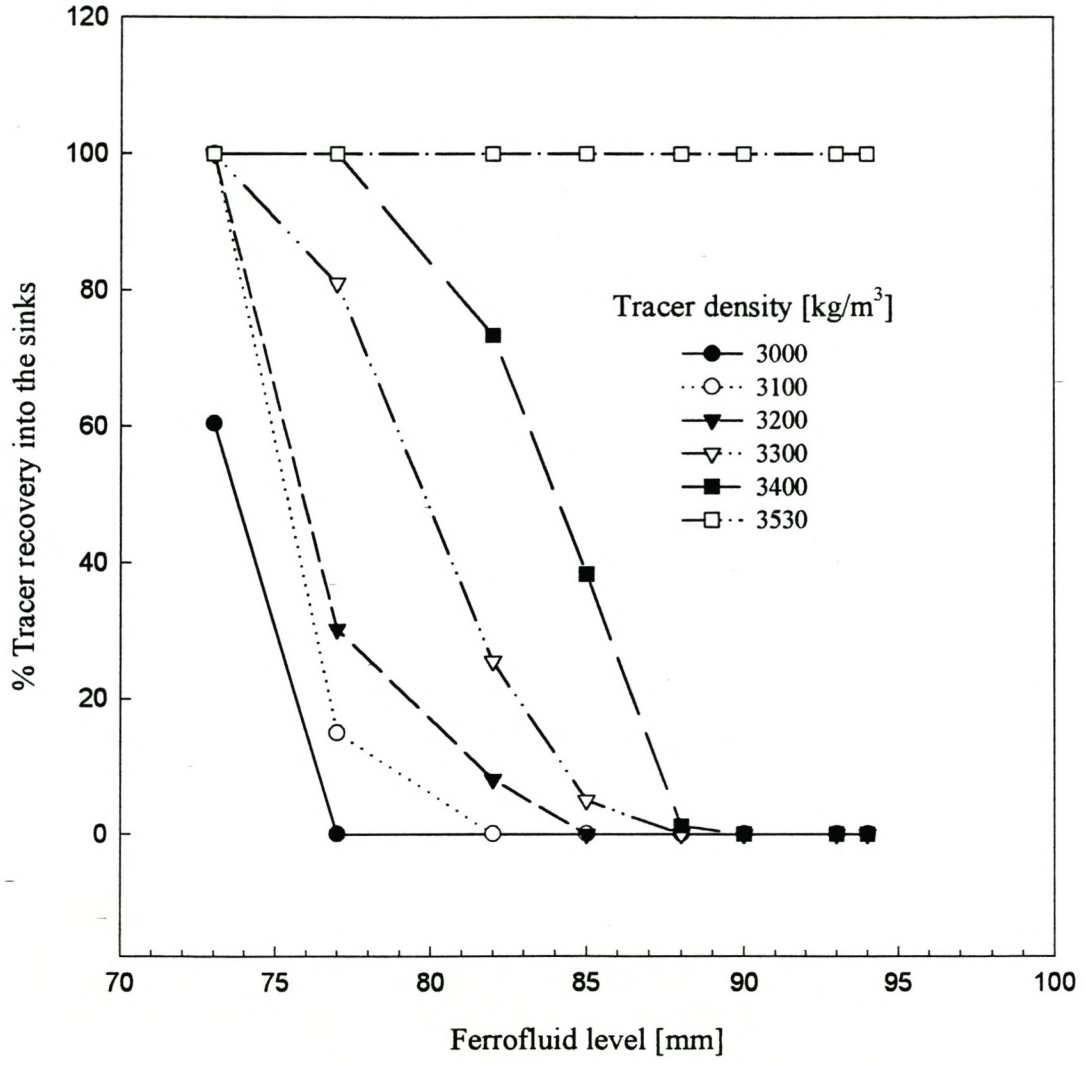

Figure 5.10 Separation as a function of fluid level using 2 mm tracers at a cut-point density of 3450 kg/m^3.

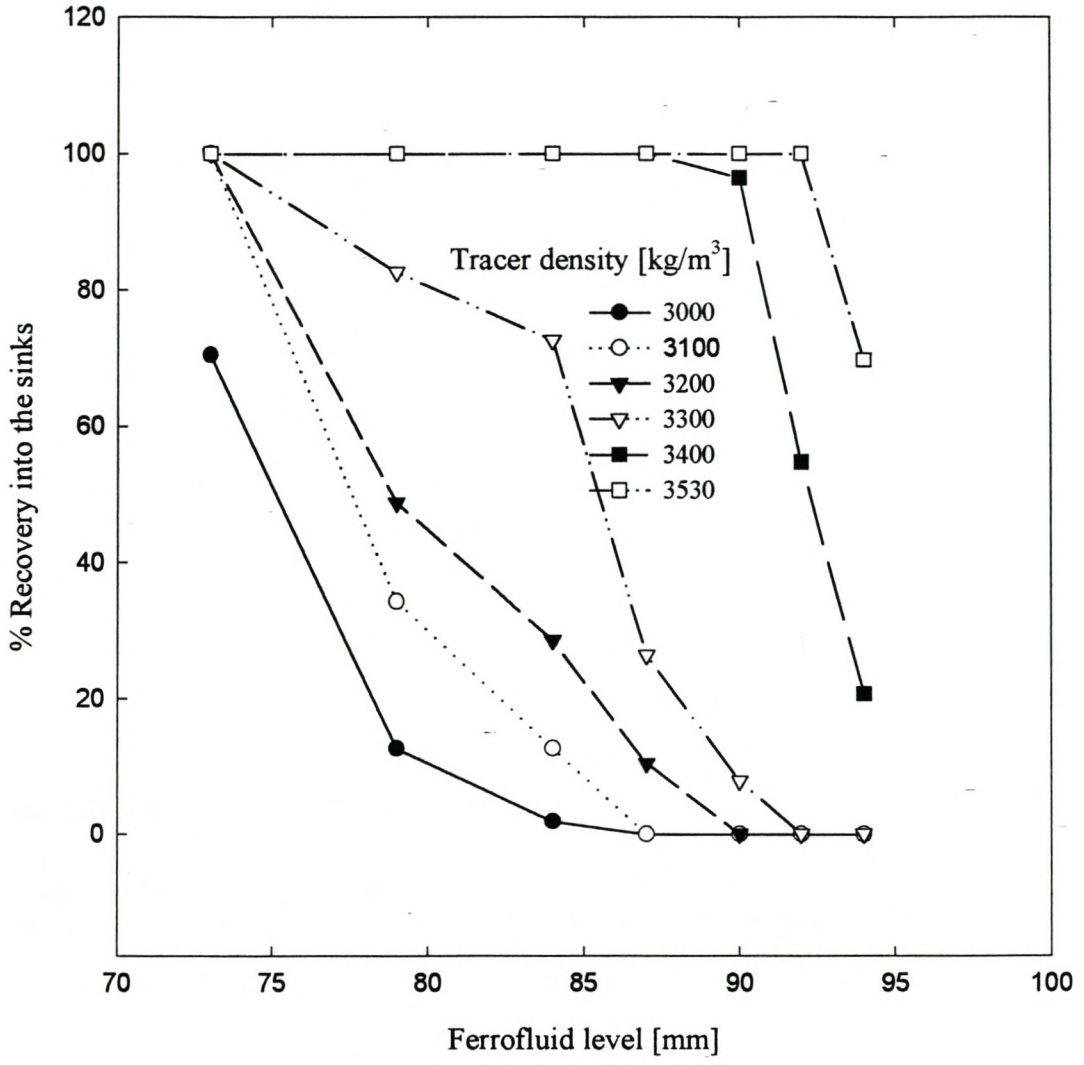

Figure 5.11 Separation as a function of ferrofluid level using 6 mm tracers at a cut-point density of 3450 kg/m^3

5.3.5 Separation as a Function of Density Distribution

The density distribution of 2 mm density tracers used is shown in Table 4.1 in Chapter 4 and the separation results at different cut-point densities are shown in Figure 5.12.

It was found that misplaced tracers have a density close to the cut-point density. This is due to the accuracy of density tracers (±30 kg/m^3) described in detail in Section 5.3.2. This can also be ascribed to the short residence time spent in the separation pool and the ways these close density tracers hit the splitter that separates float and sink product. If the tracers hit the splitter, with the greater volume of tracer exposed to the float side, they are likely to float and will sink when the greater volume is exposed to the sink product.

The other effect not necessarily appreciated in the above analysis is that a wide density distribution could lead to interference of a particle's motion in the separator, i.e. many particles moving to the floats could entrain particles trying to report to the sinks.

5.3.6 The Effective Cut-point Density of Different Size Tracers

The effective cut-point density of different size tracers is shown in Figure 5.13.

It was found that the effective cut-point density generally decreases with an increase in the tracer size. As detailed in Section 5.3.3, large tracers, due to their weight, follow a deeper and longer trajectory than small ones. Coarse tracers may also find themselves in a low apparent density zone and thus report as sink products. It can also be seen (from Figure 5.13) that the difference in the effective cut-point density of different size tracers is more pronounced for low cut-point densities. It was found that at a cut-point density of 3450 kg/m^3, 0.85 mm to 6 mm tracers can be treated together as one batch whilst at 3150 kg/m^3 only 2 mm to 4 mm can be treated together as one batch. The increase in the particle size range that can be treated with an increase in cut-point density might be due to the increase in ferrofluid viscosity caused by an increase in the magnetic field. This is compounded by the fact that 2 mm tracers were used to set the cut-point density as opposed to coarse ones, for instance 6 mm.

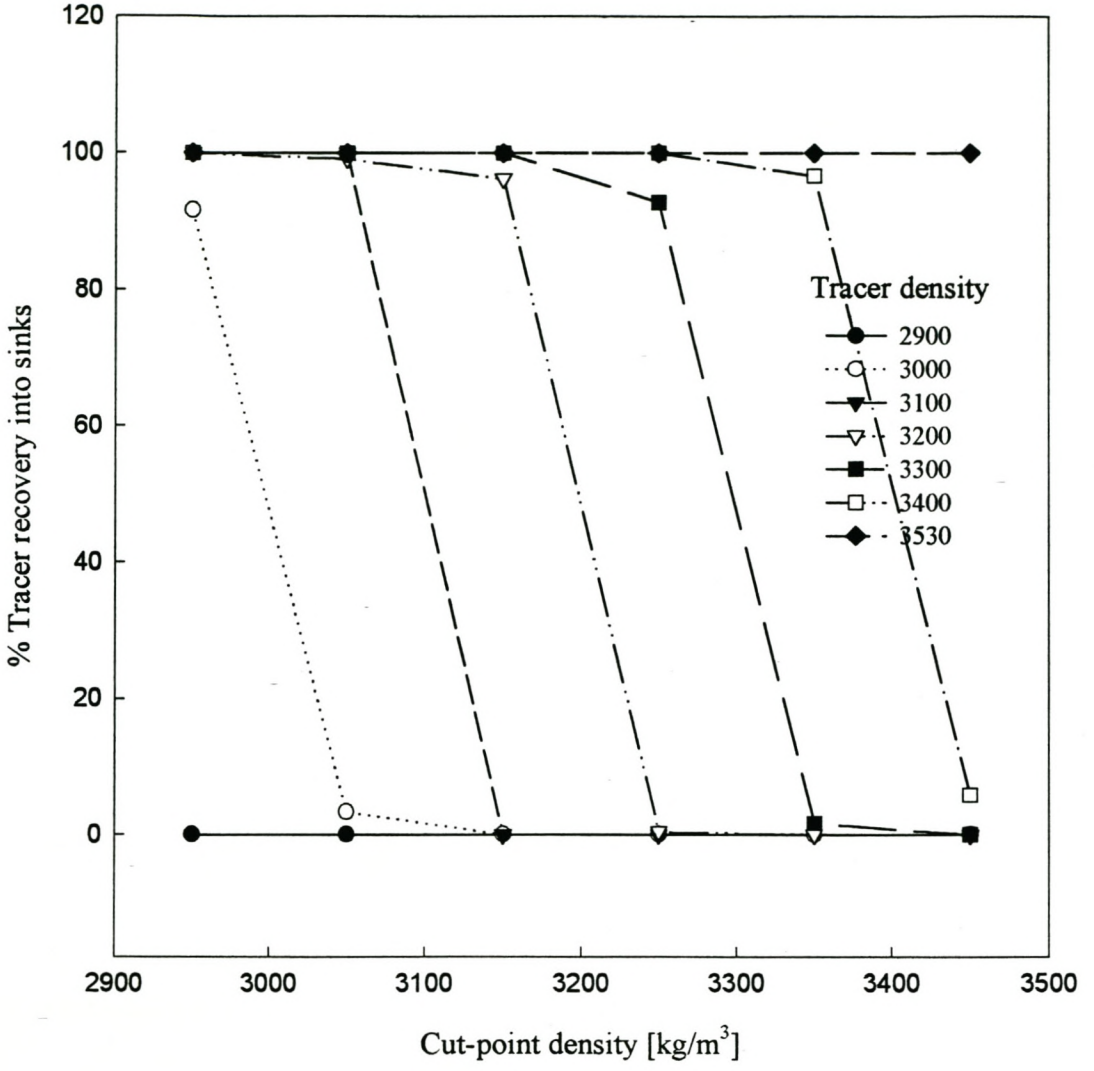

Figure 5.12 Separation as a function of density distribution using 2 mm density tracers

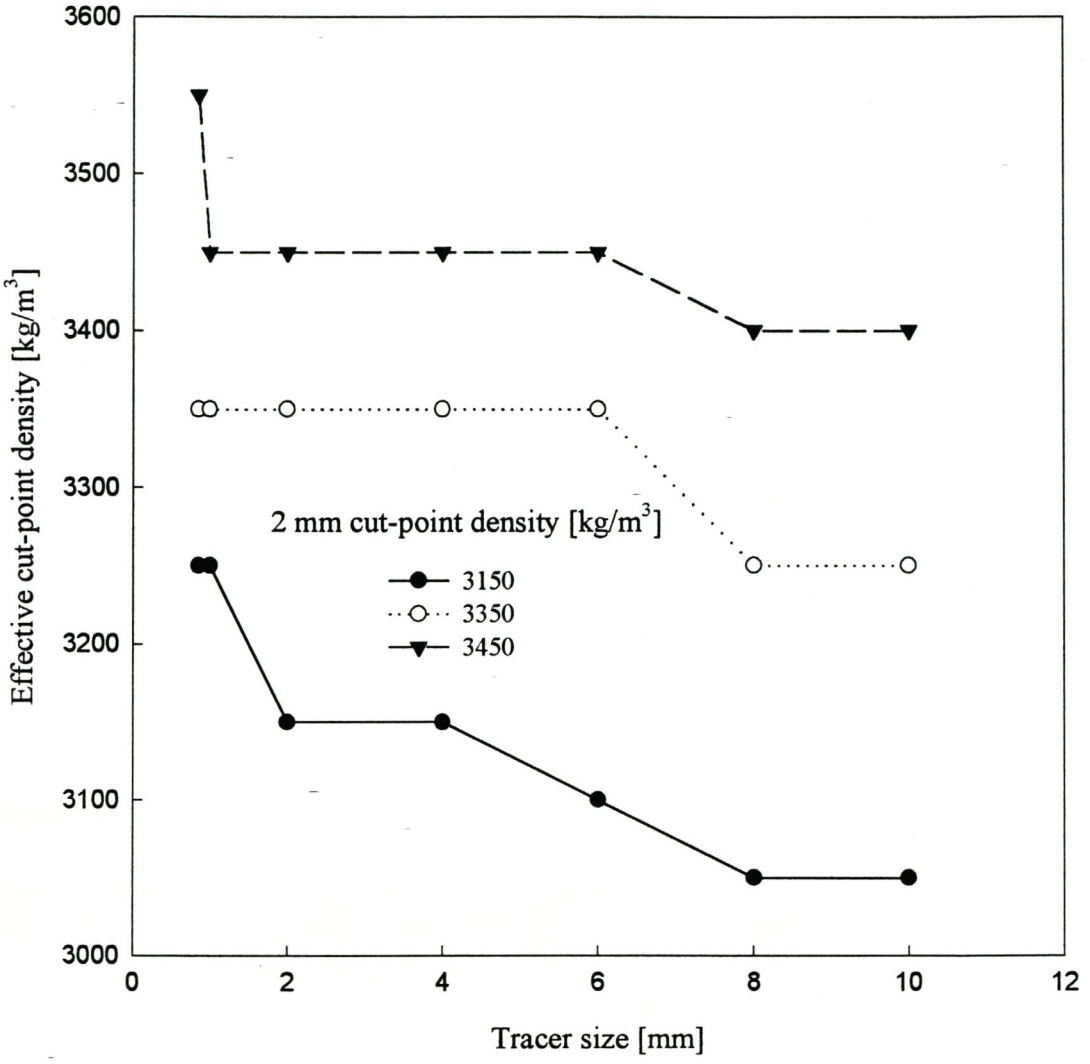

Figure 5.13 Effective density of different size tracers. Tracer size used to set cut-point density was 2 mm

5.3.7 Separation as a Function of Moisture Content

Material separation as a function of material moisture content is shown in Figure 5.14.

For fine particles, smaller than 2.8 mm, it was found that separation efficiency is highly dependent on the moisture content. For –12+8 mm and –8+4 mm particles, the percent recovery into sinks is almost constant for the varying material moisture content. In contrast for –2.8 mm material, there is a significant decrease in the amount of material recovered into the sink product. This is due to the immiscibility of water coating the particles and ferrofluid. When a small particle is completely surrounded by water, water reduces the wettability of the particle and causes it to float. These water-coated small particles have difficulty in breaking ferrofluid surface tension. With coarse particles of the same density, because of their weight, they break the surface tension and once the particle / water is in the ferrofluid pool, the particle might sink or float depending on the apparent density of the combined particle / water density.

Also, when a coarse particle enters the ferrofluid pool, water coating the particle is removed (from the particle) and the particle is then recovered in the correct fraction. This was evident as some water droplets were observed floating on the ferrofluid surface.

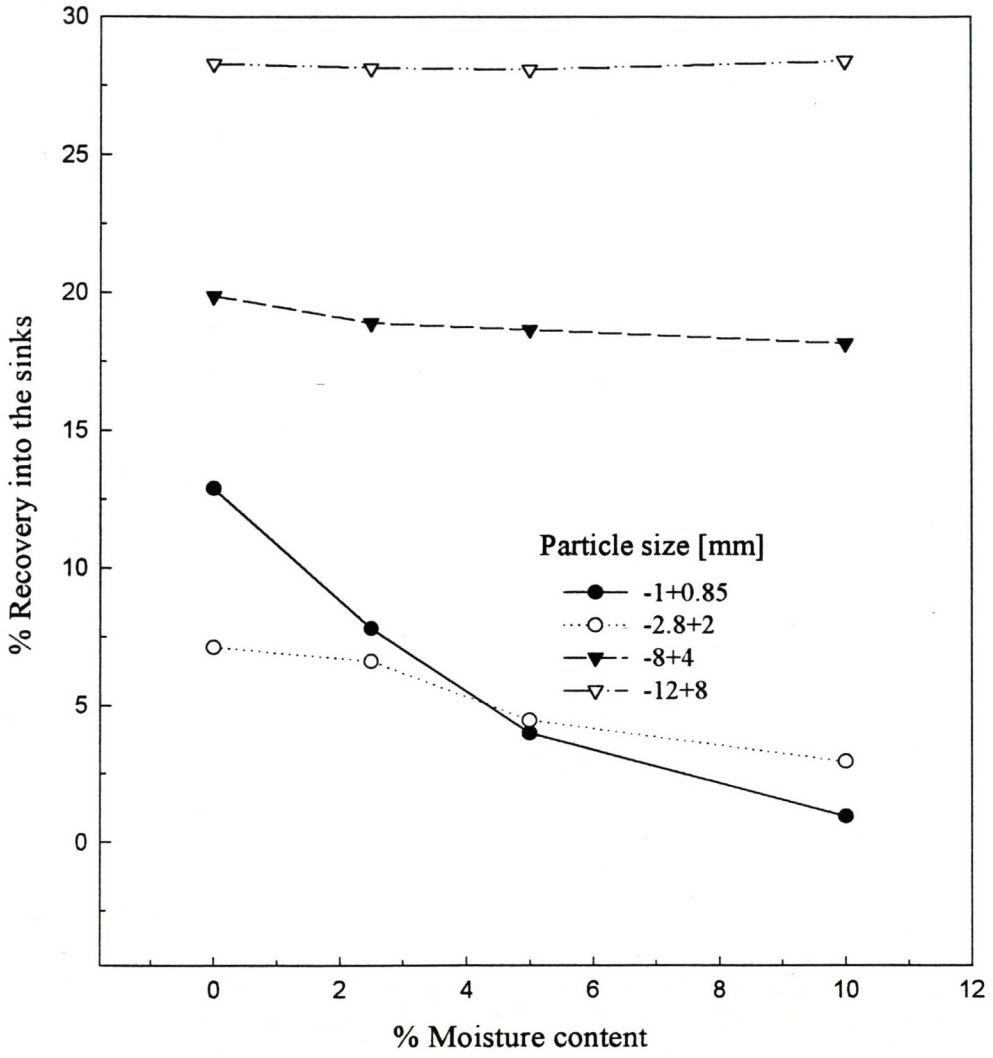

Figure 5.14 Separation as a function of moisture content. Premier Mine gravel was used for the test at 3350 kg/m^3.

5.3.8 Comparison of FHS with Heavy Liquids

The sink and float products from the FHS separator at a cut-point density of 3250 kg/m^3 were treated in heavy liquids and the results from the heavy liquid are shown in Table 5.1.

Table 5.1 Heavy Liquid Tests on Density Fractions from FHS. The sample particle size was –0.5+0.3 mm.

FHS Fraction at a Cut-point Density of 3250 kg/m^3	% Misplaced Material	Heavy Liquid Cut-point Density [kg/m^3]
Floats 1	3.3	3300
Floats 2	3.1	3300
Sinks 1	1.7	3200
Sinks 2	1.9	3200

It was found that there was more misplaced material in the floats than in the sink products. This might be due to the following:

- The FHS cut-point density was set using tracers with a density difference of 100 kg/m^3. The cut-point density could be closer to the lower density tracer or to the upper density one while with heavy liquids the cut-point density is more accurate, +-10 kg/m^3, which is the accuracy of the hydrometer.
- Small particles and flaky shaped ones failing to break the surface tension of ferrofluid.
- The cut-point density might be higher for the particle size treated as the cut-point density was set using 2 mm tracers.
- Limited residence time of small particles in the separator due the hydrodynamic drag as explained in detail in Chapter 3.

This implies that it is important to design a separating system with a wetting stage prior to FHS separation. The wetting of particles can be accomplished by increasing the length of the poles and installing some agitation mechanism at the feed point. Treating them with a suitable surfactant that will make them wet easily in ferrofluid can also enhance the wetting of particles.

5.3.9 Viscosity of Different Ferrofluids and the Effect on Separation

The normalised viscosity measurements at shear rates of 300 s^{-1} and 1000 s^{-1} are shown in Figure 5.15.

It can be seen that the normalised values follow the same trend for both shear rates. It can also be seen that there is an increase in viscosity with an increase in ferrofluid density. This increase in viscosity might affect separation of small particles as described in detail in Chapter 3.

The results of a –1.0+0.3 mm sample treated at a cut-point density of 3900 kg/m^3 are shown in Table 5.2.

Table 5.2 Separation as a Function of Ferrofluid Density.

Density of Ferrofluid [kg/m^3]	Recovery into Sinks %
1.11	4.00
1.00	9.00
0.98	18.00
0.95	20.00

It was found that there was a decrease in the amount of sink product with an increase in the density of ferrofluid. This might be ascribed to an increase in viscosity of high-density ferrofluids. The effect of the hydrodynamic drag force is high for small particles and the residence time is limited due to the limited size of the separator (195 mm).

5.3.10 Comparison of Water-based with Kerosene-based Ferrofluids

The cut-point density that can be attained by different ferrofluids at different currents is shown in Figure 5.16.

It can be seen from Figure 5.16 that higher cut-point densities can be achieved using kerosene based ferrofluids at lower currents than water based ones. This is due to the low magnetisation of water-based ferrofluids. This implies that water based ferrofluids can only be used for low density separations e.g. coal preparation. It was also found that water based ferrofluids are non-homogeneous in the FHS. Due to the decrease in magnetic field along the vertical axis between the pole tips (see Appendix A), the density of water-based ferrofluids varies with the magnetic field as shown in Table 5.3. The density of water-based ferrofluid was high at the point of highest magnetic field and low at the surface. This was due to the magnetite particles being attracted to the region of highest magnetic field. These different density regions might affect selectivity of separation hence water-based ferrofluids should not be used for separating particles with narrow density differences (fine separation).

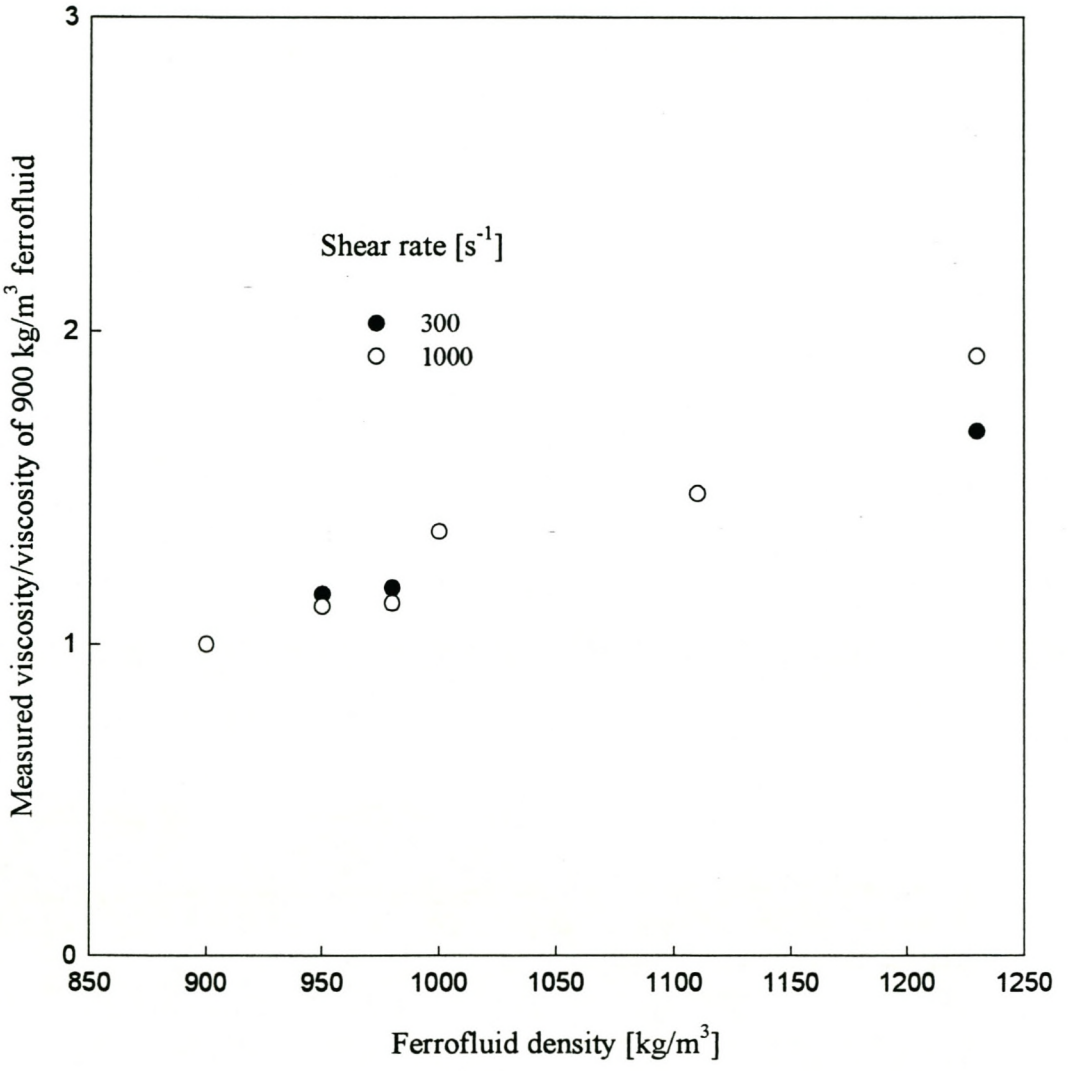

Figure 5.15 Viscosity measurements for different density ferrofluids

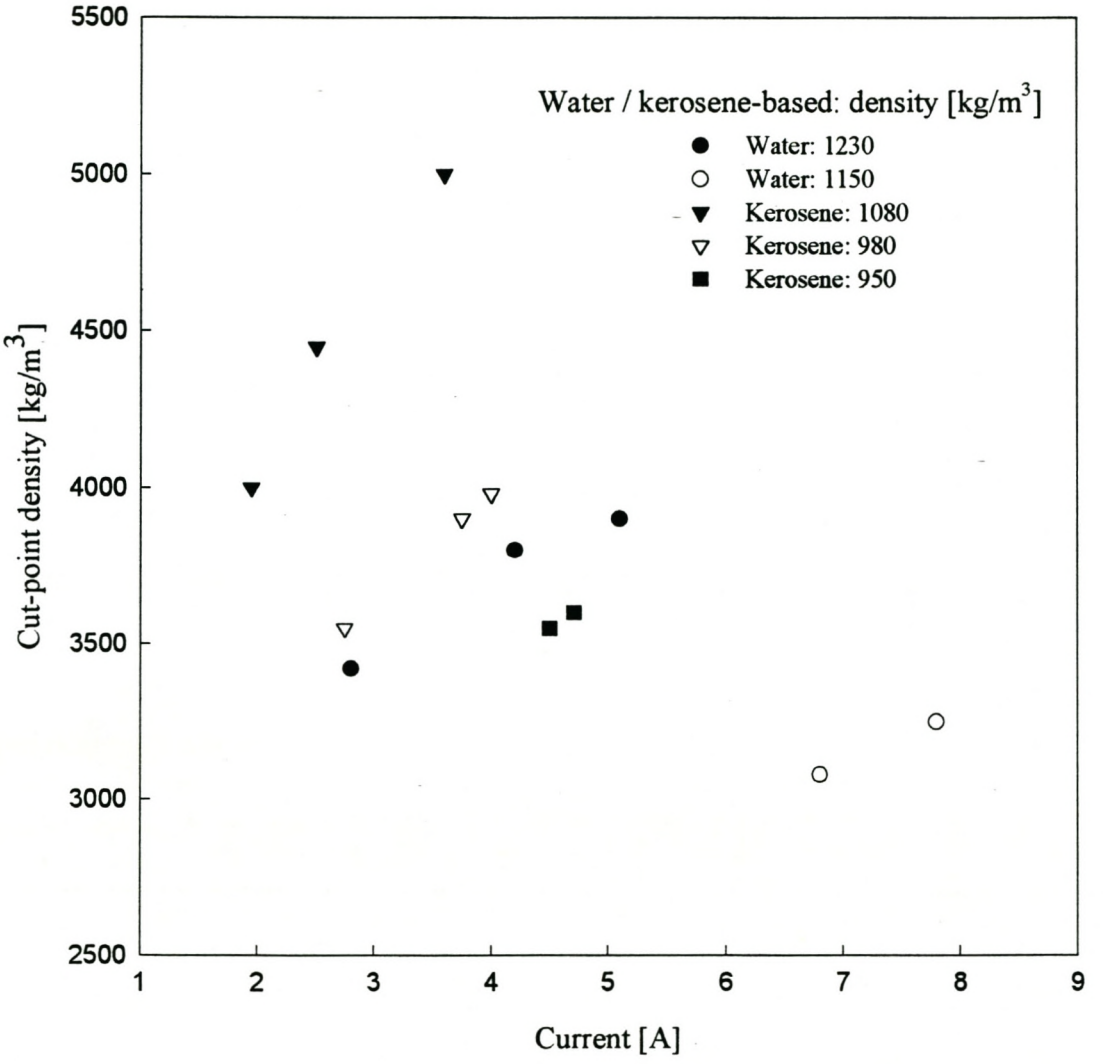

Figure 5.16 Cut-point density as a function of current. The cut-point density was determined using 2 mm tracers.

Table 5.3 Comparison of Water and Kerosene-based Ferrofluids in FHS.

Ferrofluid Base	Initial Density [kg/m^3]	Ferrofluid Density at Highest Magnetic Field Point [kg/m^3]	Ferrofluid Density at the Surface [kg/m^3]
Water	1150	1200	1130
Water	1050	1080	1030
Kerosene	980	980	980
Kerosene	950	950	950

5.4 Ferrofluid Recovery Results

5.4.1 Amount of Ferrofluid Drawn from the FHS

The amount of ferrofluid drawn by the products from the FHS mainly depends on the particle size of the material being treated and the density at which the FHS is operated as depicted in Figure 5.17.

It was found for –12+8 mm particles that more ferrofluid (162 kg per tonne of feed) was removed at a cut-point density of 2600 kg/m^3 than at 3250 kg/m^3 where only 23 kg per tonne of feed was drawn. This was due to the fact that the ferrofluid was just about to flow out of the separation chamber at 2600 kg/m^3. The magnetic field at 3250 kg/m^3 is higher and it attracted more ferrofluid back to the separator than that at 2600 kg/m^3. There was an increase in the amount of ferrofluid drawn with a decrease in particle size. This is due to an increase in surface area in small particles. At a cut-point density of 3250 kg/m^3, 164 kg of ferrofluid per tonne of feed was drawn by –1.0+0.85 mm particle size, while 23 kg of ferrofluid per tonne of feed were drawn for –12+8 mm at the same cut-point density.

The amount of ferrofluid, adsorbed by the particles after draining, was almost the same as that which remains attached after separation at high cut-point density and magnetic field. This implies that a rinse screen after the FHS (for ferrofluid to drain) might be necessary to reduce ferrofluid losses.

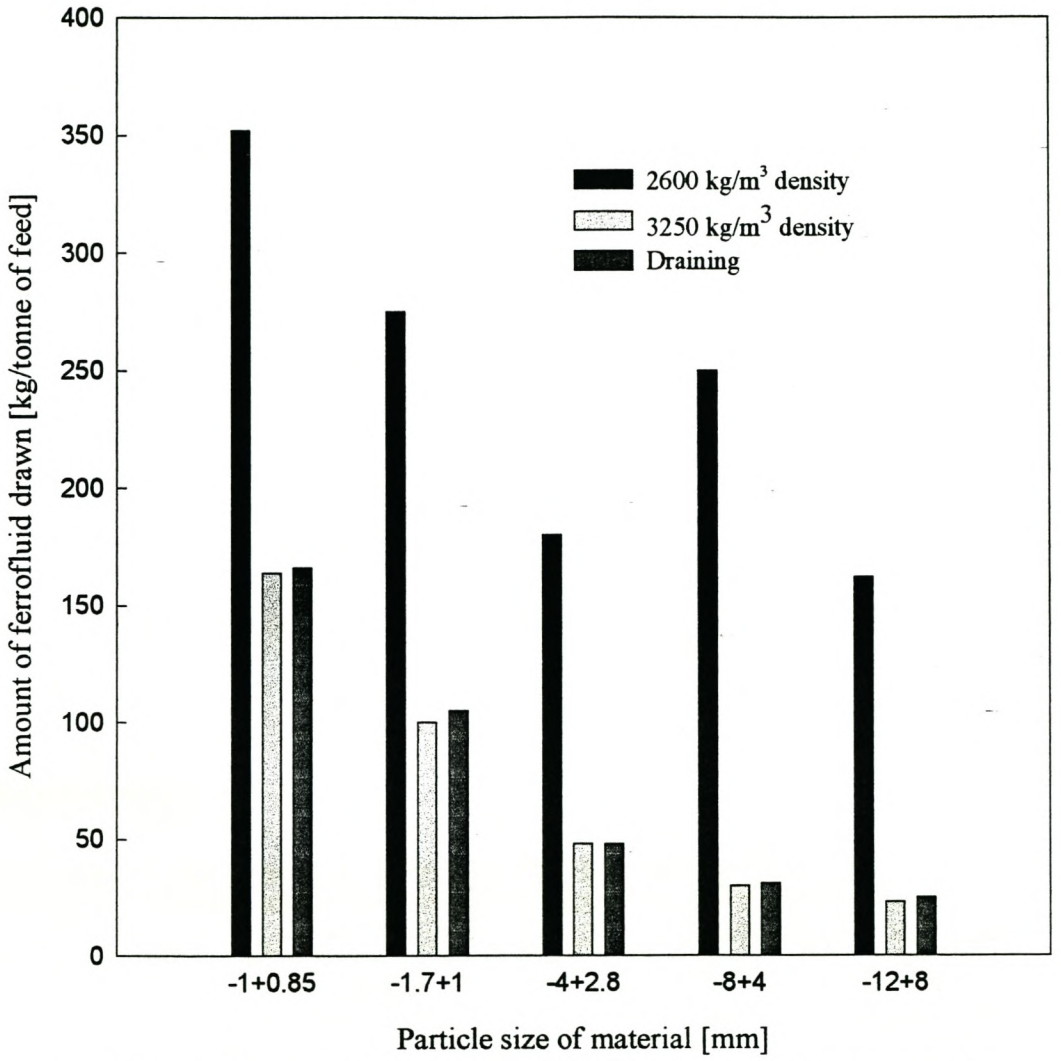

Figure 5.17 Ferrofluid drawn from the separator at different operating conditions.

5.4.2 The Effect of Particle Size on Ferrofluid Losses

The amount of ferrofluid lost as a function of particle size is shown in Figure 5.18. The density of ferrofluid used was 960 kg/m^3.

It was found that for –0.85+0.5 mm to –12+8 mm particles, the amount of ferrofluid lost per tonne of feed ranged from 0.56 kg to 0.73 kg. As described in Chapter 2, an increase in the amount of ferrofluid lost, with a decrease in particle size, is due to an increase in surface area in fine particles. The amount of ferrofluid lost could be lower than that shown in Figure 5.18 due to the following:

- Error in the mass of the dried sample due to inadequate drying.
- Experimental error from varying washing efficiencies due to blockages of sprays and material flow. More ferrofluid can be removed from a monolayer of material than a lumped one.

5.4.3 Effect of Material Moisture Content on Ferrofluid Loses

The amount of ferrofluid lost as a function of material moisture content (0 to 10 %) is shown in Figure 5.19. The density of ferrofluid used was 960 kg/m^3.

It was found that the amount of ferrofluid lost per tonne of feed decreases significantly with an increase in moisture content. This might be as a result of water droplets occupying the vacant pores in the particles. The decrease in ferrofluid lost with an increase in moisture is also enhanced by the fact that water coating the particles makes them adsorb less ferrofluid than dry ones as water is immiscible with kerosene-based ferrofluids.

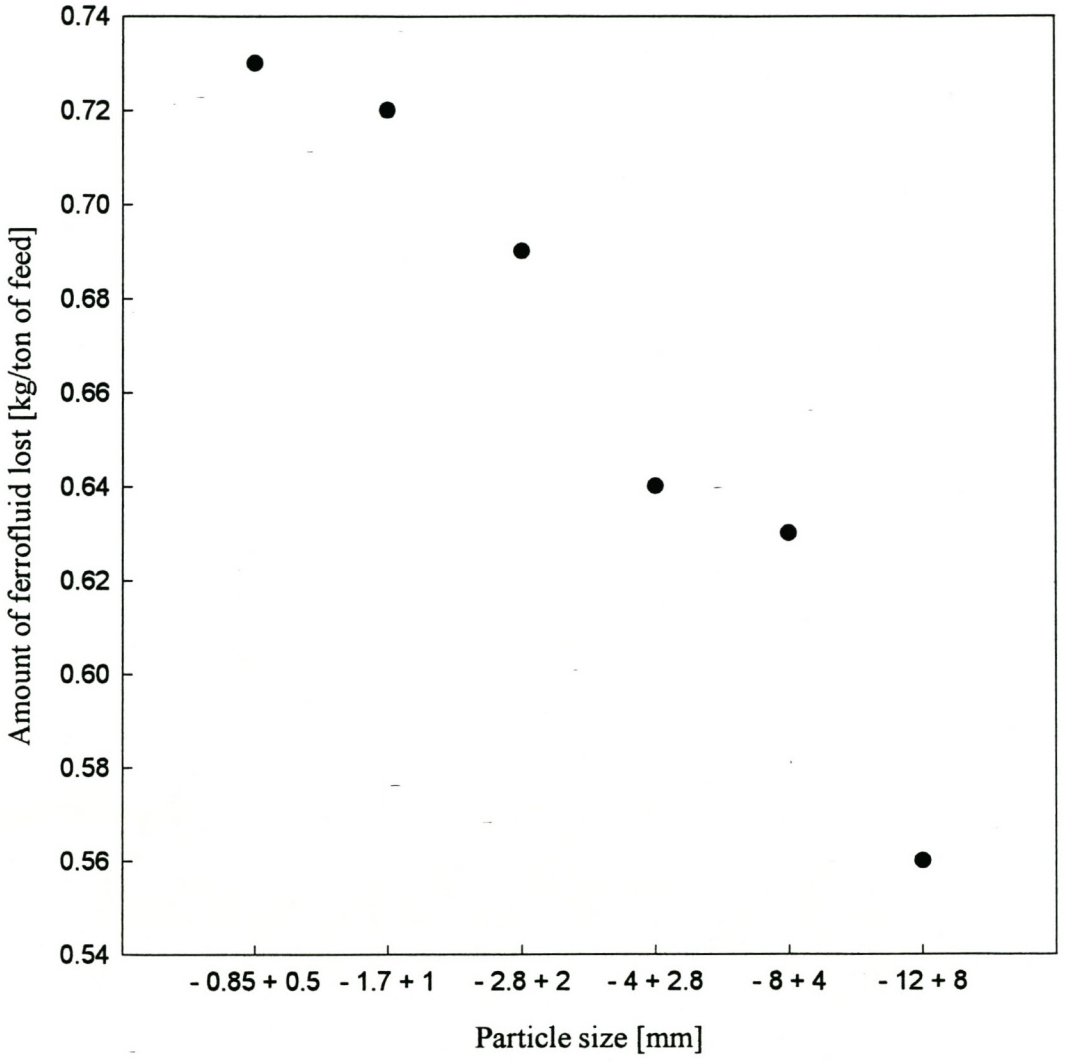

Figure 5.18 Ferrofluid loss as a function of particle size.

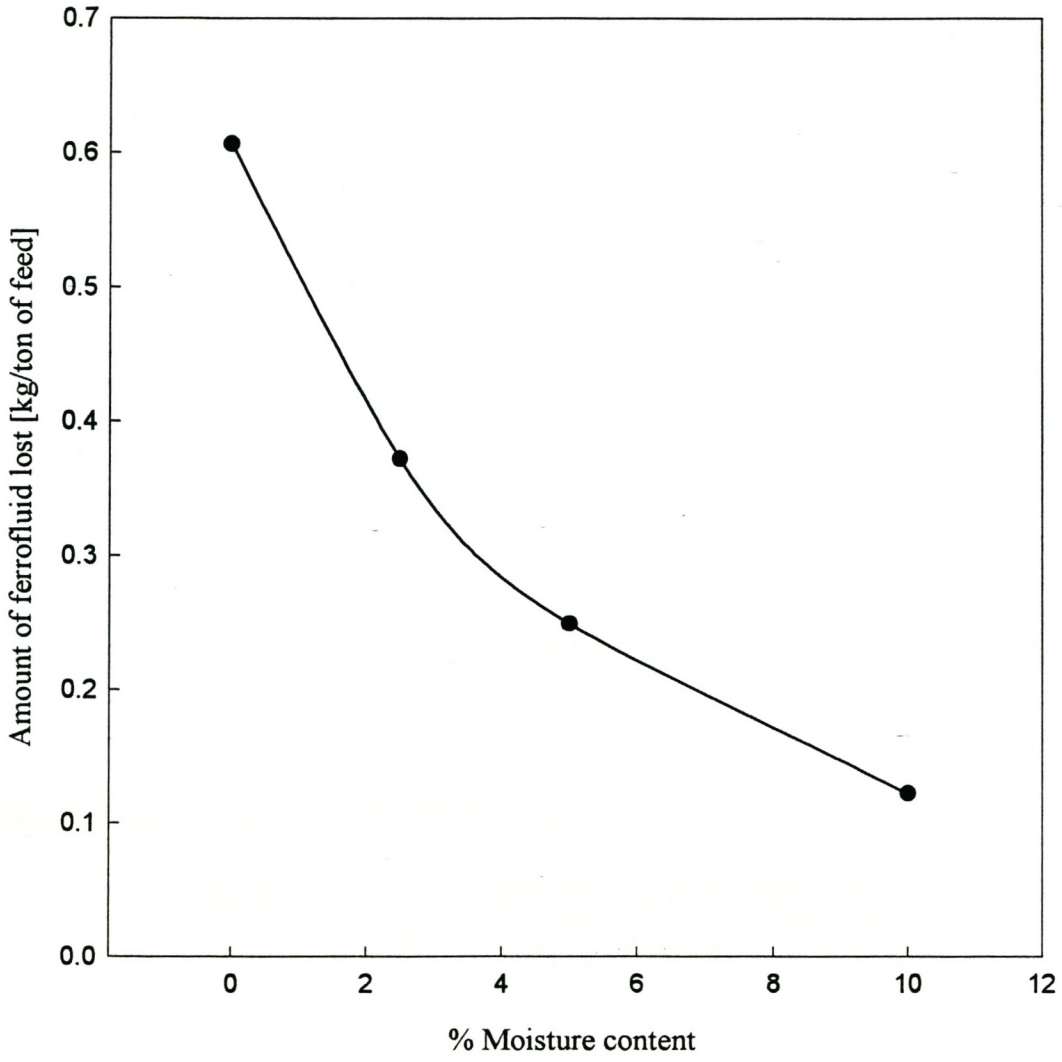

Figure 5.19 Ferrofluid losses as a function of material moisture content. Particle size was -8+4 mm.

This shows that treating wet material would reduce the amount of ferrofluid lost but this should not be done at the expense of separation efficiency. This implies that only coarse material can be wetted to reduce ferrofluid consumption, as fine material should be treated dry as described in Section 5.3.7.

5.4.4 Effect of Porosity on Ferrofluid Losses

The loss of ferrofluid as a function of material porosity (0.18 to 11.34 %) is shown in Figure 5.20.

It can be seen that ferrofluid lost per tonne of feed increases with an increase in porosity. This might be due to an increase in the amount of ferrofluid adsorbed and absorbed by the particles. The ferrofluid is embedded in the vacant pores of the particles and is difficult to wash off using water. This is enhanced by the fact that water and ferrofluid are immiscible.

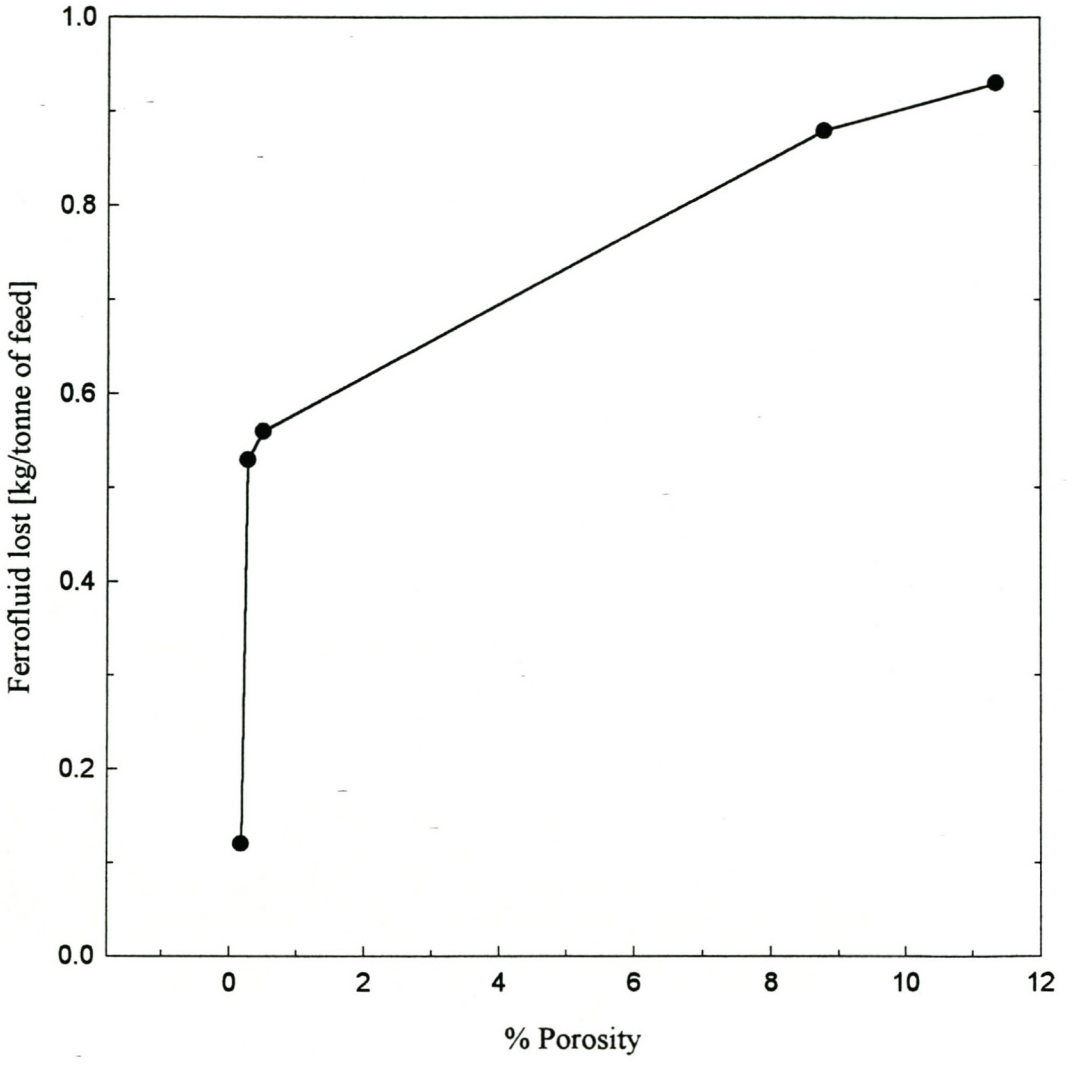

Figure 5.20 Ferrofluid losses as a function of material porosity. Particle size was - 1.75 mm + 0.85 mm

5.5 Summary and Conclusions

The experimental results obtained in this research are applicable to the separator used in this study and they should not be taken as generic to all FHS separators. Different design in the profile of the pole tips and the length of the separation chamber could result in better results.

Experimental results indicate that ferrohydrostatic separation is an efficient way of separating material based on density. It was found from the FHS Tromp curve that the Ep is smaller than 0.008, which leads to efficient material separation. The separation was found to depend on feed rate, especially for near density materials. It was found that 2700 kg/m^3 and 3530 kg/m^3, 2mm density tracers, were separated (100 %) at a feed rate of 20 kg/h and a cut-point density of 3150 kg/m^3 while 2700 kg/m^3 and 3400 kg/m^3 could only be separated at a feed rate of 2 kg/h.

Gravel feed rate tests indicated that coarse particles tend to sink at high feed rates while small particles tend to float. This is due to reduced residence time for small particles to report to the sink product. For coarse particles, due to the deeper and longer trajectory path that they follow in the separator, they exit the separator before reporting to the float product. This was also confirmed by density tracers where it was found that coarse tracers were sinking, for instance, 10 mm 3200 kg/m^3 density tracers sank at a cut-point density of 3350 kg/m^3 set using 2 mm density tracers.

The separation efficiency was found to deteriorate with a decrease in ferrofluid level. At a cut-point density of 3450 kg/m^3 and ferrofluid level of 94 mm, there was 100 % separation of 3530 kg/m^3 and 3400 kg/m^3 density tracers, while all sixty 3400 kg/m^3 density tracers sank at a ferrofluid level of 79 mm. This is also due to the trajectory path followed as coarse tracers are collected in the sink product before reporting to the float product.

From the magnetic field measurements it was found that the magnetic field gradient is lower at the lower part of the separation region. This enhances the sinking of coarse particles as they reach this low-density region.

There was a reduction in the sink product when moisture content was increased for gravel of particle size smaller than 2.8 mm. This is due to water coated particles failing to break the ferrofluid surface tension because of the immiscibility of water and kerosene-based ferrofluid. This implies that small particles should be treated dry for efficient recovery of the sought minerals.

For small particles, for instance –0.5+0.3 mm, it was found that there was more misplaced material in the floats than in the sinks. This is due to their failure to break the surface tension and the limited residence time for them to be collected in the sink product. The tracers used to set the cut-point density were larger than

the particle size treated. In this instance, the effective cut-point density was higher than the 2 mm density tracer determined hence the cut-point density should be calculated from the modified FHS equation that incorporates the hydrodynamic drag (described in detail in Chapter 3). It was also found that there was a decrease in the amount of sink product with an increase in the density of ferrofluid used for separation due to an increase in the hydrodynamic drag.

Water-based ferrofluids are inferior to kerosene based ones due to their lower magnetisation and the density regions which they exhibit in the separation volume. This implies that only low cut-point densities can be attained and different apparent density regions leads to poor separation, which is detrimental to diamond and geological applications. For diamond applications, high cut-point densities of 3650 kg/m^3 are required in order to float diamonds which average density is 3520 kg/m^3.

The amount of ferrofluid drawn from the separator by products of separation was found to be higher at low magnetic fields than at higher ones. For instance for material of particle size 12+8 mm, 162 kg of ferrofluid per tonne of feed was drawn at a cut-point density of 2600 kg/m^3, compared to 23 kg of ferrofluid per tonne of feed at a cut-point density of 3250 kg/m^3. The amount of ferrofluid lost per tonne of feed ranges from 0.56 kg to 0.73 kg for –0.85+0.50 mm to –12+8 mm respectively. This is due to an increase in surface area in small particles. There was a decrease in the amount of ferrofluid lost with an increase in material moisture content and a decrease in porosity, which is due to the reduction in vacant pores in the material.

CHAPTER 6

CONCLUSIONS AND RECOMMENDATIONS

6.1 Conclusions

The research conducted in this thesis pertains to a Ferrohydrostatic separator (FHS) imported from the Ukraine. Consequently, the results are not directly applicable to other designs of FHS separators.

The ferrohydrostatic separation technology is potentially a highly efficient means of separating minerals based on density. It is superior to DMS and heavy liquids in that:

(1) it can attain higher separation densities.
(2) it is safer than heavy liquids due to non-toxicity of the ferrofluid medium used.
(3) it has higher separation efficiency.
(4) a wide range of separation densities can be attained without changing the medium.
(5) it is easy to recover and recycle the ferrofluid used for material separation.

Theoretical Considerations

Chapter 3 extended the FHS equation and investigated various scenarios. In particular it was shown that;

- The effect of hydrodynamic drag in FHS separation is significant for particles smaller than 100 μm in radius. This is good news for diamond operations, which typically treat material greater than 1 mm.
- The treatment of nonmagnetic material together with magnetic material would result in misplaced material in the sinks.
- The maximum volume magnetic susceptibility that can be treated in the FHS separator is 20×10^{-4}.
- The misplacement of magnetic material into the sinks can be beneficial if the sinks products are to be discarded and the misplaced magnetic material are part of the gangue. The result is that there is a reduction in the gangue material reporting to the float concentrate.

Separation Efficiency

The investigation into the factors affecting FHS separation efficiency yielded the following results:

- It was found from the FHS tromp curve (using 2 mm tracers) that the Ep is less than 0.008 which is smaller than the cyclone's Ep (0.02). This makes the ferrohydrostatic separation more efficient than the DMS.
- The separation was found to depend on feed rate, especially for near density materials. It was found that 2700 kg/m^3 and 3530 kg/m^3, 2mm density tracers, could be separated with a 100% efficiency at a feed rate of 20 kg/h and a cut-point density of 3150 kg/m^3, while 2700 kg/m^3 and 3400 kg/m^3 could only be separated with the same efficiency at a feed rate of 2 kg/h.
- Gravel feed rate tests indicates that coarse particles tend to sink at high feed rates while small particles tend to float. Small particles float as a result of finite length (195 mm) of the separation chamber (hydrodynamic drag effect), while coarse particles sink due to the their extended trajectory, viz. they exit the separator before reporting to the float product. This was also confirmed by density tracer tests, where it was found that coarse tracers reported to the sinks product, i.e. 10 mm 3200 kg/m^3 density tracers sank at a cut-point density of 3350 kg/m^3 set using 2 mm density tracers.
- The separation efficiency deteriorates with a decrease in ferrofluid level. The effect of ferrofluid level is negligible if the ferrofluid level is kept within 7 mm from the feed plate level when a density difference of 130 kg/m^3 is to be separated with a 100% efficiency. If the particles to be separated have a wide density difference, for instance 2700 kg/m^3 and 3530 kg/m^3, the effective drop height of the particles into the fluid should be no more than 15 mm.
  At a cut-point density of 3450 kg/m^3 and ferrofluid level of 94 mm (6mm below drop level), there was 100 % separation of 3530 kg/m^3 and 3400 kg/m^3 density tracers, while all sixty 3400 kg/m^3 density tracers sank at a ferrofluid level of 79 mm (21 mm below drop level). This is due to the trajectory path followed as coarse tracers are collected in the sink product before reporting to the float product.
- It was found that FHS separation efficiency is highly dependent on material moisture content for particles smaller than 2.8 mm and is negligible for coarser particles. This is due to water occupying vacant pores and water coating on the particles, which is immiscible with kerosene-based ferrofluid, hence small water coated particles fail to break ferrofluid surface tension. This implies that small particles should be treated dry for efficient recovery of the sought minerals. Coarser particles, because of their relatively high mass, overcome the ferrofluid surface tension and water coating the particles is removed as particles enter the ferrofluid pool.
- For small particles, i.e. –0.5+0.3 mm, it was found that there was more misplaced material in the floats than in the sinks. This is due to their failure to break

ferrofluid surface tension and the limited residence time for them to be collected in the sink product.

- Water-based ferrofluids are inferior to kerosene based ones due to their lower magnetisation and the density regions which they exhibit in the separation volume. This implies that only low cut-point densities can be attained and different apparent density regions leads to poor separation, which is detrimental to diamond and geological applications. For diamond applications, high cut-point densities of 3650 kg/m^3 are required in order to float diamonds: average density 3520 kg/m^3.

Loss and Recovery of Ferrofluid

The investigation into the loss and recovery of ferrofluid yielded the following results:

- The amount of ferrofluid adsorbed by the products of ferrohydrostatic separation decreases with an increase in the magnetic field as more ferrofluid is retained in the separator. This implies that the FHS separator should be operated at high magnetic fields to reduce ferrofluid loss, and hence, operating costs.
- The quality of ferrofluid recovered is the same as that used for material separation.
- The amount of ferrofluid lost increases with a decrease in particle size treated due to an increase in surface area. The loss was determined to be 0.56 kg of fluid per tonne of feed for –12+8 mm and 0.73 kg/tonne for –0.85+0.50 mm particles.
- It was found that the amount of ferrofluid lost decreases with an increase in material moisture content due to water occupying vacant pores of the particles. The ferrofluid loss ranges from 0.60 down to 0.14 kg/tonne for a moisture content range of 0 % to 10 %.
- The amount of ferrofluid lost increases with an increase in material porosity. For –1.70+0.85 mm particles, the ferrofluid loss range was 0.12 kg/tonne of feed for 0.18 % porosity. For a porosity of 11.34 %, this rises to 0.93 kg/tonne.

6.2 Recommendations for Further Investigations

Based on the results given above, there is a large scope of work still to be completed. In particular;

- Wetting of fine material prior to FHS separation. This is due to the fact that fine particles fail to overcome the ferrofluid surface tension.
- The determination of the maximum particle magnetisation that can be treated in the FHS without clogging.
- The drop in ferrofluid apparent density with an increase in temperature.
- During ferrofluid recycling, there is an increase in the amount of kerosene in water used for washing. The maximum amount of kerosene allowable without affecting the washing efficiency needs to be quantified.

- The economic evaluation and FHS process should be carried out. This can be done using four common investment models; namely the payback period (PBP), financial percent return on investment (%ROI), net present value (NPV), and the internal rate of return (IRR).

REFERENCES

Aldrich, C., 1994. *The Range of Susceptibilities that can be Exploited for Effective Separation of Materials with Magnetic Fluids and the Effect of the Applied Magnetic Field Strength on this Range*, University of Stellenbosch, South Africa.

Badescu, V., Muraria, V., Rotariu, O., Rezlescu, N., 1999. *Theoretical Investigation of Particle Motion in a Magnetic Fluid,* National Institute of Research and Development for Technical Physics, Romania.

Boudouvis, A. G., Puchala, J. L., Scriven, L. E., 1988. Magnetohydrostatic Equilibria of Ferrofluids Drops in External Magnetic Fields, *Chemical Engineering Communication,* **67**, pp. 129-144.

Burt, R. O., 1984. *Gravity Concentration Technology,* Elsevier, Amsterdam.

Cheney, W., Kincaid, D., 1994. *Numerical Mathematics and Computing,* Brooks / Cole, 3rd edition, California.

Chikazumi, S., Taketomi, S., Ukita, M., Mizukami, M., Miyajima, H., Setogawa, M., Kurihara, Y., 1987. Physics of Magnetic Fluids, *Magnetism and Magnetic Materials,* **65**, pp. 245 – 251.

Dababneh, M. S., Ayoub, N. Y., Odeh, I., Laham, N. M., 1993. Viscosity, Resistivity and Surface Tension Measurements of Fe_3O_4 Ferrofluid, *Magnetism and Magnetic Materials,* **125**, pp. 34-38.

Dumbu, S., 1999. *Development of a Technique for the Recovery of Ferrofluid from Ferrofluid / Water Mixture*, De Beers, DebTech, South Africa.

Felix, J., Krüger, L., Dumbu, S., Svoboda, J., 1998. *Development of a System for the Production of Ferrofluids and a Mine Test Unit for the Treatment of Geological Samples by Ferrohydrostatic Separation,* De Beers 18th Metallurgical Conference, Vanderbijlpark, South Africa, pp.126-155.

Fofana, M., 1997. *Evaluation and Design of Magnetic Fluid Separators for Density Separations*, Ph.D. Thesis, Pennysylvania State University, U.S.A.

Freeman, R. J., Rowson, N. A., Veasey, T. J., 1994. The Development of a Magnetic Hydrocyclone for Processing Finely Ground Magnetite, *IEE Transactions on Magnetics,* **30**, p. 465.

Fujita, T., Mamiya, M., 1987. Interaction Forces Between Nonmagnetic Particles in the Magnetised Magnetic Fluid, *Magnetism and Magnetic Materials,* **65**, pp. 207 – 210.

Glass, H. J., de Bakker, J., Leest, P. A., Dalmijn, W. L., 1996. New Possibilities for Magnetohydrostatic Separation of Particles, *Institute of Mining and Metallurgy,* **105**, pp. C145-C149.

Gogosov, V. V., Smolkin, R. D., Krokhmal, V. S., Saiko, O. P., Mangov, L. I., Nozkodubov, V. I., 1994. Industrial Separators Based on Magnetic Fluids, *Magnetic Hydrodynamic,* **1,** pp. 111-120.

Gogosov, V. V., Smolkin, R. D., Krokhmal, V. S., Garin, Yu, M., Shaposhnikova, G. A., 1983. Some Theoretical and Practical Problems of Separation in Magnetic Fluids, *Magnetism and Magnetic Materials,* **39**, pp. 169–172.

Gubarevich, V. N., 1995. Method and Equipment for Final Concentration of the Gold-bearing Alluvial Sands, *Magnetic and Electrical Separation,* **6**, pp. 229-234.

Gubarevich, V. N., 1987. Separation of Materials in Magnetic Fluids, Nedra, Moscow.

Gubarevich, V. N., Vidsota, S. V., 1994. Theoretical Principles, Present Status and Prospects for Development of Material Separation in Magnetic Fluids, *Magnetic* and *Electrical Separation,* **5**, pp. 169-192.

Kaiser, R., 1975. Hyperbolic Magnet Poles for Sink-float Separators, *United States Patent,* 3898156.

Kelly, E. G., Spottiswood, D. J., 1992. *Introduction to Mineral Processing,* Wiley, New York.

Khalafalla, S. E., 1985. Beneficiation with Magnetic Fluids – Magnetic Separation of the Second Kind, *Mineral Processing and Extractive Metallurgy Review,* **2**, pp. 21–55.

Khalafalla, S. E., Reimers, G. W., 1973. Magneto-Gravimetric Separation of Non-magnetic Solids, *Society of Mining Engineers, AIME,* **254**.

Krüger, L., 1999. *Formulation of a Detergent for the Cleaning of Ferrofluid–coated Particles,* De Beers, DebTech, South Africa, pp. 9-10.

Lepekhin, V. M., Borzov, V. L., Yaramenko, V. N., 1995. The Centrifugal Separation of Fine Materials, *Magnetic and Electrical Separation,* **6**, pp. 235-242.

Lin, D., Leroux, M., Finch, J. A., 1994. Batch Magnetohydrostatic Separations with a Modified Frantz Separator, *Minerals Engineering,* **8**, pp. 283-291.

Luxon, S. G., 1992. *Hazards in the Chemical Laboratory,* 5th Edition, Royal Society of Chemistry, Cambridge.

Moskowitz, R., 1975. Designing with Ferrofluids, *Mechanical Engineering,* pp. 30-36.

Reimers, G. W., Rholl, S. A., Snyder, R. W., Khalafalla, S. E., 1974. Cell Design to Separate Nonferrous Metals in Incinerator Residue with Magnetic Fluids, *Material Science and Engineering,* **15**, pp. 129-135.

Reitz, J. R., 1993. *Foundations of Electromagnetic Theory,* 4th edition, Addison-Wesley, USA.

Robert, P., 1988. *Electrical and Magnetic Properties of Materials*, Artech House, USA.

Rosenweig, R. E., 1966. Buoyancy and Stable Levitation of a Magnetic Body Immersed in a Magnetisable Fluid, *Nature,* **210,** p. 6.

Shimoiizaka, J., Nakatsuka, K., Kounosu, A., 1980. Sink-float Separators using Permanent Magnets and Water Based Magnetic Fluid, *IEE Transactions,* **2**, pp. 368-371.

Süße, W., 1979. SOL Separator – A New Development in the Field of High-Intensity Wet Magnetic Separation, *Erzmetal*, pp. 321-324.

Svoboda, J., 1996. A Contribution to the Theory of Separation in a Rotating Ferrofluid, *Minerals Engineering,* **9**, pp. 743-752.

Svoboda, J., Coetzee, C., Campbell, Q. P., 1998. Experimental Investigation into the Application of a Magnetic Cyclone for Dense Medium Separation, *Minerals Engineering,* **11**, pp. 501-509.

Svoboda, J., Krüger, L., Felix, J., Dumbu, S., Phakathi, Z., 1996. *Experimental Investigation of Ferrohydrostatic Separation and Development of its Control System,* De Beers, DebTech, South Africa.

Svoboda, J., 1995. *History of Magnetohydrostatic Separation at DRL and the Current Status of this Technology,* TN 95/09/01, De Beers, DebTech, South Africa.

Svoboda, J., 1987. *Magnetic Methods for the Treatment of Minerals*, Elsevier, Amsterdam.

Svoboda, J., 1998. Separation of Materials in Magnetic Fluids: Principles, Applications and the Future Developments, *Waste Processing and Recycling in Mineral and Metallurgical Industries,* **3**, pp. 31-46.

Tarjàn, G., 1986. Concentration, Flotation, Separation Backup Processes, *Mineral Processing*, **2** Akademiai Kiadio, Budapest.

Wills, B. A., 1992. *Mineral Processing Technology,* 5th Edition, Pergamon, Oxford.

Zimmels, Y., 1983. Application of Ferrofluids to Separation of Particulates, *Magnetism and Magnetic Materials*, **39**, pp. 173-177.

Appendix A

Magnetic Field Measurements at Different Currents

Distance from the Point of Highest Magnetic Field [mm]	Magnetic Field Induction [T]					Magnetic Field Gradient [T/m]				
	2.8 A	3.3 A	4.3 A	5.0 A	6.0 A	2.8 A	3.3 A	4.3 A	5.0 A	6.0 A
0	0.21	0.22	0.24	0.24	0.26	-	-	-	-	-
10	0.20	0.21	0.23	0.24	0.25	0.86	0.82	0.85	0.93	0.93
20	0.19	0.20	0.22	0.22	0.23	1.32	1.32	1.43	1.51	1.54
30	0.17	0.18	0.20	0.20	0.21	1.58	1.63	1.77	1.84	1.92
40	0.16	0.16	0.18	0.18	0.19	1.74	1.82	1.99	2.05	2.15
50	0.14	0.14	0.16	0.16	0.17	1.85	1.94	2.12	2.17	2.29
60	0.12	0.12	0.13	0.14	0.15	1.93	2.02	2.20	2.26	2.38
70	0.10	0.10	0.11	0.12	0.12	1.99	2.08	2.25	2.32	2.43
80	0.08	0.08	0.09	0.09	0.10	2.05	2.12	2.28	2.37	2.46
90	0.06	0.06	0.07	0.07	0.07	2.11	2.15	2.29	2.4	2.48
100	0.03	0.04	0.04	0.04	0.05	2.16	2.18	2.31	2.45	2.50

Appendix B

Separation as a Function of Feed rate

Ferrofluid of density 960 kg/m^3 was used and the level was kept constant at 94 mm. Sixty tracers of each density were used.

(1) Test carried out using 2 mm tracers. The cut-point density was set at 3400 kg/m^3.

Feed rate [kg/h]	3000 kg/m^3 Sinks	3100 kg/m^3 Sinks	3200 kg/m^3 Sinks	3300 kg/m^3 Sinks	3400 kg/m^3 Sinks	3530 kg/m^3 Sinks
1.3	0.00	0.00	0.00	0.00	46.67	100.00
1.3	0.00	0.00	0.00	0.00	68.33	96.67
1.3	0.00	0.00	0.00	0.00	71.67	95.00
1.3	0.00	0.00	0.00	0.00	56.67	96.67
1.3	0.00	0.00	0.00	0.00	33.33	98.33
1.3	0.00	0.00	0.00	0.00	25.00	100.00
1.3	0.00	0.00	0.00	0.00	26.67	96.67
1.6	0.00	0.00	0.00	5.00	68.33	95.00
1.6	0.00	0.00	0.00	0.00	56.67	100.00
1.6	0.00	0.00	0.00	5.00	58.33	95.00
1.6	0.00	0.00	0.00	6.67	40.00	93.33
1.6	0.00	0.00	0.00	8.33	33.33	91.67
1.6	0.00	0.00	0.00	5.00	33.33	96.67
1.6	0.00	0.00	0.00	5.00	38.33	98.33
3.6	0.00	0.00	0.00	5.00	33.33	90.00
3.6	0.00	0.00	0.00	5.00	33.33	91.67
3.6	0.00	0.00	1.67	6.67	41.67	90.00
3.6	0.00	0.00	1.67	8.33	25.00	88.33
3.6	0.00	0.00	0.00	5.00	50.00	88.33
3.6	0.00	0.00	0.00	10.00	46.67	90.00
3.6	0.00	0.00	0.00	8.33	45.00	90.00
13.0	0.00	1.67	5.00	11.67	26.67	65.00
13.0	0.00	1.67	6.67	5.00	26.67	71.67
13.0	0.00	0.00	5.00	6.67	33.33	83.33
13.0	0.00	0.00	3.33	8.33	30.00	86.67
13.0	0.00	0.00	3.33	5.00	41.67	80.00
13.0	0.00	1.67	5.00	5.00	48.33	90.00
13.0	0.00	0.00	5.00	6.67	21.67	93.33
34.0	1.67	5.00	3.33	10.00	21.67	48.33
34.0	0.00	0.00	5.00	6.67	48.33	80.00
34.0	0.00	6.67	5.00	10.00	30.00	81.67
34.0	1.67	3.33	6.67	11.67	23.33	83.33
34.0	0.00	3.33	3.33	11.67	41.67	73.33
34.0	0.00	3.33	6.67	13.33	48.33	71.67
34.0	0.00	1.67	6.67	6.67	48.33	80.00

(2) Test carried out using 2 mm tracers. The cut-point density was set at 3150 kg/m^3.

Feed rate [kg/h]	2700 kg/m^3 Sinks	2800 kg/m^3 Sinks	3000 kg/m^3 Sinks	3100 kg/m^3 Sinks	3200 kg/m^3 Sinks	3300 kg/m^3 Sinks	3400 kg/m^3 Sinks	3530 kg/m^3 Sinks
1.6	0.00	0.00	0.00	1.67	100.00	96.67	96.67	100.00
1.6	0.00	0.00	0.00	0.00	98.33	100.00	100.00	100.00
1.6	0.00	0.00	0.00	0.00	98.33	96.67	100.00	100.00
1.6	0.00	0.00	0.00	0.00	96.67	100.00	100.00	100.00
1.6	0.00	0.00	0.00	3.33	98.33	100.00	100.00	100.00
1.6	0.00	0.00	0.00	1.67	100.00	100.00	100.00	100.00
1.6	0.00	0.00	0.00	3.33	100.00	100.00	100.00	100.00
1.9	0.00	0.00	3.33	11.67	95.00	98.33	100.00	100.00
1.9	0.00	0.00	0.00	8.33	96.67	91.67	100.00	100.00
1.9	0.00	0.00	1.67	11.67	96.67	88.33	100.00	100.00
1.9	0.00	0.00	1.67	15.00	95.00	90.00	100.00	100.00
1.9	0.00	0.00	0.00	11.67	96.67	98.33	100.00	100.00
1.9	0.00	0.00	3.33	13.33	93.33	91.67	100.00	100.00
1.9	0.00	0.00	3.33	10.00	91.67	98.33	100.00	100.00
2.0	0.00	0.00	0.00	28.33	91.67	93.33	100.00	100.00
2.0	0.00	0.00	0.00	16.67	86.67	96.67	100.00	100.00
2.0	0.00	0.00	5.00	18.33	90.00	91.67	100.00	100.00
2.0	0.00	0.00	6.67	28.33	90.00	96.67	100.00	100.00
2.0	0.00	0.00	1.67	20.00	95.00	93.33	100.00	100.00
2.0	0.00	0.00	3.33	23.33	86.67	93.33	100.00	100.00
2.0	0.00	0.00	6.67	25.00	85.00	93.33	100.00	100.00
6.7	0.00	5.00	3.33	31.67	86.67	95.00	98.33	100.00
6.7	0.00	3.33	6.67	36.67	88.33	96.67	93.33	100.00
6.7	0.00	3.33	10.00	30.00	80.00	90.00	91.67	100.00
6.7	0.00	6.67	3.33	35.00	86.67	88.33	98.33	100.00
6.7	0.00	5.00	5.00	31.67	90.00	83.33	98.33	100.00
6.7	0.00	3.33	6.67	31.67	86.67	95.00	96.67	100.00
6.7	0.00	3.33	6.67	33.33	86.67	83.33	100.00	100.00
20.2	1.67	11.67	18.33	45.00	75.00	85.00	91.67	100.00
20.2	3.33	6.67	23.33	48.33	75.00	88.33	91.67	100.00
20.2	1.67	13.33	16.67	43.33	80.00	81.67	96.67	100.00
20.2	0.00	10.00	13.33	45.00	68.33	80.00	93.33	100.00
20.2	0.00	11.67	18.33	45.00	65.00	85.00	83.33	100.00
20.2	1.67	11.67	15.00	46.67	73.33	85.00	90.00	100.00
20.2	1.67	6.67	18.33	41.67	76.67	83.33	90.00	100.00

(3). Test carried out using 4 mm tracers. The cut-point density was set at 3350 kg/m^3.

Feed rate [kg/h]	3000 kg/m^3 Sinks	3100 kg/m^3 Sinks	3200 kg/m^3 Sinks	3300 kg/m^3 Sinks	3400 kg/m^3 Sinks	3530 kg/m^3 Sinks
6.6	0.00	1.67	6.67	23.33	65.00	100.00
6.6	0.00	3.33	1.67	21.67	65.00	100.00
6.6	0.00	0.00	0.00	16.67	63.33	96.67
6.6	0.00	0.00	0.00	21.67	65.00	100.00
6.6	0.00	0.00	8.33	20.00	63.33	100.00
6.6	0.00	0.00	3.33	21.67	66.67	96.67
6.6	0.00	0.00	1.67	20.00	63.33	95.00
7.2	0.00	0.00	1.67	25.00	56.67	100.00
7.2	0.00	0.00	0.00	20.00	58.33	100.00
7.2	0.00	0.00	10.00	26.67	61.67	96.67
7.2	0.00	0.00	6.67	26.67	61.67	95.00
7.2	0.00.	0.00	1.67	25.00	56.67	100.00
7.2	0.00	0.00	10.00	25.00	58.33	96.67
7.2	0.00	0.00	8.33	20.00	58.33	91.67
12.6	0.00	0.00	5.00	28.33	55.00	93.33
12.6	0.00	3.33	11.67	30.00	56.67	91.67
12.6	0.00	1.67	6.67	31.67	65.00	90.00
12.6	0.00	3.33	10.00	28.33	53.33	85.00
12.6	0.00	1.67	8.33	26.67	51.67	91.67
12.6	0.00	0.00	8.33	28.33	55.00	93.33
12.6	0.00	0.00	6.67	28.33	55.00	81.67
25.2	0.00	5.00	13.33	33.33	45.00	91.67
25.2	0.00	5.00	16.67	41.67	43.33	85.00
25.2	1.67	6.67	15.00	33.33	55.00	95.00
25.2	3.33	6.67	15.00	31.67	63.33	93.33
25.2	0.00	5.00	13.33	35.00	48.33	85.00
25.2	0.00	5.00	13.33	33.33	48.33	86.67
25.2	0.00	5.00	13.33	33.33	48.33	83.33
50.0	6.67	11.67	31.67	43.33	53.33	81.67
50.0	13.33	21.67	23.33	48.33	45.00	71.67
50.0	6.67	11.67	25.00	35.00	45.00	85.00
50.0	6.67	13.33	26.67	41.67	53.33	71.67
50.0	10.00	21.67	31.67	48.33	53.33	81.67
50.0	11.67	21.67	23.33	43.33	45.00	83.33
50.0	13.33	20.00	23.33	41.67	45.00	83.33

Appendix C

Separation as a Function of Particle Size

Two millimetre tracers were used to set cut-point density at 3350 kg/m^3. The feed rate was kept constant at 1.3 kg/h.

Tracer Size [mm]	3000 kg/m^3 Sinks	3100 kg/m^3 Sinks	3200 kg/m^3 Sinks	3300 kg/m^3 Sinks	3400 kg/m^3 Sinks	3530 kg/m^3 Sinks
0.5	0.00	0.00	0.00	0.00	91.67	100.00
0.5	0.00	0.00	0.00	0.00	93.33	100.00
0.5	0.00	0.00	0.00	0.00	95.00	100.00
0.5	0.00	0.00	0.00	0.00	83.33	100.00
0.5	0.00	0.00	0.00	0.00	88.33	100.00
0.5	0.00	0.00	0.00	0.00	93.33	100.00
0.5	0.00	0.00	0.00	0.00	91.67	100.00
1	0.00	0.00	0.00	0.00	93.33	100.00
1	0.00	0.00	0.00	0.00	96.67	100.00
1	0.00	0.00	0.00	0.00	93.33	100.00
1	0.00	0.00	0.00	0.00	93.33	100.00
1	0.00	0.00	0.00	0.00	98.33	100.00
1	0.00	0.00	0.00	0.00	95.00	100.00
1	0.00	0.00	0.00	0.00	96.67	100.00
2	0.00	0.00	0.00	0.00	100.00	100.00
2	0.00	0.00	0.00	0.00	100.00	100.00
2	0.00	0.00	0.00	0.00	100.00	100.00
2	0.00	0.00	0.00	0.00	100.00	100.00
2	0.00	0.00	0.00	0.00	100.00	100.00
2	0.00	0.00	0.00	0.00	100.00	100.00
2	0.00	0.00	0.00	0.00	100.00	100.00
4	0.00	0.00	30.00	63.33	100.00	100.00
4	0.00	0.00	25.00	66.67	100.00	100.00
4	0.00	0.00	23.33	58.33	100.00	100.00
4	0.00	0.00	13.33	58.33	100.00	100.00
4	0.00	0.00	23.33	63.33	100.00	100.00
4	0.00	0.00	15.00	63.33	100.00	100.00
4	0.00	0.00	16.67	60.00	100.00	100.00
6	0.00	30.00	75.00	81.67	100.00	100.00
6	0.00	25.00	66.67	86.67	100.00	100.00
6	0.00	30.00	75.00	85.00	100.00	100.00
6	0.00	28.33	75.00	83.33	100.00	100.00
6	0.00	30.00	65.00	81.67	100.00	100.00
6	0.00	30.00	70.00	81.67	100.00	100.00
6	0.00	30.00	66.67	81.67	100.00	100.00
8	25.00	78.33	91.67	100.00	100.00	100.00
8	28.33	78.33	85.00	100.00	100.00	100.00
8	30	66.67	91.67	100.00	100.00	100.00

Table continued on page 107

8	31.67	70.00	98.33	100.00	100.00	100.00
8	25.00	78.33	96.67	100.00	100.00	100.00
8	31.67	78.33	81.67	100.00	100.00	100.00
8	31.67	70.00	91.67	100.00	100.00	100.00
10	31.67	83.33	100.00	100.00	100.00	100.00
10	36.67	81.67	100.00	100.00	100.00	100.00
10	35.00	80.00	100.00	100.00	100.00	100.00
10	31.67	81.67	100.00	100.00	100.00	100.00
10	31.67	81.67	100.00	100.00	100.00	100.00
10	33.33	83.33	100.00	100.00	100.00	100.00
10	33.33	78.33	100.00	100.00	100.00	100.00

Appendix D

Separation as a Function of Ferrofluid Level

(1) Two millimetre tracers were used at a cut-point density of 3450 kg/m^3 and the feed rate was kept constant at 1.3 kg/h.

Fluid Level [mm]	3000 kg/m^3 Sinks	3100 kg/m^3 Sinks	3200 kg/m^3 Sinks	3300 kg/m^3 Sinks	3400 kg/m^3 Sinks	3530 kg/m^3 Sinks
94	0.00	0.00	0.00	0.00	0.00	100.00
94	0.00	0.00	0.00	0.00	0.00	100.00
94	0.00	0.00	0.00	0.00	0.00	100.00
94	0.00	0.00	0.00	0.00	0.00	100.00
94	0.00	0.00	0.00	0.00	0.00	100.00
94	0.00	0.00	0.00	0.00	0.00	100.00
94	0.00	0.00	0.00	0.00	0.00	100.00
93	0.00	0.00	0.00	0.00	0.00	100.00
93	0.00	0.00	0.00	0.00	0.00	100.00
93	0.00	0.00	0.00	0.00	0.00	100.00
93	0.00	0.00	0.00	0.00	0.00	100.00
93	0.00	0.00	0.00	0.00	0.00	100.00
93	0.00	0.00	0.00	0.00	0.00	100.00
93	0.00	0.00	0.00	0.00	0.00	100.00
90	0.00	0.00	0.00	0.00	0.00	100.00
90	0.00	0.00	0.00	0.00	0.00	100.00
90	0.00	0.00	0.00	0.00	0.00	100.00
90	0.00	0.00	0.00	0.00	0.00	100.00
90	0.00	0.00	0.00	0.00	0.00	100.00
90	0.00	0.00	0.00	0.00	0.00	100.00
90	0.00	0.00	0.00	0.00	0.00	100.00
88	0.00	0.00	0.00	0.00	1.67	100.00
88	0.00	0.00	0.00	0.00	0.00	100.00
88	0.00	0.00	0.00	0.00	0.00	100.00
88	0.00	0.00	0.00	0.00	3.33	100.00
88	0.00	0.00	0.00	0.00	0.00	100.00
88	0.00	0.00	0.00	0.00	1.67	100.00
88	0.00	0.00	0.00	0.00	1.67	100.00
85	0.00	0.00	0.00	3.33	40.00	100.00
85	0.00	0.00	0.00	6.67	36.67	100.00
85	0.00	0.00	0.00	1.67	33.33	100.00
85	0.00	0.00	0.00	0	40.00	100.00
85	0.00	0.00	0.00	6.67	41.67	100.00
85	0.00	0.00	0.00	8.33	40.00	100.00
85	0.00	0.00	0.00	8.33	36.67	100.00
82	0.00	0.00	10.00	26.67	75.00	100.00
82	0.00	0.00	3.33	25	76.67	100.00
82	0.00	0.00	5.00	28.33	70.00	100.00

Table continued on page 109

82	0.00	0.00	11.67	25.00	66.67	100.00
82	0.00	0.00	10.00	25.00	75.00	100.00
82	0.00	0.00	8.33	23.33	75.00	100.00
82	0.00	0.00	8.33	25.00	75.00	100.00
77	0.00	15.00	20.00	80.00	100.00	100.00
77	0.00	16.67	28.33	80.00	100.00	100.00
77	0.00	13.33	30.00	83.33	100.00	100.00
77	0.00	11.67	33.33	85.00	100.00	100.00
77	0.00	15.00	33.33	80.00	100.00	100.00
77	0.00	15.00	33.33	78.33	100.00	100.00
77	0.00	18.33	33.33	80.00	100.00	100.00
73	58.33	100.00	100.00	100.00	100.00	100.00
73	63.33	100.00	100.00	100.00	100.00	100.00
73	58.33	100.00	100.00	100.00	100.00	100.00
73	60.00	100.00	100.00	100.00	100.00	100.00
73	61.67	100.00	100.00	100.00	100.00	100.00
73	63.33	100.00	100.00	100.00	100.00	100.00
73	58.33	100.00	100.00	100.00	100.00	100.00

(2) Six millimetre tracers were used at a cut-point density of 3450 kg/m^3. The feed rate was kept constant at 1.3 kg/h.

Fluid Level [mm]	3000 kg/m^3 Sinks	3100 kg/m^3 Sinks	3200 kg/m^3 Sinks	3300 kg/m^3 Sinks	3400 kg/m^3 Sinks	3530 kg/m^3 Sinks
94	0.00	0.00	0.00	0.00	25.00	60.00
94	0.00	0.00	0.00	0.00	18.33	63.33
94	0.00	0.00	0.00	0.00	23.33	83.33
94	0.00	0.00	0.00	0.00	20.00	75.00
94	0.00	0.00	0.00	0.00	16.67	80.00
94	0.00	0.00	0.00	0.00	23.33	60.00
94	0.00	0.00	0.00	0.00	18.33	66.67
92	0.00	0.00	0.00	0.00	65.00	100.00
92	0.00	0.00	0.00	0.00	50.00	100.00
92	0.00	0.00	0.00	0.00	63.33	100.00
92	0.00	0.00	0.00	0.00	16.67	100.00
92	0.00	0.00	0.00	0.00	60.00	100.00
92	0.00	0.00	0.00	0.00	63.33	100.00
92	0.00	0.00	0.00	0.00	65.00	100.00
90	0.00	0.00	0.00	0.00	100.00	100.00
90	0.00	0.00	0.00	16.67	96.67	100.00
90	0.00	0.00	0.00	10.00	93.33	100.00
90	0.00	0.00	0.00	0.00	95.00	100.00
90	0.00	0.00	0.00	8.33	100.00	100.00
90	0.00	0.00	0.00	5.00	91.67	100.00
90	0.00	0.00	0.00	15.00	98.33	100.00
87	0.00	0.00	16.67	30.00	100.00	100.00
87	0.00	0.00	8.33	25.00	100.00	100.00
87	0.00	0.00	3.33	31.67	100.00	100.00
87	0.00	0.00	13.33	36.67	100.00	100.00
87	0.00	0.00	16.67	16.67	100.00	100.00
87	0.00	0.00	1.67	13.33	100.00	100.00
87	0.00	0.00	13.33	31.67	100.00	100.00
84	0.00	1.67	35.00	80.00	100.00	100.00
84	6.67	0.00	33.33	73.33	100.00	100.00
84	0.00	16.67	30.00	83.33	100.00	100.00
84	0.00	25.00	16.67	58.33	100.00	100.00
84	1.67	13.33	25.00	65.00	100.00	100.00
84	5.00	15.00	36.67	75.00	100.00	100.00
84	0.00	16.67	23.33	73.33	100.00	100.00
79	16.67	50.00	50.00	85.00	100.00	100.00
79	8.33	41.67	66.67	95.00	100.00	100.00
79	6.67	33.33	53.33	70.00	100.00	100.00
79	15.00	35.00	48.33	85.00	100.00	100.00
79	18.33	23.33	35.00	98.33	100.00	100.00
79	16.67	26.67	43.33	76.67	100.00	100.00
79	6.67	30.00	45.00	68.33	100.00	100.00
73	80.00	100.00	100.00	100.00	100.00	100.00
73	78.33	100.00	100.00	100.00	100.00	100.00
73	65.00	100.00	100.00	100.00	100.00	100.00

Table continued on page 111

73	73.33	100.00	100.00	100.00	100.00	100.00
73	55.00	100.00	100.00	100.00	100.00	100.00
73	66.67	100.00	100.00	100.00	100.00	100.00
73	75.00	100.00	100.00	100.00	100.00	100.00

Appendix E

Ferrofluid Loss as a Function of Particle Size

The density of the ferrofluid used was 960 kg/m^3.and the mass of the sample was 1000 g.

Particle Size [mm]	Mass of Sample and Ferrofluid [g]	Mass of Magnetite in Dried Sample [g]	Mass of Ferrofluid Recovered [g]	Ferrofluid Recovered [%]	Ferrofluid Lost [kg/tonne of feed]
-0.85+0.5	1164.92	0.12	164.5	99.82	0.73
	1165.21	0.21	164.5	99.70	
	1166.63	0.53	164.8	99.21	
	1164.75	0.45	163.2	99.33	
	1165.18	0.08	164.9	99.88	
	1165.38	0.58	163.4	99.15	
	1165.72	0.12	165.3	99.82	
-1.7+1	1098.82	0.12	98.4	99.70	0.72
	1096.75	0.25	95.9	99.38	
	1096.23	0.63	94.1	98.40	
	1097.50	0.00	97.5	100.00	
	1098.38	0.58	96.4	98.57	
	1098.53	0.33	97.4	99.19	
	1098.06	0.16	97.5	99.59	
-2.8+2	1049.03	0.33	47.9	98.36	0.69
	1047.19	0.29	46.2	98.51	
	1050.61	0.41	49.2	98.01	
	1050.05	0.25	49.2	98.80	
	1048.94	0.04	48.8	99.80	
	1049.45	0.25	48.6	98.78	
	1049.01	0.41	47.6	97.94	
-4+2.8	1042.39	0.29	41.4	98.34	0.64
	1041.86	0.36	40.6	97.9	
	1042.57	0.37	41.3	97.87	
	1041.14	0.04	41.0	99.76	
	1041.85	0.25	41.0	98.56	
	1042.59	0.29	41.6	98.35	
	1042.05	0.25	41.2	98.56	
-8+4	1030.05	0.25	29.2	97.99	0.63
	1028.19	0.29	27.2	97.49	
	1030.15	0.25	29.3	97.99	
	1030.71	0.21	30.0	98.36	
	1031.35	0.25	30.5	98.07	
	1030.09	0.29	29.1	97.65	
	1030.48	0.29	29.5	97.68	

Table continued on page 113

-12+8	1022.66	0.16	22.1	98.22	0.56
	1024.15	0.25	23.3	97.49	
	1022.75	0.25	21.9	97.33	
	1022.85	0.25	22.0	97.35	
	1022.35	0.25	21.5	97.29	
	1021.09	0.29	20.1	96.63	
	1021.46	0.16	20.9	98.12	

Appendix F

Ferrofluid Recovery as a Function of Material Moisture Content

The density of ferrofluid used was 960 kg/m^3 and the mass of the sample was 1000 g.

Moisture Content [%]	Mass of Sample and Ferrofluid [g]	Mass of Magnetite in Dried Sample [g]	Mass of Ferrofluid Recovered [g]	Ferrofluid Recovered [%]
0	1042.19	0.29	41.2	98.33
	1042.07	0.37	40.8	97.84
	1042.69	0.49	41.0	97.16
	1041.24	0.04	41.1	99.76
	1040.88	0.08	40.6	99.51
	1042.59	0.29	41.6	98.35
	1039.96	0.16	39.4	98.99
2.5	1039.98	0.58	38.0	96.45
	1041.49	0.29	40.5	98.30
	1040.10	0.00	40.1	100.00
	1039.78	0.08	39.5	99.50
	1040.22	0.12	39.8	99.25
	1038.60	0.12	38.6	100.00
	1039.92	0.12	39.5	99.25
5	1039.02	0.00	38.6	99.23
	1036.04	0.04	35.9	99.72
	1037.82	0.12	37.4	99.20
	1036.44	0.04	36.3	99.73
	1036.76	0.16	36.2	98.91
	1035.94	0.04	35.8	99.72
	1035.04	0.04	34.9	99.71
10	1030.18	0.08	29.9	99.34
	1035.64	0.04	35.5	99.72
	1033.54	0.04	33.4	99.70
	1031.70	0.00	31.7	100.00
	1034.88	0.08	34.6	99.43
	1033.98	0.08	33.7	99.41
	1033.18	0.08	32.9	99.40

Appendix G

Ferrofluid Loss as a Function of Porosity

The density of ferrofluid used was 960 kg/m^3 and the mass of the sample was 1000 g.

Porosity [%]	Mass of Sample and Ferrofluid [g]	Mass of Magnetite in Dried Sample [g]	Mass of Ferrofluid Recovered [g]	Ferrofluid Recovered [%]	Ferrofluid Lost [kg/tonne of feed]
11.34	1164.92	0.12	164.5	99.82	
	1165.21	0.21	164.5	99.7	
	1166.63	0.53	164.8	99.22	
	1164.75	0.45	163.2	99.33	
	1165.18	0.08	164.9	99.88	
	1165.38	0.58	163.4	99.15	
	1166.30	0.70	163.9	98.97	0.93
8.78	1158.35	0.25	157.5	99.62	
	1158.74	0.74	156.2	98.86	
	1154.85	0.25	154.0	99.61	
	1157.50	0.70	155.1	98.92	
	1155.31	0.21	154.6	99.68	
	1157.45	0.25	156.6	99.62	
	1154.36	0.16	153.8	99.74	0.88
0.5	1149.22	0.12	148.8	99.80	
	1150.04	0.04	149.9	99.93	
	1146.32	0.12	145.9	99.79	
	1147.35	0.25	146.5	99.59	
	1150.31	0.41	148.9	99.33	
	1147.97	0.37	146.7	99.39	
	1155.29	0.29	154.3	99.55	0.56
0.27	1144.62	0.12	144.2	99.79	
	1141.42	0.12	141.0	99.79	
	1142.81	0.21	142.1	99.65	
	1139.36	0.16	138.8	99.71	
	1140.34	0.04	140.2	99.93	
	1138.85	0.25	138.0	99.57	
	1138.62	0.62	136.5	98.91	0.53
0.18	1125.94	0.04	125.8	99.92	
	1128.68	0.08	128.4	99.84	
	1132.54	0.04	132.4	99.92	
	11133.6	0.00	133.6	100.00	
	1134.64	0.04	134.5	99.93	
	1130.32	0.12	129.9	99.77	
	1132.10	0.00	132.1	100.00	0.12

Porosity Results as Obtained from the CSIR

CSIR Specimen Number	Rock Type	Mass [g]	Density [kg/m^3]	Pre-Test Condition			Porosity Test					
				Mass before Drying [g]	Dry OD 60 °C Mass [g]	Water Loss [%]	Saturation Mass [g]	Density of Fluid [kg/m^3]	Pore Volume [cm^3]	Total Volume [cm^3]	Rock Porosity [%]	Average Porosity [%]
OD No 21	Kimberley	208.45	2460	208.45	200.16	3.98	206.98	750	9.06	81.32	11.12	11.34
		207.08	2450	207.08	198.34	4.22	205.34	750	9.36	81.11	11.54	
OD No 24	Venetia	223.89	2620	223.89	223.83	0.03	224.10	750	0.36	85.38	0.42	0.50
		223.46	2620	223.46	223.40	0.03	223.77	750	0.50	85.38	0.58	
OD No 28	Local Sand	238.97	2850	238.97	238.93	0.02	239.03	750	0.13	83.98	0.16	0.18
		239.31	2850	239.31	239.27	0.02	239.40	750	0.17	83.98	0.21	
1678A	Kimberlite	72.52	2370	74.59	72.52	2.78	74.59	750	2.74		8.95	8.78
	OD76	59.98	2370	61.63	59.98	2.68	61.63	750	2.18		8.61	
1678B	Basalt	64.45	2800	64.50	64.45	0.08	64.50	750	0.07		0.29	0.27
	OD83	63.88	2800	63.92	63.88	0.06	63.92	750	0.05		0.24	

Appendix H

Magnetisation Curve of some Kerosene-based Ferrofluids

1) Ferrofluid of density 950 kg/m^3.

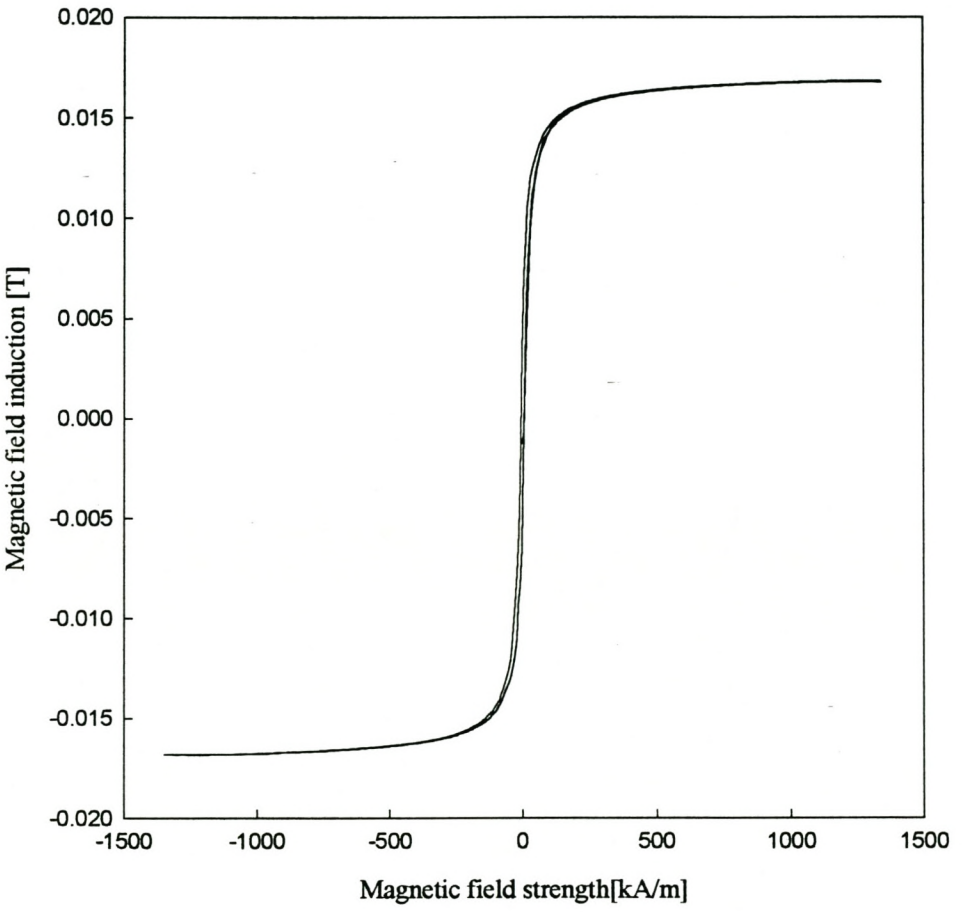

2) Ferrofluid of density 980 kg/m^3.

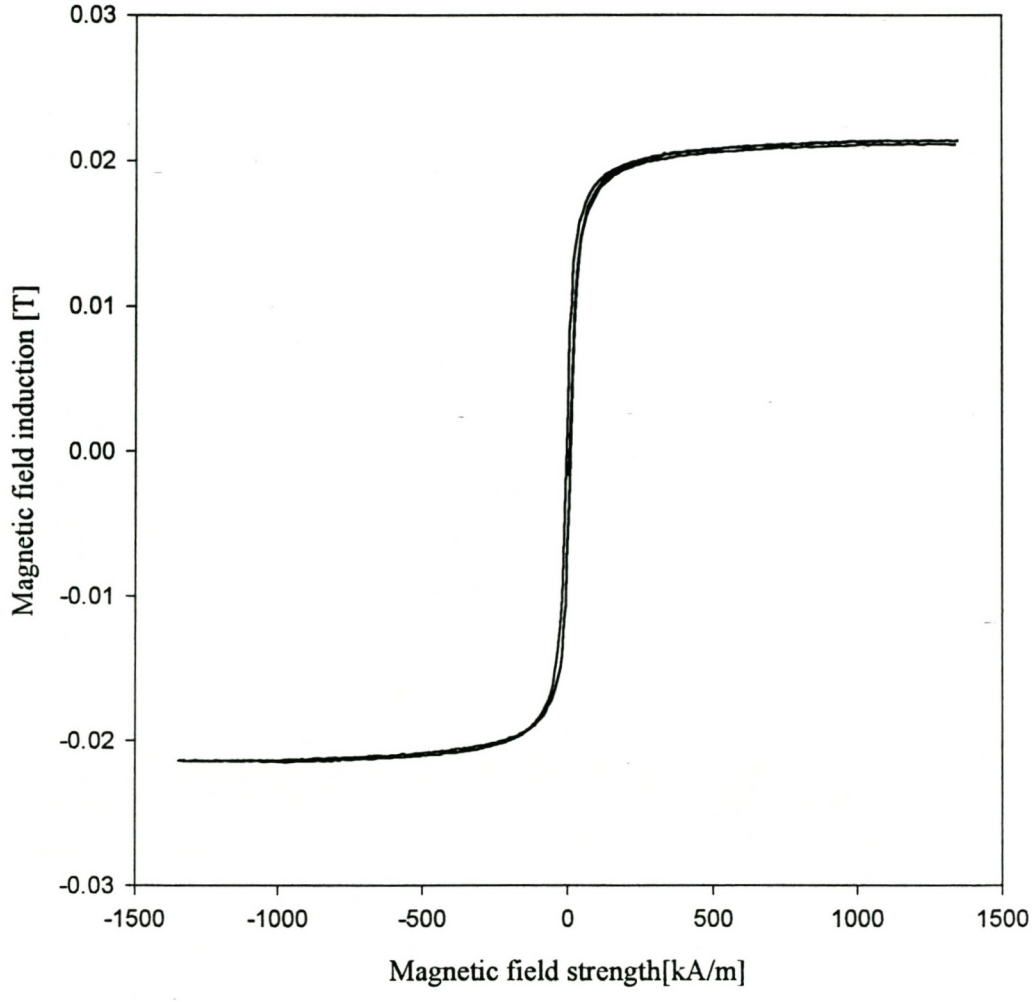

Appendix I

Viscosity of Different Density Ferrofluids in a Magnetic Field

Data from Gubarevich, 1987.